1-1-2011

Interactions between BMP and Canonical Wnt Signaling Regulate Critical Stages of the Osteoblast Lifecycle

Valerie Salazar
Washington University in St. Louis

WASHINGTON UNIVERSITY

Division of Biology and Biomedical Sciences

Program in Molecular Cell Biology

Dissertation Examination Committee:
Thomas Baranski
Kendall Blumer
Roberto Civitelli, Chairperson
Daniel Link
Fanxin Long
Gregory Longmore
Gabriel Mbalaviele

INTERACTIONS BETWEEN BMP AND CANONICAL WNT SIGNALING REGULATE CRITICAL STAGES OF THE OSTEOBLAST LIFECYCLE

By

Valerie Suzzette Salazar

A dissertation presented to the
Graduate School of Arts and Sciences
of Washington University in
partial fulfillment of the
requirements for the degree of
Doctor of Philosophy

August 2011
St. Louis, Missouri

ABSTRACT OF THE DISSERTATION

Interactions between BMP and Canonical Wnt Signaling
Regulate Critical Stages of the Osteoblast Lifecycle

by

Valerie Suzzette Salazar

Doctor of Philosophy in Biology and Biomedical Sciences
(Molecular Cell Biology)
Washington University in St. Louis, 2011
Professor Roberto Civitelli, MD., Chairperson

Skeletal development and post-natal bone homeostasis are dependent on the coordinated activity of bone-forming cells called osteoblasts and bone-resorbing cells called osteoclasts. Over 10 million people in the US currently suffer from osteoporosis, which increases the risk of low-trauma fractures and accounts for health care expenditures exceeding $14 billion per year. Osteoporosis is often treated with anti-resorptive compounds, primarily bisphosphonates, which inhibit osteoclast-mediated bone destruction. However, these drugs do not restore bone mass, which can only be accomplished by activation new bone formation, as with intermittent parathyroid hormone therapy. The development of additional bone “anabolic” therapies will require genetic and mechanistic information about other signaling pathways that can potently stimulate osteoblast differentiation and/or function. A wealth of genetic evidence in humans and mice clearly demonstrates that the canonical Wnt pathway is intimately involved in skeletal development and post-natal bone homeostasis. In fact, neutralizing antibodies to antagonists of the canonical Wnt pathway, such as Sclerostin and Dickkhopf1, are currently in clinical trials as potentially promising bone anabolic agents. However, it is still unclear how Wnt signaling provides such a strong osteogenic stimulus and how it interacts with BMP signaling, another pro-osteogenic pathway, to generate accurate and timely cues during the osteoblast differentiation process. Previous work in our lab showed that β-catenin, an essential mediator of canonical Wnt

signaling, synergizes with BMP2 to stimulate osteoblast differentiation and bone formation. My work was designed to conduct a full evaluation of how BMP and Wnt signals interact at discrete stages of the osteoblast lifecycle to regulate cell fate, establish a mitotic/post-mitotic boundary, stimulate production of the skeletal extracellular matrix, and prevent programmed cell death. Using an in vitro model of osteoblast differentiation, we find that β-catenin acts downstream of BMP2 signaling to promote an osteoblast and suppress an adipocyte cell fate decision in multipotent progenitors, a lineage allocation mechanism requiring both Tcf/Lef-dependent and Tcf/Lef–independent mechanisms. We next examined BMP/Wnt interactions during proliferation of osteoprogenitors, by focusing on Smad4, a central mediator of the greater TGFβ/BMP pathway. Acute, tamoxifen-induced deletion of Smad4 in otherwise normal osteoblasts in mice activates proliferation of predominantly post-mitotic Osterix+ cells on trabecular bone surfaces. Manipulation of Smad4 in osteoprogenitor cell lines indicates this effect is accomplished, at least in part, by the ability of BMP signals to stimulate physical recruitment of β–catenin to the DNA-binding Smad4 transcription complex, occurring in a manner that antagonizes Tcf/Lef-dependent transcription and the pro-mitotic effects of canonical Wnts. This led us to hypothesize that deficiency of Smad4 could enhance the anabolic effects of anti-Dkk1 therapy. Using a genetic mouse model with constitutive embryonic deletion of Smad4 in Osterix+ cells, we instead find that long-term deficiency of Smad4 in Osterix+ cells causes a lethal impairment of post-natal skeletal development characterized by defective osteoblasts which are insensitive to anabolic effects of BMP2 and canonical Wnts. This cell-autonomous osteoblast defect is explained by disruption of p38 MAPK signaling, which causes premature apoptosis and Caspase-3-mediated inactivation of β-catenin, and therefore resistance to anabolic Wnt signaling. Thus, acute removal of Smad4 directly favors canonical Wnt signaling and mitosis, while long-term deficiency of Smad4 indirectly impairs Wnt signaling and osteoblast function. In summary, these studies provide evidence that multifaceted interactions between BMP and Wnt signaling regulate cell fate, proliferation, function, and survival of osteoblasts.

For Irene and Petra, my two greatest mentors

The work was supported the National Institute of Arthritis, Musculoskeletal and Skin Diseases
Award Numbers F31 AR056586, R01 AR043470,
R01 AR055913, and R01 AR056678

And from The Center for Musculoskeletal Biology and Medicine, Award Number P30 AR057235
from the National Institute of Arthritis, Musculoskeletal and Skin Diseases.

The content is solely the responsibility of the authors
and does not necessarily represent the official views of the National Institute of Arthritis,
Musculoskeletal and Skin Diseases or the National Institutes of Health

TABLE OF CONTENTS

Abstract of the Dissertation ii

List of Figures and Tables viii

Chapter 1 Introduction 1

1.1 Skeletal Development 2

1.2 Genetic Markers of Connective Tissue Cells and Osteoblast Ontogeny 3

1.3 Premise and Overall Objective 4

1.4 The BMP Signaling Pathway 5

1.5 The Wnt/β-catenin Signaling Pathway 6

1.6 Wnt/β-catenin Signaling in Cell Fate Specification 6

1.7 Wnt/β-catenin Signaling in Proliferation 7

1.8 Wnt/β-catenin Signaling in Bone Formation 8

1.9 BIBLIOGRAPHY 10

Chapter 2 β-catenin Acts Downstream of BMP2 to Suppress Adipocyte Cell Fate and Promote Osteoblast Differentiation 14

2.1 ABSTRACT 15

2.2 INTRODUCTION 16

2.3 METHODS 18

2.4 RESULTS 21

2.4.1 Generation of a β-catenin mutant library and expression in C3H10T1/2 mouse embryonic fibroblasts 21

2.4.2 Transactivation of Tcf/Lef by over expression of β-catenin directly correlates with suppression of adipocyte differentiation but does not predict its ability to stimulate osteoblast formation 21

2.4.3 BMP2/4 signals are required upstream of β-catenin to promote differentiation of osteoblasts or adipocytes 23

2.5 DISCUSSION 24

2.6 ACKNOWLEDGMENTS 27

2.7 BIBLIOGRAPHY 28

2.8 FIGURE LEGENDS 32

2.9 FIGURES 35

Chapter 3 Smad4 Attenuates Proliferation and Canonical Wnt Signaling In the Osteogenic Lineage 40

3.1 ABSTRACT 41

3.2 INTRODUCTION 42

3.3 METHODS 45

3.4 RESULTS 49

3.4.1 BMP2 stimulates the formation of a Smad4/β-catenin DNA-binding complex 49

3.4.2 Smad4 expression inversely correlates with Tcf/Lef-dependent transcription and proliferation 51

3.4.3 Smad4 antagonizes transcriptional activity on the human CCND1 promoter via DNA-binding activity but not Smad-dependent transcription 53

3.4.4 Acute postnatal ablation of Smad4 in Osterix+ cells enhances proliferation in bone 55

3.4.5 Postnatal ablation of Smad4 in Osterix+ Cells enhances osteoblast proliferation more than inhibition of Dkk1 57

3.5 DISCUSSION 59

3.6 BIBLIOGRAPHY 65

3.7 FIGURE LEGENDS 69

3.8 FIGURES 72

Chapter 4 Smad4 Coordinates p38 Signaling in Osteoblasts and is Required for a Bone Anabolic Response to Canonical Wnt Signaling 77

4.1 ABSTRACT 78

4.2 INTRODUCTION 79

4.3 METHODS 81

4.4 RESULTS 83

4.4.1 Progressive skeletal phenotype in mice with 83

deficiency of Smad4 in Osx1+ cells

4.4.2 Loss of Smad4 impairs R-Smad and p38 MAPK pathways in osteoblasts 85

4.4.3 Bone anabolic responses to canonical Wnt signaling require Smad4 in osteoblasts 87

4.5 DISCUSSION 90

4.6 BIBLIOGRAPHY 93

4.7 FIGURE LEGENDS 101

4.8 FIGURES 105

4.9 TABLE 114

Chapter 5 Summary and Future Directions 114

5.1 CONCLUSIONS 115

5.2 Summary of Chapter 2 116

5.3 Summary of Chapter 3 117

5.4 Summary of Chapter 4 118

5.5 FUTURE DIRECTIONS 119

5.6 CLOSING REMARKS 121

5.7 BIBLIOGRAPHY 122

Curriculum Vitae 123

LIST OF FIGURES AND TABLES

Chapter 1 Introduction

Figure 1.1 Endochondral and intramembranous ossification 2

Figure 1.2 Genetic markers of connective tissue types 3

Chapter 2 β-catenin acts downstream of BMP2 to suppress adipocyte cell fate and promote osteoblast differentiation

Figure 2.1 Structure and expression of β-catenin mutants. 35

Figure 2.2 Tcf/Lef-dependent transcriptional activity of β-catenin mutants and C3H10T1/2 differentiation. 36

Figure 2.3 The C-terminal transactivation domain of β-catenin is necessary for Tcf/Lef transcriptional activity and for suppression of adipogenesis, but is dispensable for osteogenic stimulation. 37

Figure 2.4 A Tcf/Lef-defective β-catenin mutant stimulates both osteoblasts and adipocytes under osteogenic conditions and enhances BMP-2 effects. 38

Figure 2.5 C3H10T1/2 cells express endogenous BMP-4 which accounts for most of the “intrinsic” pro-osteogenic β-catenin activity 39

Chapter 3 Smad4 Attenuates Canonical Wnt Signaling and Proliferation In the Osteogenic Lineage

Figure 3.1 β-catenin translocates to the nucleus and physically associates with Smad4 to modulate the transcriptional response to BMP2 72

Figure 3.2 Smad4 expression inversely correlates with Tcf/Lef-dependent transcription 73

Figure 3.3 Antagonism of CCND1 promoter activity is partially dependent on Smad4 DNA-binding activity, but independent of Smad transcriptional activity or autocrine regulation of the canonical Lrp5/6 pathway 74

Figure 3.4 Post-natal tamoxifen-dependent ablation of Smad4 in Osterix+ cells activates proliferation of osteoblasts 75

Figure 3.5 The Mitotic Response to Ablation of Smad4 in Osterix+ cells is Stronger than Mitotic Response to Inhibition of Dkk1 76

Chapter 4 Smad4 Coordinates p38 Signaling in Osteoblasts and is Required for a Bone Anabolic Response to Canonical Wnt Signaling

Figure 4.1 Progressive skeletal phenotype in Smad4$^{F/F}$; Osx1-EGFP::Cre mice 105

Figure 4.2 Abnormal Architecture and Quality of Long Bones in Smad4$^{F/F}$; Osx1-Cre mice 106

Figure 4.3 Non-cell autonomous regulation of osteoclastogenesis by Smad4 in Osx1+ cells is not explained by RankL/Opg 108

Figure 4.4 Smad4 is required in Osx1+ cells for expression of collagen-processing enzymes in bone 109

Figure 4.5 Smad4 integrates with p38 MAPK to regulate expression of Lox and Bcl-2 110

Figure 4.6 Ablation of Smad4 Curtails Osteoanabolic Response to Canonical Wnt signaling 111

Figure 4.7 Smad4 protects osteoblasts from apoptosis and deactivating cleavage of β-catenin 112

Table 4.1 Antibodies used in Chapter 4 113

Chapter 5 Summary and Future Directions

Figure 5.1 Interactions between BMP and canonical Wnt signaling regulate critical stages of the osteoblast lifecycle 115

CHAPTER 1

Introduction

1.1 SKELETAL DEVELOPMENT - The skeleton forms during late stages of development from three embryonic lineages. Migration of neural crest and paraxial mesoderm contributes to form the cranial vault [1]. The spine of the axial skeleton derives from paraxial mesoderm and is formed by a precisely timed process of sclerotome divisions known as the somite clock [3]. The limbs of the appendicular skeleton are formed by progenitors from lateral plate mesoderm. During development, these progenitors migrate to their final destinations and proliferate to form organized cellular condensations at sites where bone will be formed by either endochondral bone development (Figure 1A) or intramembranous ossification (Figure 1B; see review [2]). Membranous skeletal tissues of the skull, jaw, and innermost layer of long bones are formed in sheets-like fragments by differentiation of mesenchymal progenitors into **osteoblasts**, the bone-producing cells of the body. By contrast, the formation of endochondral bones of the appendicular skeleton is a multistep process where mesenchymal progenitors first generate **chondrocytes**, or cartilage-producing cells that form a template of the skeleton known as the anlagen. This anlagen is then patterned and elongated largely via a Hedgehog and Parathyroid Hormone Related Protein regulatory network [4] before the

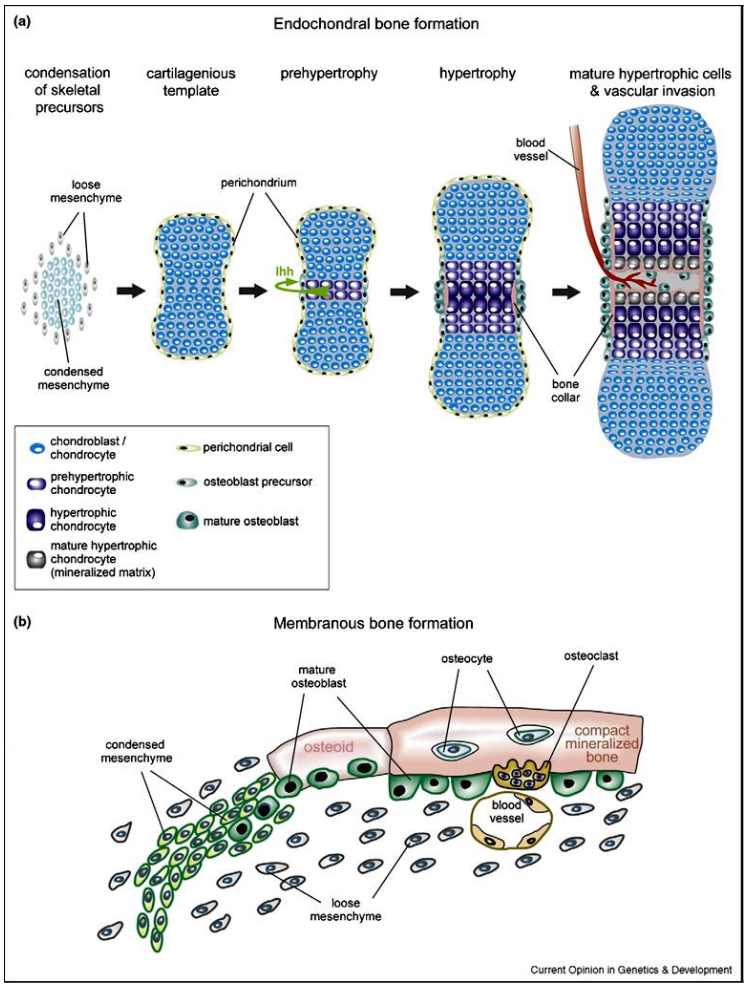

Figure 1.1 Schematic showing the processes of endochondral (a) and intramembranous (b) ossification [2].

appearance of mesenchymally-derived osteoblast progenitors on the perichondral surfaces. Finally, the avascular cartilage template is then converted to a mature mineralized bone with a medullary cavity by an orchestrated invasion of blood vessels, cartilage-resorbing cells of the hematopoietic lineage known as **osteoclasts**, and bone forming osteoblasts [5]. Though initially formed during development, the skeleton is a dynamic tissue that undergoes remodeling in response to physiologic and environmental factors for the remainder of post-natal life. A greater understanding of the cellular and molecular factors contributing to differentiation and function of skeletal cells will contribute to the identification of molecules and pathways which may be employed as pharmacologic targets in therapeutic intervention of skeletal disease.

1.2 GENETIC MARKERS OF OSTEOBLASTS AND RELATED CONNECTIVE TISSUE CELLS- Skeletal progenitors of the mesenchymal lineage are multipotent and can adopt a chondrocyte or osetoblast cell fate during development, in addition to an adipocyte cell fate in postnatal skeletal tissues. Mesenchymal progenitors actually co-express a wide variety of "lineage-specific" transcription factors. And the process of cell fate determination is characterized by the ability of the multipotent progenitors to process positional and intracellular cues in a manner that ultimately favors dominant action by mediators of one lineage over others (Figure 1.2). For example, the transcription factor Sox9 promotes formation of chondrocytes at the expense of osteoblasts by direct negative regulation of

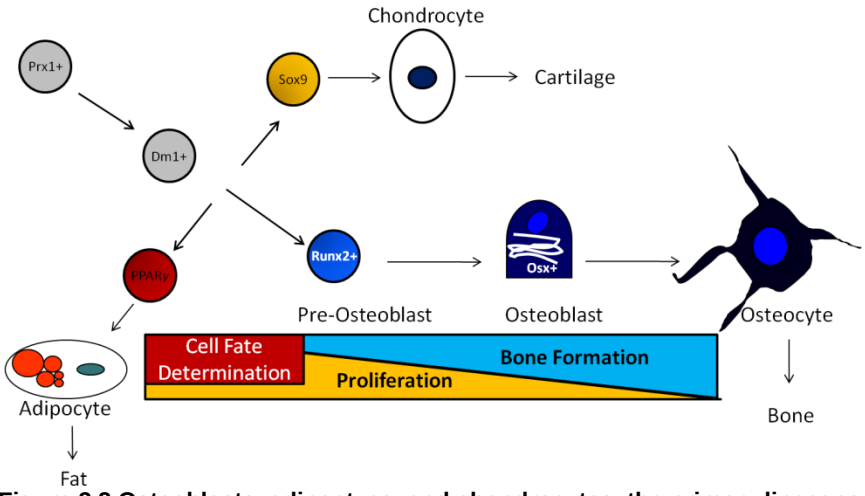

Figure 2.2 Osteoblasts, adipoctyes, and chondrocytes, the primary lineages of connective tissue, are derived from common mesenchymal progenitors and are characterized by expression of specific genetic markers

β-catenin [6,7], an essential mediator of the canonical Wnt pathway. By contrast, high Wnt/β-catenin activity can favor osteoblast formation at the expense of chondrocyte [8,9,10] or adipocyte cell fate [11]. And conditions favoring adipogenesis promote dominance by PPARγ proteins, which are critical for the differentaion of fat cells [12]. This body of the research focuses on the osteoblast, whose lineage is characterized by tissue-restricted transcription factors such as Runx2 and Osterix, as well as the ubiquitious transcription factor, β-catenin.

1.3 PREMISE AND OVERALL OBJECTIVE - A large body of data demonstrates that β-catenin signaling is critically involved in bone development and cell fate determination of osteoblasts. Although the importance of β-catenin in favoring osteoblast over chondrocyte differentiation during embryonic skeletogenesis has been demonstrated [8,9,10,13,14], the molecular mechanisms by which Wnt/β-catenin signaling stimulates osteogenesis and bone formation in the post-natal skeleton require further evaluation. Cumulative work by many labs indicates that β-catenin provides temporally-specific regulatory cues during critical stages of the osteoblast differentiation program. For example, in committed by still immature osteoprogenitors, β-catenin favors maturation into matrix secreting osteoblasts [15]. Curiously however, when β-catenin is activated in this same differentiating population, it stimulates cell cycle, resulting in expansion of progenitors which are supposed to be exiting cell cycle to progress through differentiation. In mature osteoblasts, β-catenin inhibits terminal differentiation [15] and has non-cell autonomous control of osteoclastogenesis [16]. Genetic evidence in both mice and humans further indicates that elevated Lrp5/ β-catenin signaling protects osteoblasts from programmed cell death. β-catenin therefore functions as a mediator of cell fate decisions, a stimulator of proliferation, a driver of osteoblast maturation, and protector from cell death. Using multipotent embryonic mouse fibroblast cell lines and in vivo models of bone formation, our lab previously found that β-catenin synergistically interacts with Bone Morphogenetic Protein-2 and (BMP-2) to producing new bone [17]. **The central focus of this work is to examine the epistatic and molecular**

interactions between β-catenin and the BMP pathway that contribute to coordinate cell fate allocation, proliferation, matrix synthesis, and the death of osteoblasts.

1.4 THE BMP SIGNALING PATHWAY - Bone Morphogenetic Proteins (BMPs), are members of the Transforming Growth Factor-β (TGFβ) superfamily. BMPs signal in diverse organisms to regulate proliferation, differentiation, and tissue morphogenesis. TGFβ ligands activate heterodimeric serine/threonine kinase receptors to stimulate a variety of intracellular signal transduction cascades including PI-3K/Akt, ERK, p38, and JNK, which are non-specific to the TGFβ pathway, and Smads, which are TGFβ-specific [18]. Distinct groups of receptor-activated Smads (RA-Smads) are phospho-activated in response to different classes of TGFβligands. For example, ligand-mediated activation of the BMP Type I (BMPRI) and BMP Type II (BMPRII) heterodimeric receptor induces phosphorylation and dimerization of Smads-1, -5, and -8. In all cases however, pathway activation results in RA-Smad homodimerization and recruitment of an additional, non-receptor activated, Smad4. Smads contain intrinsic protein domains facilitating both nucleocytoplasmic shuttling and DNA-binding, enabling Smad complexes to function as transcription factors which induce gene expression at promoters containing Smad-binding elements (SBEs) [19]. Physical association of Smad protein complexes with other co-activators such as forkhead proteins [20], OAZ [21], Runx2/Cbfa1 [22], and Schnurri [23] confers considerable plasticity and tissue specificity to Smad-dependent transcription. Interestingly, Smads have been demonstrated to integrate with β-catenin/Tcf4, components of the canonical Wnt pathway, on the msx-2 [24], gastrin [25], and c-myc [26] promoters, or with β-catenin/Lef1 during formation of the embryonic Spemann organizer [27]. Abundant evidence therefore indicates that the BMP and Wnt pathways can interact via intracellular signaling mechanisms involving Smads and β-catenin.

1.5 THE WNT/β-CATENIN SIGNALING PATHWAY - β-catenin and plakoglobin are two vertebrate homologs of Drosophila armadillo, which serve as a bridge between cadherins and the actin-

based cytoskeleton. Through binding to α-catenin, they stabilize intercellular adherens junctions [28]. In addition to its function in cell-cell adhesion, β-catenin also functions as a transcriptional activator within the Wnt signaling pathway, a system involved in regulation of many embryonic processes, including limb development and growth [29]. In the Wnt pathway, β-catenin is downstream of Frizzled (Fz) and LRP-5 or LRP-6, two co-receptors that transduce signals upon binding to their extracellular ligands, Wnts. In the absence of Wnts, β-catenin is phosphorylated by glycogen synthase kinase-3 (GSK-3), and thus targeted for degradation through the ubiquitin-proteasome pathway. Upon activation of the Wnt pathway, phosphorylation of β-catenin by GSK-3β is inhibited, causing accumulation of β-catenin in the cytoplasm and Rac-1 mediated translocation into the nucleus where it associates with DNA binding proteins of the T cell factor / lymphoid enhancer factor (Tcf/Lef) family to activate gene transcription (for reviews, see [30,31,32]). Tcf/Lefs function as transcriptional repressors in the absence of β-catenin.

1.6 WNT/β-CATENIN SIGNALING IN CELL FATE SPECIFICATION - The Wnt/β-catenin signaling system is involved cell fate determination in many tissues. Studies using conditional deletion of the β-catenin gene (Catnb) in the epidermis demonstrate that in the absence of β-catenin skin stem cells fail to differentiate into follicular keratinocytes, but instead adopt an epidermal phenotype [33]. Importantly, this study also concluded that although β-catenin is necessary for stem cells to form follicular keratinocytes, β-catenin is not sufficient to induce follicular differentiation of keratinocytes, and additional mesenchymal signals are required [33,34,35]. Using the same strategy, others have demonstrated that ablation of the β-catenin gene in epithelial cells of the embryonic lungs disrupts lung morphogenesis while enhancing formation of the conducting airways [36]. Expression of constitutively a activated β-catenin mutant can result in precocious lobuloalveolar development and differentiation of mammary glands [37]. While BMP signals are well known to regulate tissue morphogenesis during development, the BMP pathway is not typically associated with cell fate decisions per se, such as the Wnt pathway is well known. Our finding that activated β-catenin synergizes with BMP2 to stimulate osteoblast

formation from multipotent progenitors suggests that combined β-catenin and BMP2 signaling amplifies the osteoblast cell fate decision normally attributed to β-catenin alone. **Chapter 2 examines how β-catenin interacts with BMP signals to promote and amplify allocation of progenitor cells to the osteoblast and not adipocyte lineage.**

1.7 WNT/β-CATENIN SIGNALING IN PROLIFERATION - In addition to mediating cell fate decisions, β-catenin stimulates cell cycle via Tcf/Lef-dependent expression of Cyclin-D1[9]. In the intestine, β-catenin can even favor proliferation of crypt cells over villous differentiation [38], demonstrating its ability to act on both cell fate and mitotic potential. While β–catenin normally acts in immature Runx2+ cells to expand the osteoprogenitor pool, it generally does not provide mitotic signals in progenitors once they begin progressing through the Runx2+/Osterix+ transition. Osterix+ cells of the osteoblast lineage are typically bone-adherent or bone-embedded cells, and have a diminished proliferative index, as would be expected for acquisition of their specialized function as bone producing cells. Curiously, while β–catenin is required in Osterix+ cells for acquisition of their matrix mineralizing function, genetic activation of canonical β–catenin activity in the Osterix+ population inappropriately reactivates cell cycle [15] and causes pathologic levels of bone growth [15]. This strongly suggests that there is mechanism acting in the osteogenic lineage to govern whether β–catenin is providing pro-mitotic or pro-differentation cues.

We considered this in the context of tumorigenesis where activating mutations of β-catenin, or upstream Wnt components, lead to loss of cell cycle control and increased proliferation [30,39,40,41,42,43]. A similar effect is often seen by loss of Smad4 or loss of Smad4 DNA-binding activity [44,45,46,47]. The mechanism by which Smad4 attenuates proliferation and protects against pathophysiologic hyperplasia remains poorly understood, but intriguing clues can be taken from experiments in Drosophila melanogaster demonstrating that phenotypes normally associated with Wingless (the fly ortholog of Wnt) or activated armadillo (the fly ortholog of β-catenin) are induced by expression of Smad4 mutants defective in DNA-binding [48]. The fact that loss of Smad4 phenocopies proliferative and cell fate cues attributed to activated β-catenin

leads us to hypothesize that loss of Smad4 antagonizes proliferation by antagonizing canonical Wnt/β-catenin activity. **Chapter 3 of this work tests the specific hypothesis that pro-mitotic Wnt/β-catenin signals are negatively regulated by BMP/Smad4 activity in osteoprogenitors.**

1.8 WNT/β-catenin SIGNALING IN BONE FORMATION. The involvement of β-catenin in osteoblast differentiation and bone formation is demonstrated by studies showing that upstream activators and downstream mediators of β-catenin signaling are essential for skeletal development. In the mouse, loss-of-function mutations of Wnt-5a [49], Wnt-7a [50], LRP-6 [51], or the transcription factors Lef1 and Tcf1 [52], cause a variety of malformations whose common denominator is abnormal skeletal development or lack of skeletal elements. A number of in vivo studies further defined the critical role of this signaling system in bone development. Loss-of-function mutations of LRP-5 have been linked to osteoporosis pseudoglioma syndrome, a rare condition characterized by congenital severe osteoporosis [53]. Accordingly, LRP-5 null mice are osteopenic since birth owing to an osteoblast defect [54]. By contrast, "gain-of-function" mutations of LRP-5 have been identified in two separate kindred with a high bone mass phenotype [55,56]. Since β-catenin is an integral component of the Wnt pathway, these observations would support the notion that β-catenin is involved in controlling bone development and bone mass acquisition. Recent work cast doubts about β-catenin involvement in mediating the bone anabolic effect of LRP-5 activation, pointing instead to an endocrine loop involving serotonin secretion from the duodenum [57]. While the role of endocrine signaling on regulation of bone mass is under intense study by many groups, it was recently demonstrated that osteoblast-specific gene ablation of both Lrp5 and Lrp6 are catastrophic to bone formation, thereby solidifying a role for Wnt signaling through Lrp5/6 receptors specifically in osteoblasts.

Whereas developmental studies clearly demonstrate that β-catenin is necessary for osteoblast differentiation and bone formation, complex and sometimes seemingly contradictory interactions between BMP and Wnt signaling have been reported in the skeletal system. For example, β-catenin was shown to be both upstream and downstream of BMP signaling in mice

with Catnb ablation in neural crest cells [13]. On the other hand, lack of Catnb blocks the osteogenic effect of BMP-2 in ex vivo mouse calvaria cultures [8], while β-catenin contributes to formation of new ectopic bone in response to BMPs [58], leading to the notion that canonical Wnt signaling, via β-catenin, may be downstream of BMP signaling, as proposed by earlier in vitro studies [59,60]. Recent data on conditional BMPR1A inactivation in osteoblasts seem to support this view, suggesting BMPs up-regulate Wnt signaling via upregulation of Sclerostin [61,62]. However, others found that blockade of BMP signaling actually impedes Wnt-induced osteoblast differentiation, suggesting instead that Wnt is upstream of BMPs [63]. Clearly, simple epistatic models do not satisfactory explain the many discrepant data on BMP and Wnt/β-catenin interactions. We hypothesize that Wnt/β-catenin activation and BMP signaling are required simultaneously to deliver timely and accurate osteogenic cues. **In Chapter 4, we specifically examine the requirement for Smad4 in osteogenic BMP signaling, and then continue by utilizing in vivo and in vitro experiments to test whether anabolic responses to canonical Wnt signaling require integrity of the BMP signaling pathway.**

1.9 BIBLIOGRAPHY

1. Minoux M, Rijli FM Molecular mechanisms of cranial neural crest cell migration and patterning in craniofacial development. Development 137: 2605-2621.
2. Hartmann C (2009) Transcriptional networks controlling skeletal development. Curr Opin Genet Dev 19: 437-443.
3. Aulehla A, Pourquie O Signaling gradients during paraxial mesoderm development. Cold Spring Harb Perspect Biol 2: a000869.
4. Vortkamp A, Lee K, Lanske B, Segre GV, Kronenberg HM, et al. (1996) Regulation of rate of cartilage differentiation by Indian hedgehog and PTH-related protein. Science 273: 613-622.
5. Maes C, Kobayashi T, Selig MK, Torrekens S, Roth SI, et al. Osteoblast precursors, but not mature osteoblasts, move into developing and fractured bones along with invading blood vessels. Dev Cell 19: 329-344.
6. Akiyama H, Lyons JP, Mori-Akiyama Y, Yang X, Zhang R, et al. (2004) Interactions between Sox9 and beta-catenin control chondrocyte differentiation. Genes Dev 18: 1072-1087.
7. Topol L, Chen W, Song H, Day TF, Yang Y (2009) Sox9 inhibits Wnt signaling by promoting beta-catenin phosphorylation in the nucleus. J Biol Chem 284: 3323-3333.
8. Hill TP, Spater D, Taketo MM, Birchmeier W, Hartmann C (2005) Canonical Wnt/β-catenin signaling prevents osteoblasts from differentiating into chondrocytes. Developmental Cell 8: 727-738.
9. Hu H, Hilton MJ, Tu X, Yu K, Ornitz DM, et al. (2005) Sequential roles of Hedgehog and Wnt signaling in osteoblast development. Development 132: 49-60.
10. Day TF, Guo X, Garrett-Beal L, Yang Y (2005) Wnt/β-catenin signaling in mesenchymal progenitors controls osteoblast and chondrocyte differentiation during vertebrate skeletogenesis. Developmental Cell 8: 739-750.
11. Ross SE, Hemati N, Longo KA, Bennett CN, Lucas PC, et al. (2000) Inhibition of adipogenesis by Wnt signaling. Science 289: 950-953.
12. Takada I, Kouzmenko AP, Kato S (2009) Wnt and PPARgamma signaling in osteoblastogenesis and adipogenesis. Nat Rev Rheumatol 5: 442-447.
13. Brault V, Moore R, Kutsch S, Ishibashi M, Rowitch DH, et al. (2001) Inactivation of the β-catenin gene by Wnt1-Cre-mediated deletion results in dramatic brain malformation and failure of craniofacial development. Development 128: 1253-1264.
14. Holmen SL, Zylstra CR, Mukherjee A, Sigler RE, Faugere MC, et al. (2005) Essential role of β-catenin in postnatal bone acquisition. Journal of Biological Chemistry 280: 21162-21168.
15. Rodda SJ, McMahon AP (2006) Distinct roles for Hedgehog and canonical Wnt signaling in specification, differentiation and maintenance of osteoblast progenitors. Development 133: 3231-3244.
16. Glass DA, Bialek P, Ahn JD, Starbuck M, Patel MS, et al. (2005) Canonical wnt signaling in differentiated osteoblasts controls osteoclast differentiation. Developmental Cell 8: 751-764.
17. Mbalaviele G, Sheikh S, Stains JP, Salazar VS, Cheng SL, et al. (2005) β-catenin and BMP-2 synergize to promote osteoblast differentiation and new bone formation. Journal of Cellular Biochemistry 94: 403-418.
18. Chen D, Zhao M, Mundy GR (2004) Bone morphogenetic proteins. Growth Factors 22: 233-241.

19. Shi Y, Wang YF, Jayaraman L, Yang H, Massague J, et al. (1998) Crystal structure of a Smad MH1 domain bound to DNA: insights on DNA binding in TGF-beta signaling. Cell 94: 585-594.
20. Seoane J, Le HV, Shen L, Anderson SA, Massague J (2004) Integration of Smad and forkhead pathways in the control of neuroepithelial and glioblastoma cell proliferation. Cell 117: 211-223.
21. Hata A, Seoane J, Lagna G, Montalvo E, Hemmati-Brivanlou A, et al. (2000) OAZ uses distinct DNA- and protein-binding zinc fingers in separate BMP-Smad and Olf signaling pathways. Cell 100: 229-240.
22. Javed A, Afzal F, Bae JS, Gutierrez S, Zaidi K, et al. (2009) Specific residues of RUNX2 are obligatory for formation of BMP2-induced RUNX2-SMAD complex to promote osteoblast differentiation. Cells Tissues Organs 189: 133-137.
23. Zwijsen A, Verschueren K, Huylebroeck D (2003) New intracellular components of bone morphogenetic protein/Smad signaling cascades. FEBS Letters 546: 133-139.
24. Hussein SM, Duff EK, Sirard C (2003) Smad4 and β-catenin coactivators functionally interact with LEF1 to regulate graded expression of Msx2. Journal of Biological Chemistry 278: 48805-48814.
25. Lei S, Dubeykovskiy A, Chakladar A, Wojtukiewicz L, Wang TC (2004) The murine gastrin promoter is synergistically activated by transforming growth factor-β/Smad and Wnt signaling pathways. Journal of Biological Chemistry 279: 42492-42502.
26. Hu MC, Rosenblum ND (2005) Smad1, β-catenin and Tcf4 associate in a molecular complex with the Myc promoter in dysplastic renal tissue and cooperate to control Myc transcription. Development 132: 215-225.
27. Nishita M, Hashimoto MK, Ogata S, Laurent MN, Ueno N, et al. (2000) Interaction between Wnt and TGF-beta signalling pathways during formation of Spemann's organizer. Nature 403: 781-785.
28. Nagafuchi A (2001) Molecular architecture of adherens junctions. Current Opinions in Cell Biology 13: 600-603.
29. Cadigan KM, Nusse R (1997) Wnt signaling: a common theme in animal development. Genes Dev 11: 3286-3305.
30. Barker N, Clevers H (2000) Catenins, Wnt signaling and cancer. Bioessays 22: 961-965.
31. Huelsken J, Behrens J (2002) The Wnt signalling pathway. Journal of Cell Science 115: 3977-3978.
32. Nelson WJ, Nusse R (2004) Convergence of Wnt, β-catenin, and cadherin pathways. Science 303: 1483-1487.
33. Huelsken J, Birchmeier W (2001) New aspects of Wnt signaling pathways in higher vertebrates. Current Opinions in Genetics and Development 11: 547-553.
34. DasGupta R, Rhee H, Fuchs E (2002) A developmental conundrum: a stabilized form of β-catenin lacking the transcriptional activation domain triggers features of hair cell fate in epidermal cells and epidermal cell fate in hair follicle cells. Journal of Cell Biology 158: 331-344.
35. Merrill BJ, Gat U, DasGupta R, Fuchs E (2001) Tcf3 and Lef1 regulate lineage differentiation of multipotent stem cells in skin. Genes Dev 15: 1688-1705.
36. Mucenski ML, Wert SE, Nation JM, Loudy DE, Huelsken J, et al. (2003) β-Catenin is required for specification of proximal/distal cell fate during lung morphogenesis. Journal of Biological Chemistry 278: 40231-40238.

37. Imbert A, Eelkema R, Jordan S, Feiner H, Cowin P (2001) Delta N89 β-catenin induces precocious development, differentiation, and neoplasia in mammary gland. Journal of Cell Biology 153: 555-568.
38. Batlle E, Henderson JT, Beghtel H, van den Born MM, Sancho E, et al. (2002) β-catenin and TCF mediate cell positioning in the intestinal epithelium by controlling the expression of EphB/ephrinB. Cell 111: 251-263.
39. Harada N, Tamai Y, Ishikawa T, Sauer B, Takaku K, et al. (1999) Intestinal polyposis in mice with a dominant stable mutation of the β-catenin gene. EMBO Journal 18: 5931-5942.
40. Castellone MD, Teramoto H, Williams BO, Druey KM, Gutkind JS (2005) Prostaglandin E2 promotes colon cancer cell growth through a Gs-axin-beta-catenin signaling axis. Science 310: 1504-1510.
41. Korinek V, Barker N, Morin PJ, van Wichen D, de Weger R, et al. (1997) Constitutive transcriptional activation by a beta-catenin-Tcf complex in APC -/- colon carcinoma. Science 275: 1784-1787.
42. Yang M, Zhong WW, Srivastava N, Slavin A, Yang J, et al. (2005) G protein-coupled lysophosphatidic acid receptors stimulate proliferation of colon cancer cells through the β-catenin pathway. Proceedings of the National Academy of Sciences of the USA 102: 6027-6032.
43. van Es JH, Barker N, Clevers H (2003) You Wnt some, you lose some: oncogenes in the Wnt signaling pathway. CurrOpinGenetDev 13: 28-33.
44. Xu X, Kobayashi S, Qiao W, Li C, Xiao C, et al. (2006) Induction of intrahepatic cholangiocellular carcinoma by liver-specific disruption of Smad4 and Pten in mice. JClinInvest 116: 1843-1852.
45. Li W, Qiao W, Chen L, Xu X, Yang X, et al. (2003) Squamous cell carcinoma and mammary abscess formation through squamous metaplasia in Smad4/Dpc4 conditional knockout mice. Development 130: 6143-6153.
46. Xu X, Brodie SG, Yang X, Im YH, Parks WT, et al. (2000) Haploid loss of the tumor suppressor Smad4/Dpc4 initiates gastric polyposis and cancer in mice. Oncogene 19: 1868-1874.
47. Qiao W, Li AG, Owens P, Xu X, Wang XJ, et al. (2006) Hair follicle defects and squamous cell carcinoma formation in Smad4 conditional knockout mouse skin. Oncogene 25: 207-217.
48. Takaesu NT, Herbig E, Zhitomersky D, O'Connor MB, Newfeld SJ (2005) DNA-binding domain mutations in SMAD genes yield dominant-negative proteins or a neomorphic protein that can activate WG target genes in Drosophila. Development 132: 4883-4894.
49. Yamaguchi TP, Bradley A, McMahon AP, Jones S (1999) A Wnt5a pathway underlies outgrowth of multiple structures in the vertebrate embryo. Development 126: 1211-1223.
50. Parr BA, McMahon AP (1995) Dorsalizing signal Wnt-7a required for normal polarity of D-V and A-P axes of mouse limb. Nature 374: 350-353.
51. Pinson KI, Brennan J, Monkley S, Avery BJ, Skarnes WC (2000) An LDL-receptor-related protein mediates Wnt signalling in mice. Nature 407: 535-538.
52. Galceran J, Farinas I, Depew MJ, Clevers H, Grosschedl R (1999) Wnt3a-/--like phenotype and limb deficiency in Lef1(-/-)Tcf1(-/-) mice. Genes Dev 13: 709-717.
53. Gong Y, Slee RB, Fukai N, Rawadi G, Roman-Roman S, et al. (2001) LDL receptor-related protein 5 (LRP5) affects bone accrual and eye development. Cell 107: 513-523.

54. Kato M, Patel MS, Levasseur R, Lobov I, Chang BH, et al. (2002) Cbfa1-independent decrease in osteoblast proliferation, osteopenia, and persistent embryonic eye vascularization in mice deficient in Lrp5, a Wnt coreceptor. Journal of Cell Biology 157: 303-314.
55. Boyden LM, Mao J, Belsky J, Mitzner L, Farhi A, et al. (2002) High bone density due to a mutation in LDL-receptor-related protein 5. New England Journal of Medicine 346: 1513-1521.
56. Little RD, Carulli JP, Del Mastro RG, Dupuis J, Osborne M, et al. (2002) A mutation in the LDL receptor-related protein 5 gene results in the autosomal dominant high-bone-mass trait. American Journal of Human Genetics 70: 11-19.
57. Yadav VK, Ryu JH, Suda N, Tanaka KF, Gingrich JA, et al. (2008) Lrp5 controls bone formation by inhibiting serotonin synthesis in the duodenum. Cell 135: 825-837.
58. Chen Y, Whetstone HC, Youn A, Nadesan P, Chow EC, et al. (2007) β-catenin signaling pathway is crucial for bone morphogenetic protein 2 to induce new bone formation. Journal of Biological Chemistry 282: 526-533.
59. Rawadi G, Vayssiere B, Dunn F, Baron R, Roman-Roman S (2003) BMP-2 controls alkaline phosphatase expression and osteoblast mineralization by a Wnt autocrine loop. Journal of Bone and Mineral Research 18: 1842-1853.
60. Bain G, Muller T, Wang X, Papkoff J (2003) Activated β-catenin induces osteoblast differentiation of C3H10T1/2 cells and participates in BMP2 mediated signal transduction. Biochemical and Biophysical Research Communications 301: 84-91.
61. Kamiya N, Ye L, Kobayashi T, Mochida Y, Yamauchi M, et al. (2008) BMP signaling negatively regulates bone mass through sclerostin by inhibiting the canonical Wnt pathway. Development 135: 3801-3811.
62. Kamiya N, Ye L, Kobayashi T, Lucas DJ, Mochida Y, et al. (2008) Disruption of BMP signaling in osteoblasts through type IA receptor (BMPRIA) increases bone mass. J Bone Miner Res 23: 2007-2017.
63. Winkler DG, Sutherland MS, Ojala E, Turcott E, Geoghegan JC, et al. (2005) Sclerostin inhibition of Wnt-3a-induced C3H10T1/2 cell differentiation is indirect and mediated by bone morphogenetic proteins. Journal of Biological Chemistry 280: 2498-2502.

CHAPTER 2

β-catenin acts downstream of BMP2 to suppress adipocyte cell fate and promote osteoblast differentiation

2.1 ABSTRACT

The role of β-catenin in skeletal development and osteogenic cell differentiation is well established, but the molecular mechanisms attending these effects remain largely unknown. We conducted a structure/function analysis of β-catenin to gain further insights on these mechanisms. Retroviral transduction of a full-length, constitutively active β-catenin mutant inhibited adipogenesis and stimulated osteoblast differentiation from multipotent embryonic fibroblasts (C3H10T1/2). However, N-terminal truncated β-catenin mutants with weak Tcf/Lef activity retained their pro-osteogenic action, as did a constitutively stabilized mutant lacking the C-terminal Tcf/Lef transactivation domain. Importantly, this Tcf/Lef-defective β-catenin did not suppress adipogenesis, and even elicited spontaneous adipogenesis when expressed in cells cultured in osteogenic conditions. Thus, Tcf/Lef transcriptional activity of β-catenin is critical for inhibition of adipogenesis, while it is dispensable for its pro-osteogenic effect. BMP-2 greatly enhanced both osteogenesis and adipogenesis in the presence of the C-terminally truncated mutant, though it selectively enhanced only osteoblast differentiation in cells transduced with the full-length, Tcf/Lef active β-catenin mutant. C3H10T1/2 cells produce BMP-4, and inhibition of endogenous BMP signaling by Noggin curtailed osteogenic differentiation by constitutively active β-catenin. Therefore, BMP signaling must be active for full induction by β-catenin of osteogenic differentiation from multipotent precursors. These data suggest that cooperative interactions between β-catenin and BMP signaling systems drive osteoblast cell fate specification and differentiation.

2.2 INTRODUCTION

β-catenin orchestrates cell fate decisions in diverse tissues and organisms. In vertebrates, β-catenin directs lineage allocation of intestinal stem cells, favoring proliferation of crypt cells over villous differentiation (Batlle et al., 2002). In the epidermis, it determines the differentiation of follicular keratinocytes while inhibiting epidermal lineages (Huelsken et al., 2001). During skeletal development, β-catenin favors osteoblast over chondrocyte fate in mesodermal and neural crest progenitors, thereby bearing an essential role in both endochondral and intramembranous ossification (Hu et al., 2005a;Day et al., 2005;Hill et al., 2005). In the adult skeleton, new osteoblasts are recruited from bone marrow stromal cells, which also give rise to adipocytes. In vitro studies demonstrate that canonical Wnts, via β-catenin and Tcf/Lef transcription factors, effectively block adipogenesis (Ross et al., 2000); and we previously showed a postnatal osteogenic to adipogenic shift in bone marrow stromal cells derived from transgenic mice expressing a dominant-negative N-cadherin, which sequesters β-catenin on the cell surface (Castro et al., 2004). This differentiation defect was rescued by expression of activated β-catenin, suggesting β-catenin favors osteoblast over adipocyte commitment from undifferentiated precursors in the adult bone marrow microenvironment.

As an integral component of adherens junctions, β-catenin stabilizes cell-cell adhesion by binding to cadherins (Nelson et al., 2004). β-catenin is also part of canonical Wnt signaling, a cascade initiated by binding of Wnt(s) to low-density lipoprotein receptor-related protein-5 or 6 (LRP-5/6) and Frizzled co-receptors, resulting in inhibition of GSK-3β-mediated degradation of β-catenin. Stabilized β-catenin accumulates in the nucleus, stimulating transcription via the Tcf/Lef family of DNA-binding proteins (Cadigan et al., 1997;van Es et al., 2003). Abundant genetic and epidemiological data support a role for canonical Wnt signaling in skeletal development (Hartmann, 2006) and post-natal bone mass acquisition (Gong et al., 2001;Little et al., 2002;Boyden et al., 2002). However, ablation or activation of the Cttnb gene in the mouse does not phenocopy genetic ablation or constitutive activation of Lrp5 (Kato et al., 2002;Babij et al., 2003), resulting in severe skeletal malformations (Hu et al., 2005a;Hill et al., 2005;Day et al., 2005). Furthermore, many components of the canonical Wnt pathway are involved in Wnt-

independent signal transduction pathways (Xu et al., 2004;Nam et al., 2006;Fujino et al., 2003;Jia et al., 2005); and Wnt-independent transactivation of Tcf/Lefs by β-catenin can be stimulated by lysophosphatidic acid (Yang et al., 2005) or by prostaglandin E2 (Castellone et al., 2005). Therefore, while Wnts can certainly provide osteogenic signals, it is possible that the osteogenic role of β-catenin may not derive exclusively from generation of canonical Wnt (Tcf/Lef-dependent) signals.

Bone morphogenetic proteins (BMPs) are important in osteoblast specification, bone formation and maintenance (Zhao et al., 2002;Wan et al., 2005;Mishina et al., 2004;Mishina et al., 2004), but can elicit the development of multiple mesenchymal skeletal lineages (Ahrens et al., 1993). Interactions between BMPs and Wnt signaling have been studied by others in a variety of mesenchymal cell lines, suggesting that such interactions are essential for osteoblast differentiation (Rawadi et al., 2003). We previously demonstrated that β-catenin synergizes with BMP-2 to stimulate osteoblast differentiation in the mouse embryonic fibroblast cell line C3H10T1/2, and to induce new bone formation in mouse calvaria (Mbalaviele et al., 2005). More recently, β-catenin signaling has been shown to be critical for BMP-2 stimulation of ectopic bone formation in vivo (Chen et al., 2007). We hypothesized that interaction with BMP signaling offers one potential mechanism by which β-catenin, a ubiquitous signaling system, provides osteogenic cues to undifferentiated multipotent cells.

To test this hypothesis, we performed a structure/function analysis of β-catenin in C3H10T1/2 cells, which differentiate into osteoblasts or adipocytes in response to BMP treatment (Ahrens et al., 1993). Our results indicate that Tcf/Lef-dependent transcriptional activity of β-catenin is not required for its pro-osteogenic action, despite that it is necessary for inhibition of adipogenesis. Furthermore, we show that BMP signaling is required for full osteogenic stimulation by β-catenin, as well as adipogenesis.

2.3 METHODS

Reagents. β-catenin antibody was purchased from BD Transduction Laboratories (San Diego, CA); KT3-tag antibody from Covance (Princeton, NJ); TCF4 antibody from Upstate (Charlottesville, VA); BMP-2/4 antibody from R&D Systems (Minneapolis, MN). Purified recombinant human BMP-2 and murine Noggin were purchased from Sigma (St. Louis, MO) and R&D systems, respectively. pTopFlash (Tcf/Lef-luc) was purchased from Promega (Madison, WI) and consists of the luciferase open reading frame preceded by 6 tandemly-arranged Tcf/Lef binding elements. p12X-SBE-Luc (SBE-luc) was a kind gift from Dr. Di Chen (University of Rochester, NY) and consists of 12 tandem Smad binding elements upstream of an osteocalcin minimal promoter and the luciferase open reading frame (Zhao et al., 2002). Primers were purchased from Invitrogen (Carlsbad, CA). Unless otherwise indicated, all other chemicals and reagents were purchased from Sigma.

Cell Culture and Differentiation Assays. C3H10T1/2 murine embryonic fibroblast cells, obtained from ATCC (Manassas, VA) were maintained in basal medium of Eagle (BME; Gibco; Carlsbad, CA) containing 10% fetal bovine serum (Atlas Biologicals; Fort Collins, CO), 40 mM L-glutamine, 100 U/ml penicillin-G, and 100 mg/ml streptomycin, and incubated at 37°C in a humidified atmosphere with 5% CO_2. To stimulate differentiation, we applied well-established methods, already described for the C3H10T1/2 cell line (Mbalaviele et al., 2005;Shin et al., 2000). Briefly, for osteogenic differentiation cells were seeded in 24-well dishes (10^5 cells per well) and cultured in osteogenic medium (10 mM β-glycerophosphate and 50 μg/ml ascorbic acid). As a marker of osteoblast lineage, ALP activity was assessed after 6-7 days in culture using a biochemical assay and normalized to protein content. In some experiments, enzyme activity was detected by direct staining in fixed cells (Mbalaviele et al., 2005). For adipogenic differentiation, C3H10T1/2 cells were cultured in adipogenic medium (5 μg/ml insulin, 50 μM indomethacin, and 0.1 μM dexamethasone) for 10 days, and adipocytes were identified after fixation by the presence of lipid droplets stained using Oil Red O (Mbalaviele et al., 2005;Shin et al., 2000).

Expression of β-catenin mutants in C3H10T1/2. β-catenin cDNAs for wild type, mutGSK, ΔN90, and ΔN151 were kind gifts from Dr. James Nelson (Stanford University, Stanford, CA). mutGSK is full length β-catenin containing four point mutations in the CK1 (S45A) and GSK3β (33/37T41A) phosphorylation domain. ΔN90, and ΔN151 are N-terminal truncation mutants that include the phosphorylation domain (Barth et al., 1997). The cDNAs encoding β-catenin mutants were subcloned into the polylinker site of pIRES2-EGFP (BDBiosciences; San Diego, CA) using SacII and BamHI. IRES-EGFP or bicistronic β-catenin-IRES-EGFP constructs were subcloned into pLNCX2 retroviral vector (BD Biosciences; San Diego, CA) using XhoI and NotI. We also generated a C-terminally truncated β-catenin, mutGSKΔC, using a modified PCR strategy (Byrappa et al., 1995) and the pLNCX2-mutGSK-IRES-EGFP plasmid as a template. Briefly, amino acids 675-781 of mutGSK β-catenin were deleted in frame from the pLNCX2-mutGSK-IRES-EGFP plasmid by amplifying the plasmid template using a high fidelity polymerase (Pfu-Turbo; Stratagene; La Jolla, CA), a forward primer complementary to the C-terminal KT3 tag of mutGSK, and a reverse primer complementary to coding sequence for β-catenin amino acids 674-668. The purified PCR product was circularized with T4 DNA ligase and cloned. Retroviral particles were generated by using Lipofectamine (Invitrogen; Carlsbad, CA) to transfect pLNCX2 retroviral vectors into 293GPG packaging cells, which express MuLV gag-pol and vesicular stomatitis virus G glycoprotein (VSV-G) under tetracycline regulation (Ory et al., 1996). Following removal of tetracycline repression, 293GPG conditioned media were collected daily and tested for ability to transduce C3H10T1/2 cells. Infectious fractions were pooled and supplemented with 6 μg/ml anionic polybrene. Subconfluent C3H10T1/2 cells were incubated in viral-conditioned media for 48 hr and selected for 7 d with 1 mg/ml G418 antibiotic. Transgene expression was assessed by both fluorescence microscopy (detection of EGFP) and SDS-PAGE/immunoblot (detection of transgenic β-catenin or C-terminal KT3 tag).

Luciferase Assay. Following a previously described method (Stains et al., 2003), cells were seeded in 24-well plates ($4x10^4$ cells per well), and the following day plasmids (0.4 μg/well of TopFlash or SBE-luc) were transfected using Lipofectamine2000 (Invitrogen; Carlsbad, CA)

per manufacturer's instructions. Transfection medium was replaced with complete medium containing additional treatments as indicated. Tcf/Lef-luc and SBE-luc were harvest after 24 hr of treatment. Luciferase activity was assessed in an Optocomp luminometer using a Luciferase kit (Promega; Madison, WI) as per manufacturer's instructions. Since the Renilla reporters commonly used for normalization of transfection efficiency were modulated by some treatments used in this study, Firefly activity is shown as a ratio over the average of the control group. Assays were repeated >3 times.

Immunoprecipitation and Immunoblotting. Whole cell protein extracts were prepared as previously described (Mbalaviele et al., 2005). Protein content was determined Pierce BCA kit, separated by SDS-PAGE, and transferred to PDVF membranes (Millipore; Billerica, MA). Membranes were blocked and probed in PBS containing 0.05% Tween-20 and 5% non-fat dry milk. Antigen-antibody complexes were visualized by horseradish peroxidase-conjugated secondary antibody (1:5000) and West-Pico detection (Pierce; Rockford, IL).

RNA Isolation and PCR. Briefly, 1 µg total RNA was isolated using RNeasy kit (Qiagen; Valencia, CA) and was reverse transcribed using Superscript II reverse transcriptase and oligo(dT)15 primers (Stains et al., 2003;Stains et al., 2005). **Quantitative real time PCR** was performed using SYBR green (Applied Biosystems; Foster City; CA) and an ABI Prism 7300 detector using these conditions: 40 cycles (95°C/10 min, 95°C/15 sec, 60°C/30 sec). Data were normalized to Gapdh expression. For **semi-quantitative RT-PCR analysis**, the following conditions were used: 95°C/5 min; 30 cycles (95°C for 30 sec, 55°C for 30 sec, and 72°C for 30 sec); 72°C for 5 min. Primers: Bmp-2 (RT-PCR) sense 5'-cggagactctctcaatggac-3' and antisense 5'-gttcctccacggcttctagt-3'; Bmp-4 (RT-PCR) sense 5'-ctcccaagaatcatggactg-3' and antisense 5'-aaagcagagctctcactggt-3'; Bmp-4 (QPCR) sense 5'-ttcctggtaaccgaatgctga-3' and antisense 5'-cctgaatctcggcgacttttt-3'.

Statistical Analysis. All data are expressed as the mean ± standard deviation. Group means were compared by unpaired t-test.

2.4 RESULTS

2.4.1 Generation of a β-catenin Mutant Library and Expression in C3H10T1/2 Mouse Embryonic Fibroblasts. We first functionally characterized the transcriptional and osteogenic activities of 3 constitutively stabilized β-catenin mutants, mutGSK, ΔN90, and ΔN151 (Figure 2.1A) in C3H10T1/2 cells. Effective expression of these mutants, achieved by retroviral transduction using bicistronic constructs that also express EGFP, was verified by both EGFP fluorescence and Western blotting using antibody to β-catenin C-terminus. G418-resistant cells exhibited fluorescence in the green spectrum (Figure 2.1B), and the level of protein expression of each mutant was similar to endogenous β-catenin (Figure 2.1C).

2.4.2 Transactivation of Tcf/Lef by Overexpression of β-catenin Directly Correlates with Suppression of Adipogenesis but does not Predict Its Ability to Stimulate Osteoblast Differentiation. Each β-catenin mutant stimulated the activity of a Tcf/Lef-dependent transcriptional reporter (Tcf/Lef-luc). However, despite the similar abundance of protein expression (Figure 2.1C), mutGSK was a far more potent transcriptional co-activator than was ΔN90 or ΔN151 (Figure 2.2A, black bars). Consistent with our previous findings (Mbalaviele et al., 2005), BMP-2 treatment for 24 h did not activate Tcf/Lef-luc alone and did not enhance the effect of any β-catenin mutant (Figure 2.2A, gray bars). As we previously reported (Mbalaviele et al., 2005), ΔN151 was at best a weak stimulator of alkaline phosphatase (ALP) activity, an early marker of osteoblast differentiation. By contrast, mutGSK or ΔN90 stimulated substantially higher levels of ALP activity after 7 days of culture (Figure 2.2B, black bars). Importantly, BMP-2 (100ng/ml) synergistically enhanced ALP stimulation by each β-catenin mutant (Figure 2.2B, gray bars). However, ΔN90 was stronger in stimulating ALP activity than was ΔN151 (Figure 2.2B), despite that ΔN90 and ΔN151 were equivalent activators of Tcf/Lef-dependent transcription (Figure 2.2A). Also, ΔN90 and mutGSK stimulated similar levels of ALP activity (Figure 2.2B) despite that ΔN90 was a weaker activator of Tcf/Lef-dependent transcription (Figure 2.2A). By contrast, after 10 days in culture with an adipogenic medium, transduction with either of the N-

terminally truncated mutants, ΔN90 or ΔN151 resulted in about 70% fewer adipocytes compared to EGFP, while mutGSK nearly abrogated adipogenesis (Figure 2.2C). Thus, inhibition of adipogenesis by β-catenin directly correlates with its Tcf/Lef transcriptional activity, whereas stimulation of ALP activity by β-catenin does not.

To better test whether induction of ALP activity can be dissociated from β-catenin transactivation of Tcf/Lef, a stabilized but transcriptionally-defective β-catenin mutant lacking the C-terminal transactivation domain was generated from the mutGSK retrovirus vector backbone (mutGSKΔC; Figure 2.3A). It was successfully expressed in C3H10T1/2 cells, as shown by immunoblots of lysates from mutGSKΔC transduced cells (Figure 2.3B). To test the biologic activity of mutGSKΔC, we first compared its ability to stimulate Tcf/Lef transcription against 80mM LiCl, a pharmacological inhibitor of GSK3 or the Tcf/Lef-active mutant, mutGSK. Exposure to 80 mM LiCl and expression of mutGSK resulted in a similar degree of Tcf/Lef-dependent promoter activity, and no further stimulation was obtained by treating mutGSK-transduced cells with LiCl. Conversely, mutGSKΔC did not autonomously transactivate Tcf/Lef-luc, and in fact, it significantly inhibited endogenous and LiCl-stimulated Tcf/Lef activity (Figure 2.3C). These results confirm that the C-terminal domain is required for canonical β-catenin transcriptional activity (Cong et al., 2003), and demonstrate that this construct functions as a dominant-negative on Tcf/Lef dependent transactivation. To determine whether loss of β-catenin's Tcf/Lef activity correlates with a loss of biological function, we monitored adipogenesis in cells transduced with either mutGSK or mutGSKΔC. As noted earlier, transduction with mutGSK prevented formation of Oil Red O positive cells in adipogenic medium, however transduction with mutGSKΔC was ineffective in this regard, yielding an abundance of adipocytes similar to those observed in EGFP control cultures (Figure 2.3D). Importantly, despite the loss of both Tcf/Lef-activity and its anti-adipogenic effect, mutGSKΔC stimulated a comparable level of ALP activity as mutGSK, an effect which was enhanced by exogenous BMP-2 (Figure 2.3E).

Consistent with quantitative biochemical results, the number of ALP positive cells in 10-day mutGSK or mutGSKΔC osteogenic cultures was much higher than in EGFP cultures,

although the number in mutGSKΔC cultures was slightly less than in mutGSK cultures (Figure 2.4A, B, and C). BMP-2 (200 ng/ml) greatly enhanced the ability of mutGSK to stimulate ALP staining (Figures 2.4A, B, D, and E). The number of ALP positive cells in mutGSKΔC plus BMP-2 cultures equaled or exceeded that of mutGSK plus BMP-2 (Figures 2.4F and 2.4E). Remarkably, adipocytes appeared among ALP-positive cells in mutGSKΔC cultures but not in mutGSK cultures (Figures 2.4B-C' and 2.4E-F'). Adipogenesis in mutGSKΔC cells ensued spontaneously, in the absence of adipogenic stimuli and the presence of osteogenic supplements (Figures 2.4C-C'); and it became vigorous with BMP-2 treatment (Figures 2.4F-F').

2.4.3 BMP2/4 Signals Act Upstream of β-catenin to Promote Differentiation Both Osteoblasts and Adipocytes. These results indicate that mutGSK, ΔN90, and mutGSKΔC, but not ΔN151, stimulate osteoblast differentiation in the absence of exogenous BMP-2. However, C3H10T1/2 cells have been reported to produce BMPs (Shea et al., 2003). To determine if endogenously produced BMPs are required for the "intrinsic" osteogenic activity of these β-catenin mutants, we first assessed BMP expression by RT-PCR in 20% and 100% confluent C3H10T1/2 cells. C3H10T1/2 cells express abundant Bmp-4 mRNA, perhaps more abundantly in confluent than non-confluent cells, whereas Bmp-2 mRNA is undetectable (Figure 2.5A). Temporal expression profiling revealed that Bmp-4 expression sharply increased >25-fold after the first 7 days post-confluence in osteogenic medium, receding by 21 d (Figure 2.5B). Neither exposure to exogenous BMP-2, nor transduction of mutGSK altered expression of Bmp-4 (Figure 2.5B) or Bmp-2 (data not shown). To ascertain the signaling activity of endogenous BMPs, a BMP-responsive transcriptional luciferase reporter (SBE-luc) was transfected into C3H10T1/2 cells. Addition of recombinant Noggin (a BMP-2/4/7 antagonist) or a BMP-2/4 neutralizing antibody significantly inhibited basal SBE-luc activity while exogenous BMP-2, used as positive control, stimulated SBE-luc activity 3-fold (Figure 2.5C).

More to the point, when cells transduced with activated mutGSK were cultured in osteogenic media in the presence of different concentrations of Noggin for 7 days, induction of

ALP activity by mutGSK was dose-dependently attenuated by BMP blockade (Figure 2.5D). Notably, at a concentration of 1.5 µg/ml, Noggin inhibited BMP-dependent SBE-luc activity by 50% (Figure 2.5C) and mutGSK-dependent ALP activity by 70% (Figure 2.5D), indicating that endogenous BMPs, probably BMP-4, contribute in great part, if not entirely, to osteoblast differentiation induced by activated β-catenin in C3H10T1/2 cells. Since adipogenesis was enhanced by BMP-2 in cells transduced with the transcriptionally inactive mutGSKΔC, we tested whether induced adipogenesis was sensitive to BMP signaling blockade. The formation of Oil Red O positive cells in cells grown in adipogenic medium for 9 days was dose-dependently stimulated by exogenous BMP-2, and dose-dependently inhibited by Noggin (Figure 2.5E). Thus, endogenous BMPs drive both adipogenic and osteogenic differentiation in C3H10T1/2 cells.

2.5 DISCUSSION

We previously reported that stabilized β–catenin synergizes with BMP-2 to stimulate in vitro osteoblast differentiation and in vivo new bone formation (Mbalaviele et al., 2005). That study evaluated the effects of a single mutant, ΔN151, which displayed little osteogenic action by itself and required exogenous BMP-2 treatment to generate an osteogenic stimulus. Here, we utilize a more comprehensive structure-function analysis to demonstrate that, when expressed on a wild type background, the ability of β-catenin to stimulate Tcf/Lef-dependent transcriptional activity is neither necessary nor sufficient to induce osteoblast differentiation, but rather requires active BMP signaling.

Previous studies reported that β-catenin contributes to formation of new ectopic bone in response to BMPs (Chen et al., 2007); that genetic ablation of β-catenin blocks the osteogenic effect of BMP-2 in ex vivo mouse calvaria cultures (Hill et al., 2005); and that canonical Wnt signaling is induced by BMPs via an autocrine loop (Rawadi et al., 2003;Bain et al., 2003). These data suggested a model whereby canonical Wnt signaling, via β-catenin, is part of the downstream events activated by BMPs to induce osteogenesis. However, others found that blockade of BMP signaling impedes Wnt-induced osteoblast differentiation (Winkler et al., 2005);

and the present work demonstrates that blockade of BMP signaling impedes the stimulatory effect of constitutively activated β-catenin, which does not require expression of canonical Wnts to stimulate Tcf/Lef-dependent transcription. Thus, while others had reported "intrinsic" osteogenic activity in various β-catenin mutants, (Rawadi et al., 2003;Bain et al., 2003), we here clarify that even a full-length β-catenin mutant with potent Tcf/Lef activity is still largely dependent on endogenously produced BMPs for its pro-osteogenic activity. Furthermore, since we find that up-regulation of endogenous BMP-4 requires at least 3 days of culture in differentiation medium, the assessment of effects by β-catenin/Wnt and BMP signaling interactions is heavily dependent on timing of experimental endpoints. This factor may in part explain some of the discrepant results from independent groups. Nonetheless, collective findings do not support a simple epistatic model of osteogenesis where Wnts are downstream mediators of BMPs. Instead, emerging data suggest that canonical Wnt signaling through β-catenin is necessary, though not sufficient in the absence of BMPs, to stimulate osteoblast differentiation (Chen et al., 2007). Although it is possible that canonical Wnts may induce expression of BMPs in a β-catenin-dependent manner to stimulate osteoblast differentiation (Winkler et al., 2005), the present results together with others' findings (Hill et al., 2005), strongly suggest that β-catenin activation and BMP signaling are required simultaneously to deliver an osteogenic cue.

Our structure-function analysis of β-catenin establishes that its anti-adipogenic and pro-osteogenic actions are separable. We find that the anti-adipogenic action of β-catenin directly correlates with Tcf/Lef-dependent transcriptional activity and requires the C-terminal transactivation domain. By contrast, the transactivation domain is dispensable for the pro-osteogenic function of β-catenin, which is not accurately predicted by Tcf/Lef activity. Although the molecular nature of this β-catenin-dependent but non-canonical pro-osteogenic mechanism remains to be determined, Tcf/Lef-independent functions of β-catenin in cell fate specification have been proposed in other cell types. For example, ablation of β-catenin in skin stem cells induces epidermal differentiation at the expense of follicular keratinocyte differentiation (Huelsken et al., 2001) while expression of a Tcf/Lef-defective β-catenin mutant instead had both dominant-

positive and dominant-negative actions, depending upon the cell context in which it was expressed (DasGupta et al., 2002). It is also worth considering why constitutive activation or ablation of β-catenin leads to severe skeletal malformations in mice (Hu et al., 2005a;Day et al., 2005;Hill et al., 2005), while ablation of Lrp5 results only in low bone mass and an osteoblast defect but no skeletal malformations (Kato et al., 2002). Thus, previous findings support the notion that the pro-osteogenic action of β-catenin can operate in a non-canonical (Tcf/Lef-independent) manner. And furthermore, mechanistically separable cell fate cues may be operative in other tissues as well.

A non-canonical mechanism could be related to cross-talk between components of the Wnt and BMP signaling systems. For example, direct interaction between Smad1 and Dvl-1 in undifferentiated mesenchymal cells decreases cell proliferation (Chen et al., 2007). Alternatively, β-catenin itself and Tcf/Lef proteins may interact with Smad-containing transcription complexes on promoters containing both Tcf/Lef and Smad-binding elements (Hussein et al., 2003;Lei et al., 2004;Hu et al., 2005b). Or, β-catenin may even directly interact with BMP-2 signaling independently of Tcf/Lef proteins. Intriguingly, canonical Wnt signals are reported to regulate gene expression in osteoblasts which are involved in osteoclast function, such as Opg (Glass et al., 2005); but to date there is no strong evidence that osteoblastic genes, such as Runx2 or Osterix, are directly activated by Tcf/Lef-dependent mechanisms (Glass et al., 2005;Kato et al., 2002). Determining if non-canonical β-catenin signaling regulates osteoblast gene expression and differentiation therefore represents an attractive hypothesis to test.

Our data support a model where β-catenin refines a BMP-2 signal into either an adipocyte or osteoblast cue, depending upon its transcriptional activity. When β-catenin is fully active, adipogenesis is inhibited and BMP signaling is fully osteogenic. When transcriptional activity is inhibited, BMP signals become ambiguous, inducing both osteogenesis and adipogenesis. Thus, both Tcf/Lef-dependent and Tcf/Lef-independent actions of β-catenin are necessary to make a BMP signal strictly osteogenic. While the anti-adipogenic function is linked to the C-terminal transactivation domain, the topology of β-catenin pro-osteogenic activity is less clear. The differences in ALP stimulatory activities between the ΔN90 and ΔN151 mutants point

to a region between residues 90 and 151 that might be critically important for β-catenin pro-osteogenic action. However, the ΔN151 mutant was still able to enhance BMP-2 induced osteoblast differentiation, implying that additional domains are involved. These do not include the transactivation domain, since C-terminal deletion of β-catenin has no detrimental effect on its pro-osteogenic function. Finer resolution of the structure-function correlates of β-catenin should be useful for understanding its pro-osteogenic action, and the mode of interaction with the BMP signaling system.

In summary, we demonstrate that when overexpresed, β-catenin employs at least two mechanistically distinct actions that control differentiation of mesenchymal lineages: a Tcf/Lef-dependent function of β-catenin operates to suppress the adipocyte lineage; and, a Tcf/Lef-independent function integrates with a BMP signal to induce osteogenesis. Our results support a model whereby β-catenin and BMP effectors act cooperatively, so full induction of an osteoblastogenesis program occurs when they signal in tandem. This cooperative interaction of two osteogenic signaling systems will now be tested in vivo.

2.6 Acknowledgements

The authors wish to express their gratitude to Drs. Adriana Di Benedetto, Joseph Stains, and previous members of the Civitelli laboratory for help with some technical aspects of the work and for critical discussion of the results. Parts of this work have been presented in abstract form at the 27th annual meeting of the American Society for Bone and Mineral Research, Nashville, TN, September 23-27, 2005.

2.7 BIBLIOGRAPHY

1. Ahrens M, Ankenbauer T, Schroder D, Hollnagel A, Mayer H, Gross G. 1993. Expression of human bone morphogenetic proteins-2 or -4 in murine mesenchymal progenitor C3H10T1/2 cells induces differentiation into distinct mesenchymal cell lineages. DNA Cell Biol 12:871-880.
2. Babij P, Zhao W, Small C, Kharode Y, Yaworsky PJ, Bouxsein ML, Reddy PS, Bodine PV, Robinson JA, Bhat B, Marzolf J, Moran RA, Bex F. 2003. High bone mass in mice expressing a mutant LRP5 gene. J Bone Miner Res 18:960-974.
3. Bain G, Muller T, Wang X, Papkoff J. 2003. Activated b-catenin induces osteoblast differentiation of C3H10T1/2 cells and participates in BMP2 mediated signal transduction. Biochem Biophys Res Commun 301:84-91.
4. Barth AI, Pollack AL, Altschuler Y, Mostov KE, Nelson WJ. 1997. NH2-terminal deletion of b-catenin results in stable colocalization of mutant β-catenin with adenomatous polyposis coli protein and altered MDCK cell adhesion. J Cell Biol 136:693-706.
5. Batlle E, Henderson JT, Beghtel H, van den Born MM, Sancho E, Huls G, Meeldijk J, Robertson J, van de WM, Pawson T, Clevers H. 2002. Beta-catenin and TCF mediate cell positioning in the intestinal epithelium by controlling the expression of EphB/ephrinB. Cell 111:251-263.
6. Boyden LM, Mao J, Belsky J, Mitzner L, Farhi A, Mitnick MA, Wu D, Insogna K, Lifton RP. 2002. High bone density due to a mutation in LDL-receptor-related protein 5. N Engl J Med 346:1513-1521.
7. Byrappa S, Gavin DK, Gupta KC. 1995. A highly efficient procedure for site-specific mutagenesis of full-length plasmids using Vent DNA polymerase. Genome Res 5:404-407.
8. Cadigan KM, Nusse R. 1997. Wnt signaling: a common theme in animal development. Genes Dev 11:3286-3305.
9. Castellone MD, Teramoto H, Williams BO, Druey KM, Gutkind JS. 2005. Prostaglandin E2 promotes colon cancer cell growth through a Gs-axin-beta-catenin signaling axis. Science 310:1504-1510.
10. Castro CH, Shin CS, Stains JP, Cheng SL, Sheikh S, Mbalaviele G, Szejnfeld VL, Civitelli R. 2004. Targeted expression of a dominant-negative N-cadherin in vivo delays peak bone mass and increases adipogenesis. J Cell Sci 117:2853-2864.
11. Chen Y, Whetstone HC, Youn A, Nadesan P, Chow EC, Lin AC, Alman BA. 2007. Beta-catenin signaling pathway is crucial for bone morphogenetic protein 2 to induce new bone formation. J Biol Chem 282:526-533.
12. Cong F, Schweizer L, Chamorro M, Varmus H. 2003. Requirement for a nuclear function of beta-catenin in Wnt signaling. Mol Cell Biol 23:8462-8470.
13. DasGupta R, Rhee H, Fuchs E. 2002. A developmental conundrum: a stabilized form of β-catenin lacking the transcriptional activation domain triggers features of hair cell fate in epidermal cells and epidermal cell fate in hair follicle cells. J Cell Biol 158:331-344.
14. Day TF, Guo X, Garrett-Beal L, Yang Y. 2005. Wnt/beta-catenin signaling in mesenchymal progenitors controls osteoblast and chondrocyte differentiation during vertebrate skeletogenesis. Dev Cell 8:739-750.
15. Fujino T, Asaba H, Kang MJ, Ikeda Y, Sone H, Takada S, Kim DH, Ioka RX, Ono M, Tomoyori H, Okubo M, Murase T, Kamataki A, Yamamoto J, Magoori K, Takahashi S, Miyamoto Y, Oishi H, Nose M, Okazaki M, Usui S, Imaizumi K, Yanagisawa M, Sakai J, Yamamoto TT. 2003. Low-density lipoprotein receptor-related protein 5 (LRP5) is

essential for normal cholesterol metabolism and glucose-induced insulin secretion. Proc Natl Acad Sci U S A 100:229-234.

16. Glass DA, Bialek P, Ahn JD, Starbuck M, Patel MS, Clevers H, Taketo MM, Long F, McMahon AP, Lang RA, Karsenty G. 2005. Canonical wnt signaling in differentiated osteoblasts controls osteoclast differentiation. Dev Cell 8:751-764.
17. Gong Y, Slee RB, Fukai N, Rawadi G, Roman-Roman S, Reginato AM, Wang H, Cundy T, Glorieux FH, Lev D, Zacharin M, Oexle K, Marcelino J, Suwairi W, Heeger S, Sabatakos G, Apte S, Adkins WN, Allgrove J, Arslan-Kirchner M, Batch JA, Beighton P, Black GC, Boles RG, Boon LM, Borrone C, Brunner HG, Carle GF, Dallapiccola B, De Paepe A, Floege B, Halfhide ML, Hall B, Hennekam RC, Hirose T, Jans A, Juppner H, Kim CA, Keppler-Noreuil K, Kohlschuetter A, LaCombe D, Lambert M, Lemyre E, Letteboer T, Peltonen L, Ramesar RS, Romanengo M, Somer H, Steichen-Gersdorf E, Steinmann B, Sullivan B, Superti-Furga A, Swoboda W, van den Boogaard MJ, Van Hul W, Vikkula M, Votruba M, Zabel B, Garcia T, Baron R, Olsen BR, Warman ML. 2001. LDL receptor-related protein 5 (LRP5) affects bone accrual and eye development. Cell 107:513-523.
18. Hartmann C. 2006. A Wnt canon orchestrating osteoblastogenesis. Trends Cell Biol 16:151-158.
19. Hill TP, Spater D, Taketo MM, Birchmeier W, Hartmann C. 2005. Canonical Wnt/beta-catenin signaling prevents osteoblasts from differentiating into chondrocytes. Dev Cell 8:727-738.
20. Hu H, Hilton MJ, Tu X, Yu K, Ornitz DM, Long F. 2005a. Sequential roles of Hedgehog and Wnt signaling in osteoblast development. Development 132:49-60.
21. Hu MC, Rosenblum ND. 2005b. Smad1, beta-catenin and Tcf4 associate in a molecular complex with the Myc promoter in dysplastic renal tissue and cooperate to control Myc transcription. Development 132:215-225.
22. Huelsken J, Vogel R, Erdmann B, Cotsarelis G, Birchmeier W. 2001. β-Catenin controls hair follicle morphogenesis and stem cell differentiation in the skin. Cell 105:533-545.
23. Hussein SM, Duff EK, Sirard C. 2003. Smad4 and β -catenin coactivators functionally interact with LEF1 to regulate graded expression of Msx2. J Biol Chem 278:48805-48814.
24. Jia J, Zhang L, Zhang Q, Tong C, Wang B, Hou F, Amanai K, Jiang J. 2005. Phosphorylation by double-time/CKIepsilon and CKIalpha targets cubitus interruptus for Slimb/beta-TRCP-mediated proteolytic processing. Dev Cell 9:819-830.
25. Kato M, Patel MS, Levasseur R, Lobov I, Chang BH, Glass DA, Hartmann C, Li L, Hwang TH, Brayton CF, Lang RA, Karsenty G, Chan L. 2002. Cbfa1-independent decrease in osteoblast proliferation, osteopenia, and persistent embryonic eye vascularization in mice deficient in Lrp5, a Wnt coreceptor. J Cell Biol 157:303-314.
26. Lei S, Dubeykovskiy A, Chakladar A, Wojtukiewicz L, Wang TC. 2004. The murine gastrin promoter is synergistically activated by transforming growth factor-beta/Smad and Wnt signaling pathways. J Biol Chem 279:42492-42502.
27. Little RD, Carulli JP, Del Mastro RG, Dupuis J, Osborne M, Folz C, Manning SP, Swain PM, Zhao SC, Eustace B, Lappe MM, Spitzer L, Zweier S, Braunschweiger K, Benchekroun Y, Hu X, Adair R, Chee L, FitzGerald MG, Tulig C, Caruso A, Tzellas N, Bawa A, Franklin B, McGuire S, Nogues X, Gong G, Allen KM, Anisowicz A, Morales AJ, Lomedico PT, Recker SM, Van Eerdewegh P, Recker RR, Johnson ML. 2002. A mutation

in the LDL receptor-related protein 5 gene results in the autosomal dominant high-bone-mass trait. Am J Hum Genet 70:11-19.
28. Mbalaviele G, Sheikh S, Stains JP, Salazar VS, Cheng SL, Chen D, Civitelli R. 2005. β-catenin and BMP-2 synergize to promote osteoblast differentiation and new bone formation. J Cell Biochem 94:403-418.
29. Mishina Y, Starbuck MW, Gentile MA, Fukuda T, Kasparcova V, Seedor JG, Hanks MC, Amling M, Pinero GJ, Harada S, Behringer RR. 2004. Bone morphogenetic protein type IA receptor signaling regulates postnatal osteoblast function and bone remodeling. J Biol Chem 279:27560-27566.
30. Nam JS, Turcotte TJ, Smith PF, Choi S, Yoon JK. 2006. Mouse cristin/R-spondin family proteins are novel ligands for the Frizzled8 and LRP6 receptors and activate beta -catenin-dependent gene expression. J Biol Chem .
31. Nelson WJ, Nusse R. 2004. Convergence of Wnt, beta-catenin, and cadherin pathways. Science 303:1483-1487.
32. Ory DS, Neugeboren BA, Mulligan RC. 1996. A stable human-derived packaging cell line for production of high titer retrovirus/vesicular stomatitis virus G pseudotypes. Proc Natl Acad Sci U S A 93:11400-11406.
33. Rawadi G, Vayssiere B, Dunn F, Baron R, Roman-Roman S. 2003. BMP-2 controls alkaline phosphatase expression and osteoblast mineralization by a Wnt autocrine loop. J Bone Miner Res 18:1842-1853.
34. Ross SE, Hemati N, Longo KA, Bennett CN, Lucas PC, Erickson RL, MacDougald OA. 2000. Inhibition of adipogenesis by Wnt signaling. Science 289:950-953.
35. Shea CM, Edgar CM, Einhorn TA, Gerstenfeld LC. 2003. BMP treatment of C3H10T1/2 mesenchymal stem cells induces both chondrogenesis and osteogenesis. J Cell Biochem 90:1112-1127.
36. Shin CS, Lecanda F, Sheikh S, Weitzmann L, Cheng SL, Civitelli R. 2000. Relative abundance of different cadherins defines differentiation of mesenchymal precursors into osteogenic, myogenic, or adipogenic pathways. J Cell Biochem 78:566-577.
37. Stains JP, Civitelli R. 2005. Gap junctions regulate extracellular signal-regulated kinase signaling to affect gene transcription. Mol Biol Cell 16:64-72.
38. Stains JP, Lecanda F, Screen J, Towler DA, Civitelli R. 2003. Gap junctional communication modulates gene transcription by altering the recruitment of Sp1 and Sp3 to connexin-response elements in osteoblast promoters. J Biol Chem 278:24377-24387.
39. van Es JH, Barker N, Clevers H. 2003. You Wnt some, you lose some: oncogenes in the Wnt signaling pathway. Curr Opin Genet Dev 13:28-33.
40. Wan M, Cao X. 2005. BMP signaling in skeletal development. Biochem Biophys Res Commun 328:651-657.
41. Winkler DG, Sutherland MS, Ojala E, Turcott E, Geoghegan JC, Shpektor D, Skonier JE, Yu C, Latham JA. 2005. Sclerostin inhibition of Wnt-3a-induced C3H10T1/2 cell differentiation is indirect and mediated by bone morphogenetic proteins. J Biol Chem 280:2498-2502.
42. Xu Q, Wang Y, Dabdoub A, Smallwood PM, Williams J, Woods C, Kelley MW, Jiang L, Tasman W, Zhang K, Nathans J. 2004. Vascular development in the retina and inner ear: control by Norrin and Frizzled-4, a high-affinity ligand-receptor pair. Cell 116:883-895.
43. Yang M, Zhong WW, Srivastava N, Slavin A, Yang J, Hoey T, An S. 2005. G protein-coupled lysophosphatidic acid receptors stimulate proliferation of colon cancer cells through the {beta}-catenin pathway. Proc Natl Acad Sci U S A 102:6027-6032.

44. Zhao M, Harris SE, Horn D, Geng Z, Nishimura R, Mundy GR, Chen D. 2002. Bone morphogenetic protein receptor signaling is necessary for normal murine postnatal bone formation. J Cell Biol 157:1049-1060.

2.8 FIGURE LEGENDS

Figure 2.1 Structure and expression of β-catenin mutants. (A) Three different β-catenin mutants (mutGSK, ΔN90 and ΔN151) are shown below the basic structure of the wild type protein. The 4 phosphorylation sites (mutated to alanine in mutGSK3) at the N-terminus are shown, as well as the Tcf/Lef-binding domain (shaded), the transactivation domain (TA, hatched), and the KT3 epitope (solid). (B) C3H10T1/2 cells were transduced with VSV-G retroviruses encoding EGFP only, or a bicistronic construct comprised of one β-catenin mutant and IRES-EGFP. Fluorescence microscopy shows G418-resistant cells expressing EGFP. (C) Western analysis detects expression of the β-catenin mutant proteins in similar abundance to endogenous β-catenin (red arrowhead).

Figure 2.2 Tcf/Lef-dependent transcriptional activity of β-catenin mutants and C3H10T1/2 differentiation. (A) After retroviral transduction, G418-resistant C3H10T1/2 cells were monitored for Tcf/Lef transcriptional activity in the absence or presence of 100 ng/ml BMP-2 for 24 hr after transfection with Tcf/Lef-luc. (B) Alkaline phosphatase (ALP) activity was quantified from cells grown in the absence or presence of 100 ng/ml BMP-2. (C) C3H10T1/2 cells transduced with EGFP or β-catenin mutants were grown in adipogenic medium for 10 d, and the number of adipocytes, defined by presence of Oil Red O positive lipid droplets, was determined in 6 random 40X microscopic fields per genotype; $p<0.05$ versus EGFP (*), versus ΔN151 (#), versus BMP-2

(‡), or versus ΔN151 plus BMP-2 (†), two-tailed Student's t-test.

Figure 2.3 The C-terminal transactivation domain of β-catenin is necessary for Tcf/Lef transcriptional activity and for suppression of adipogenesis, but is dispensable for osteogenic stimulation. (A) Schematic diagram of wild type and mutant (mutGSK, or mutGSKΔC) β-catenin constructs, with their functional domains illustrated as in Fig 1A. (B) C3H10T1/2 cells were transduced with either EGFP or mutant β-catenin (mutGSK, or mutGSKΔC) VSV-G retroviruses. Whole cell lysates were immunoblotted using either an anti-β-catenin or anti-KT3 antibody, as indicated. (C) Cells transduced with the different mutants were

monitored for Tcf/Lef transcriptional activity in the absence or presence of 80 mM LiCl after transfection with Tcf/Lef-luc; $p<0.05$ versus EGFP (*) or versus EGFP plus LiCl (#), two-tailed Student t-test. (D) Adipogenic differentiation was determined in transduced C3H10T1/2 cells by Oil Red O staining after 10 d incubation in adipogenic medium. (E) Alkaline phosphatase (ALP) activity was quantified in cell lysates in the absence or presence of 100 ng/ml BMP-2 after 7 d; $p<0.05$ versus EGFP (*) or versus EGFP plus BMP-2 (#), two-tailed Student t-test. Results are representative of 3 separate experiments. Bar, 100 μm.

Figure 2.4 A Tcf/Lef-defective β-catenin mutant stimulates both osteoblasts and adipocytes under osteogenic conditions and enhances BMP-2 effects. C3H10T1/2 cells transduced with either EGFP or mutant β-catenin (mutGSK, or mutGSKΔC) VSV-G retroviruses and selected with G418 were cultured in osteogenic medium for 10 d, stained with Oil Red O and subsequently counterstained for ALP activity (A-F'). Stained monolayers were microphotographed at 10X or 40X magnification. Adipocytes contain red-colored lipid droplets and osteoblasts are stained purple.

Figure 2.5 C3H10T1/2 cells express endogenous BMP-4 which accounts for most of the "intrinsic" pro-osteogenic β-catenin activity. (A) Expression of Bmp-2 and Bmp-4 mRNA by RT-PCR in confluent and sub-confluent cultures of C3H10T1/2 cells grown in osteogenic medium. As a control for mRNA stability and abundance, Gapdh mRNA was determined. (B) C3H10T1/2 cells were transduced with either EGFP (circles) or mutGSK (triangles) and incubated in the presence (open) or in the absence (solid) of BMP-2 for up to 21 d. Total mRNA, extracted at indicated time points, was used for determination of Bmp-4 mRNA abundance by quantitative real time PCR, relative to Gapdh. (C) C3H10T1/2 cells were transiently transfected with a BMP-specific luciferase reporter containing 12 tandem Smad-binding elements (SBE-luc), and then treated with Noggin (1.5 μg/ml), a BMP-2/4 neutralizing antibody (20 μg/ml), or BMP-2 (200 ng/ml) for 24 h; $p<0.05$ versus untreated (*), two-tailed Student's t-test. (D) Alkaline phosphatase (ALP) activity was quantified in C3H10T1/2 cells transduced with mutGSK and treated with

Noggin; $p<0.05$ versus mutGSK (*) or versus mutGSK plus 0.5 μg/ml Noggin (#), two-tailed Student t-test. (E) C3H10T1/2 cells were grown in adipogenic medium containing either BMP-2 or Noggin for 10 d and the number of adipocytes, defined by presence of Oil Red O positive lipid droplets, was determined in 6 random 20X microscopic fields; $p<0.05$ versus vehicle (*), two-tailed Student's t-test.

2.9 FIGURES

Figure 2.1

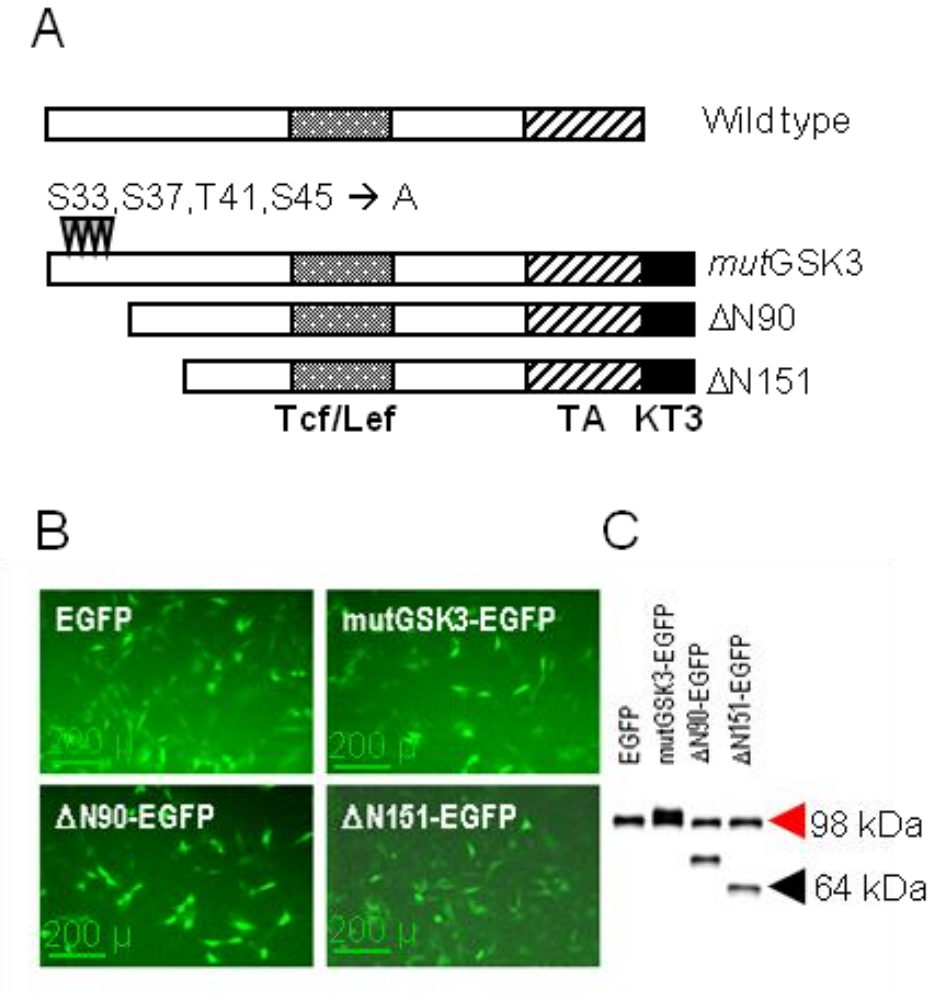

Figure 2.2

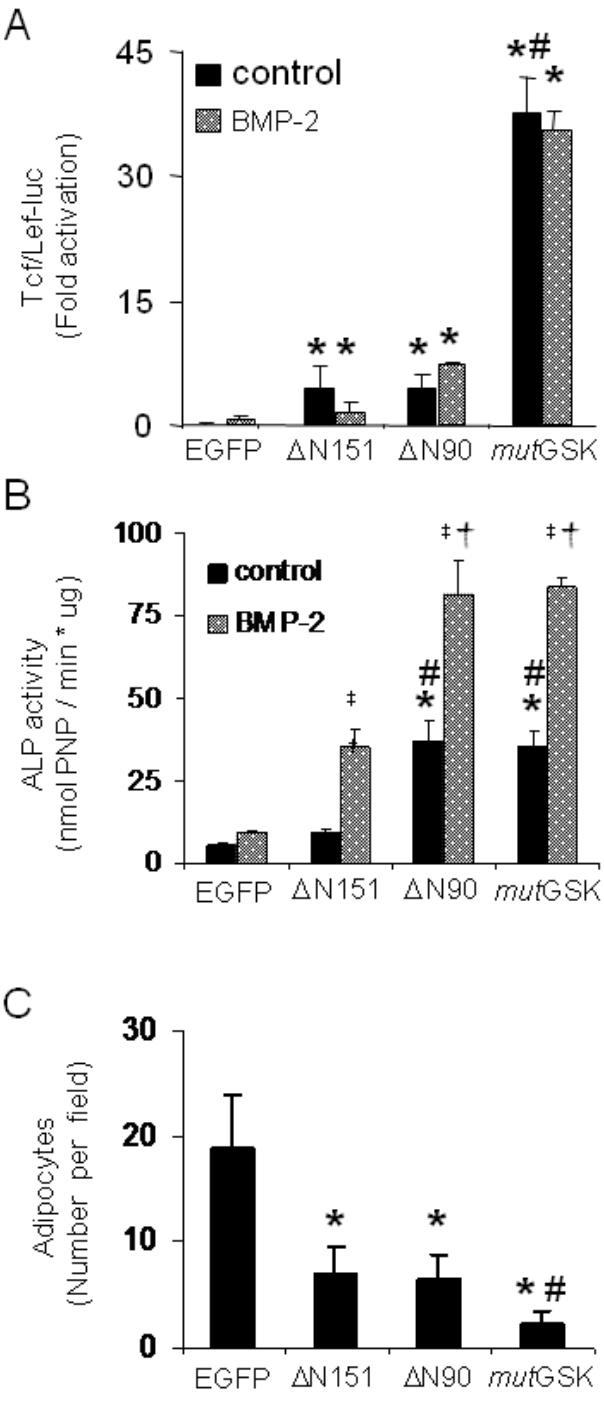
A
Tcf/Lef-luc
(Fold activation)
45
30
15
0
control
BMP-2
EGFP
ΔN151
ΔN90
mutGSK
B
ALP activity
(nmol PNP / min * ug)
100
75
50
25
0
control
BMP-2
EGFP
ΔN151
ΔN90
mutGSK
C
Adipocytes
(Number per field)
30
20
10
0
EGFP
ΔN151
ΔN90
mutGSK

Figure 2.3

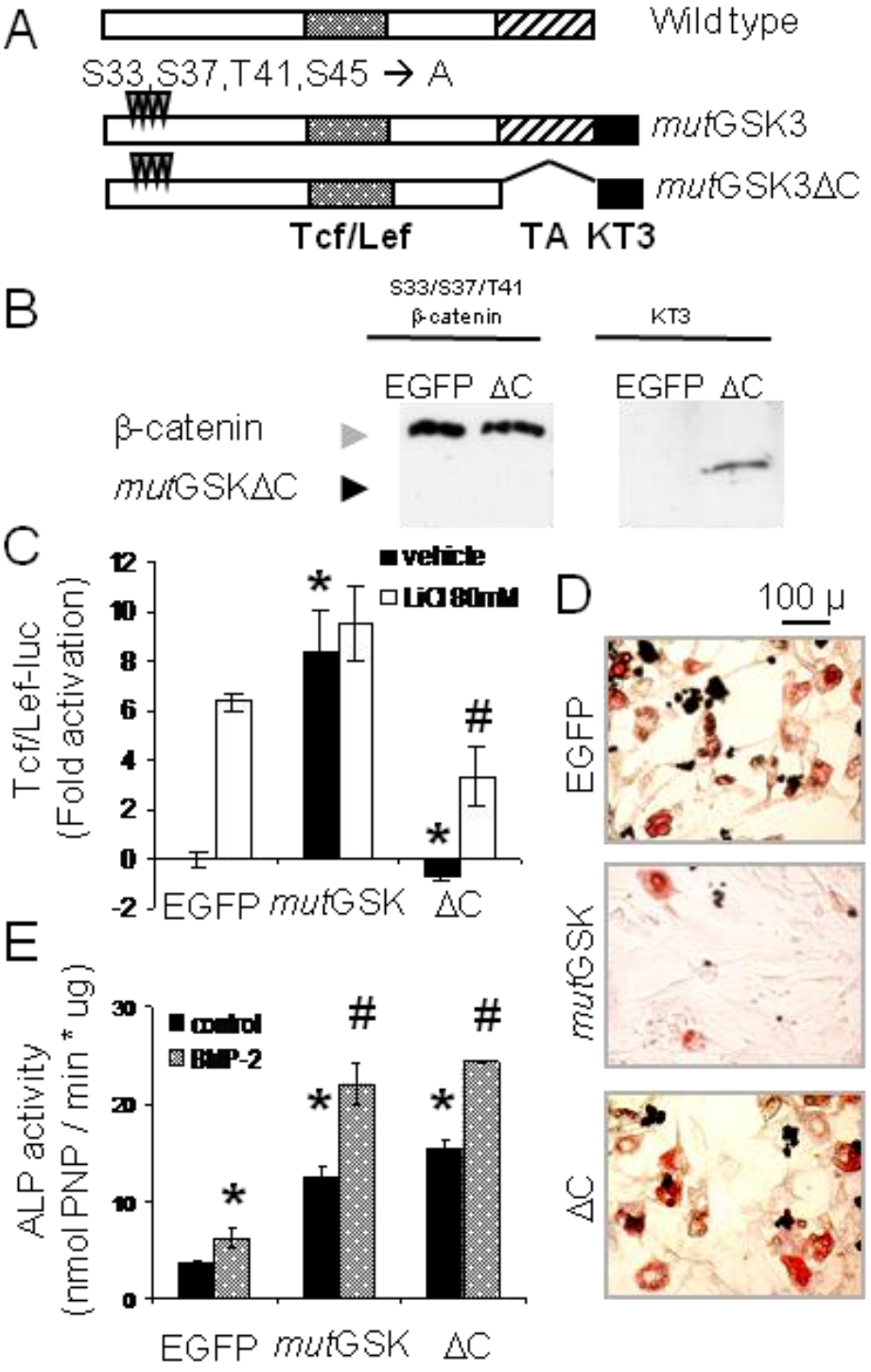
A
Wild type
S33,S37,T41,S45 → A
mutGSK3
mutGSK3ΔC
Tcf/Lef
TA
KT3
B
S33/S37/T41
β-catenin
KT3
EGFP
ΔC
EGFP
ΔC
β-catenin
mutGSKΔC
C
vehicle
LiCl 80mM
Tcf/Lef-luc
(Fold activation)
EGFP
mutGSK
ΔC
D
100 μ
EGFP
mutGSK
ΔC
E
control
BMP-2
ALP activity
(nmol PNP / min * ug)
EGFP
mutGSK
ΔC

Figure 2.4

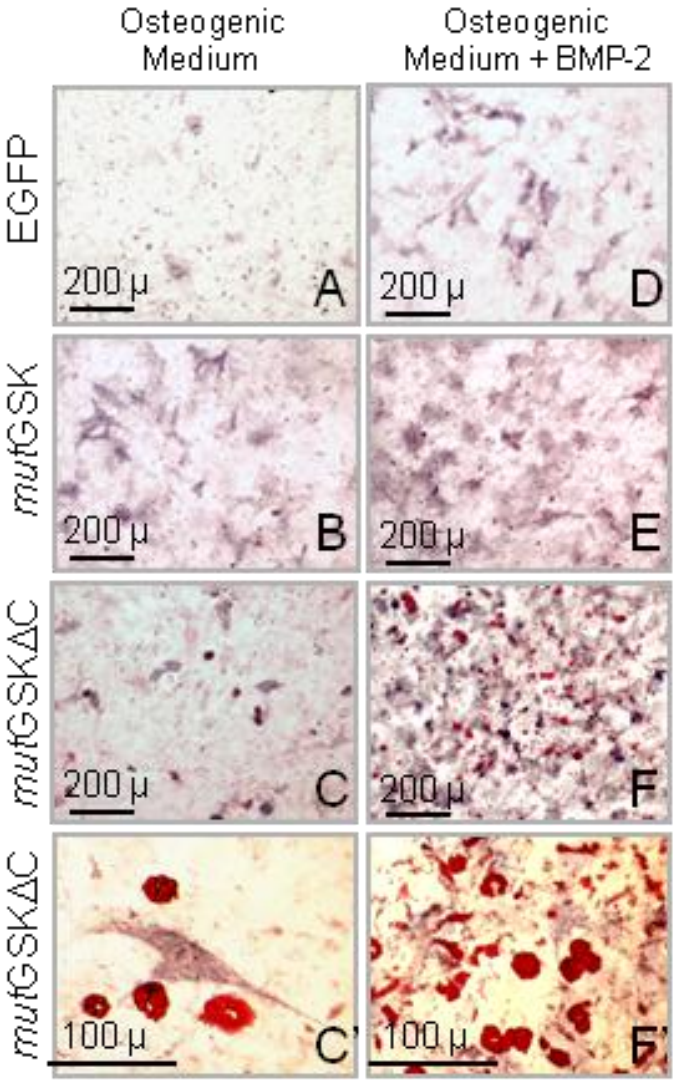
Osteogenic Medium
Osteogenic Medium + BMP-2
EGFP
mutGSK
mutGSKΔC
mutGSKΔC
200 µ
A
200 µ
D
200 µ
B
200 µ
E
200 µ
C
200 µ
F
100 µ
C'
100 µ
F'

Figure 2.5

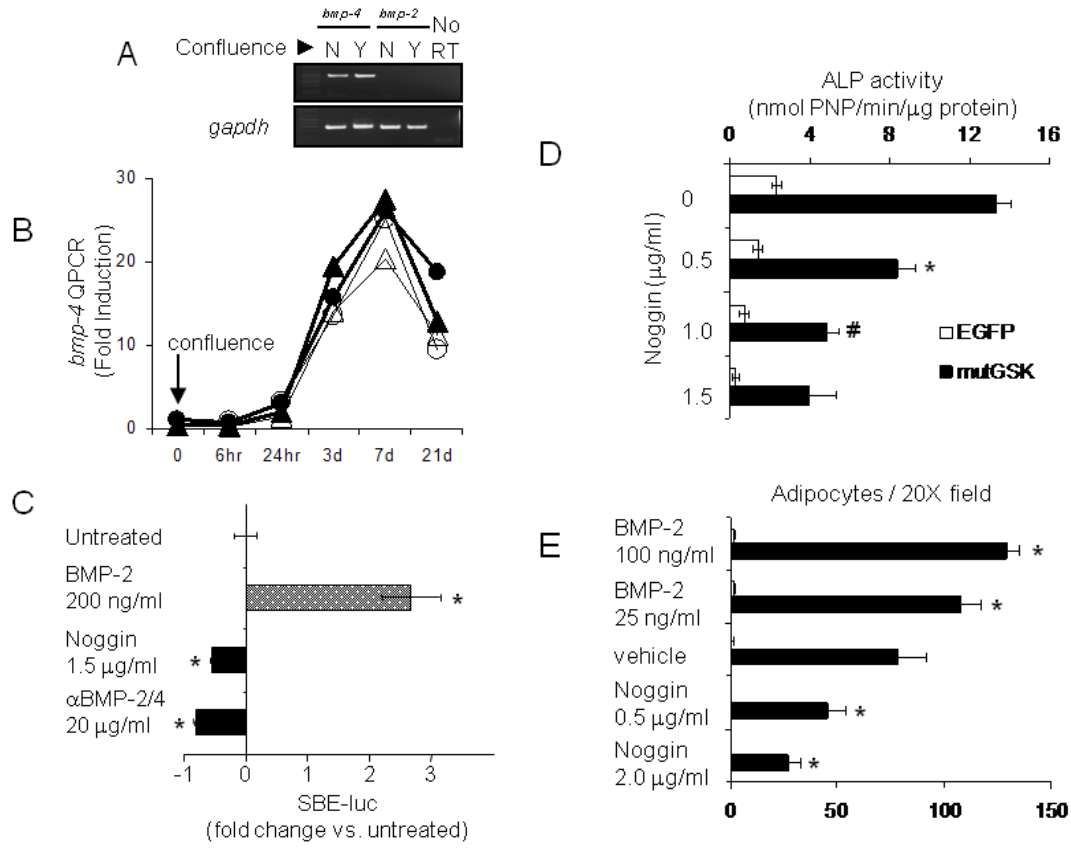
A
bmp-4
bmp-2
No RT
Confluence
N Y N Y
gapdh
B
bmp-4 QPCR (Fold Induction)
confluence
0 6hr 24hr 3d 7d 21d
C
Untreated
BMP-2 200 ng/ml
Noggin 1.5 µg/ml
αBMP-2/4 20 µg/ml
SBE-luc (fold change vs. untreated)
D
ALP activity (nmol PNP/min/µg protein)
Noggin (µg/ml)
EGFP
mutGSK
E
Adipocytes / 20X field
BMP-2 100 ng/ml
BMP-2 25 ng/ml
vehicle
Noggin 0.5 µg/ml
Noggin 2.0 µg/ml

CHAPTER 3

Smad4 Attenuates Proliferation and Canonical Wnt Signaling In the Osteogenic Lineage

3.1 ABSTRACT

Smad4, a transcription factor of the TGFβ/BMP pathway, interacts with components of the canonical Wnt pathway. In C3H10T1/2 cells, knockdown of Smad4 using siRNA stimulates Tcf/Lef-dependent transcription and enhances the ability of Wnt3a or β-catenin to stimulate CCND1 promoter activity and mitosis. In vivo, Tamoxifen-dependent gene ablation of Smad4 in Osterix^{+} cells greatly increases the number of BrdU-positive cells sitting directly on the bone surface. Using structure/function analysis, we find that the ability of Smad4 to attenuate CCND1 promoter activity is dependent on Smad4 DNA-binding activity, but independent of changes in Smad-dependent transcription. Expression of Smad4 mutants does not alter expression of or signaling through essential components of the canonical Wnt pathway in MC3T3 cells, eliminating the possibility of autocrine or paracrine mode of antagonism. Instead, we find that BMP2 rapidly induces Smad4 and β-catenin association. Consistent with a model where BMP2 signals can recruit β-catenin to an activated Smad4-based transcription complex, expression of activated or dominant-negative β-catenin mutants modulates luciferase activity driven by BMP-response elements. We provide evidence that Smad4 can physically interact with β-catenin in a manner that antagonizes canonical Wnt signaling and proliferation in the osteogenic lineage.

3.2 INTRODUCTION

Osteoblasts are dedicated bone-forming cells of the body and arise from multipotent stem cells residing in the bone marrow stroma. In the adult skeleton, these precursors provide a progenitor pool for adipocytes as well. Progression of precursors through early stages of osteoblastogenesis is demarcated by expression of Runx2, an essential pro-osteogenic transcription factor [1]. At this stage, Runx2+ precursors continue to proliferate and expand the osteogenic progenitor pool. Expression of Osterix, another essential osteogenic transcription factor, is believed to delineate the boundary between proliferative and post-mitotic osteoblasts [2,3] and indicates that osteoprogenitors have begun to acquire functional characteristics of the matrix-producing osteoblast. At the end of their life cycle, mature osteoblasts either undergo apoptosis (the majority) or become entrapped in their own extracellular matrix where they serve a post-mitotic role as a mechano-sensing osteocyte [4]. While much is known about the genetic ontogeny of the osteogenic lineage, much remains to be described about molecular mechanisms governing the transition from proliferative to post-mitotic phases in the osteoblast lifecycle.

Bone morphogenetic proteins 2, 4, and 7 (BMP2, 4, and 7) are critical regulators of osteoblast differentiation and bone homeostasis [5,6,7,8,9,10,11,12]. BMP family ligands signal through Type I and Type II heteromeric BMP receptor complexes to activate a variety of intracellular kinase cascades as well as Smads, which bind DNA-binding transcription factors[13] In addition to “canonical” activity, Smads also cooperate with lineage-specific transcription factors to drive cell-type specific gene expression programs. In this manner, a Smad-dependent transcriptional response to TGFβ or BMP signaling is refined by interaction with transcription factors expressed in a particular tissue. In bone for example, a physical interaction and cooperative transcriptional activity between BMP-specific R-Smads and Runx2 is necessary for BMP2 to stimulate osteoblast differentiation [14]. In the gastric mucosa, by comparison, an interaction between TGFβ-specific R-Smads with Runx3, a gastric tumor suppressor, induces mitotic-arrest of stomach epithelia cells and is required for prevention of gastric hyperplasia [15]. In fact, loss of Smad4 or the BMP receptor IA lead to increased cell proliferation or even

pathologic hyperplasia in a myriad of progenitor niches [16,17]. The molecular mechanism by which BMP-dependent Smad signaling attenuates proliferation remains to be fully elucidated. Experiments in Drosophila melanogaster provide intriguing evidence that Smad4 function may affect the Wnt/β-catenin signaling system. Cell fate decisions normally associated with overexpression of Wingless (the fly ortholog of Wnt) or activated armadillo (the fly ortholog of β-catenin) can be phenocopied by overexpression of Smad4 mutants defective in DNA-binding [18]. β-catenin is an essential transcription co-factor of the canonical Wnt pathway. Wnt ligands signal through heteromeric receptor complexes comprised of Frizzled and Lrp5/6 proteins to block negative regulation of β-catenin protein stability by GSK3β. Canonical Wnt signaling causes accumulation of β-catenin in the nucleus where it can bind to proteins of the Tcf/Lef family to activate gene expression. β-catenin acts in a variety of developmental and post-natal tissues to stimulate cell cycle via Tcf/Lef-dependent expression of Cyclin-D1[19] or impact cell fate. In bone, β-catenin can drive an osteoblast cell fate decision at the expense of progenitor allocation to the chondrocyte [20,21] or adipocyte [22] lineages. Curiously, while β-catenin is required for progression of an Osterix+ cell to a mature osteoblast, Cre-mediated activation of β-catenin in the same Osterix+ population reactivates proliferation of differentiating osteoblasts which should be exiting cell cycle [2]. This apparent paradox suggests that a specific molecular mechanism acts at the Runx2/Osterix transition to dampen the pro-mitotic and instead promote pro-differentiation cues provided by β-catenin.

We considered the possibility that such a molecular mechanism could explain why loss of BMP/Smad signaling can mimic the proliferative effect of Wnt/β-catenin activation. Many Smads interact with β-catenin and Tcf/Lef family members to activate gene promoters containing both Smad- and Tcf/Lef-binding elements. In the intestine, Smads interact with β-catenin/Tcf4 on the gastrin [23] and c-myc [24] promoters. In the Spemann organizer of the frog, Smads cooperate with β-catenin/Lef1 on the Xtwn promoter [25]. And in osteoblastic cells, conserved regulatory motifs for both Wnt and BMP response elements have been identified in the Dlx5, Msx2, and Runx2 promoters [26]. Outside of the nucleus, Smads can physically interact with regulatory

components of the canonical Wnt pathway such as GSKβ [27] and Dishevelled [28]. Thus, Smads have access to canonical Tcf/Lef transcriptional machinery by proximity to canonical Wnt signaling scaffolds in the cytoplasm and the ability to physically interact with β-catenin on natural promoter landscapes in the nucleus.

Here, we test the hypothesis that the molecular mechanism by which Smad4 can integrate with β-catenin and Tcf/Lef might also serve to decrease β-catenin occupancy at canonical Tcf/Lef target genes, and thereby negatively impact proliferation. Biochemical studies in the osteogenic lineage reveal that BMP2 signals quickly regulate cellular distribution of endogenous β-catenin and lead to formation of transcriptionally active Smad4/β-catenin complexes. Accordingly, the ability of Wnt3a or β-catenin to drive Tcf/Lef-dependent transcription of Cyclin-D1 is suppressed by increased levels of Smad4 and synergistically enhanced by loss of Smad4. This mechanism is at least partially dependent on the DNA-binding function of Smad4 but does not require Smad-dependent transcription or autocrine regulation of the Wnt pathway. In vivo and in vitro models indicate that loss of Smad4 is potent mitotic stimulus of osteoblast proliferation, rivaling or exceeding the mitotic effects of canonical Wnt signals. In summary, we demonstrate that Smad4 operates at the Osterix+ stage of lineage commitment to promote exit from cell cycle during osteoblast differentiation. Our study provides evidence that this is accomplished in large part via a BMP2-dependent Smad4/β-catenin interaction that antagonizes canonical Wnt signaling and Tcf/Lef-dependent transcription.

3.3 METHODS

Genetic Mouse Models For conditional Smad4 ablation, a mouse strain harboring a "floxed" Smad4 allele (Smad4^{flox}) [50] was crossed to mice expressing a Cre::ERalpha fusion protein under control of the Osterix promoter (Osx-CreERT2) [51]. Cre-mediated excision of the 8th exon of Smad4 is dependent on administration of Tamoxifen, an estrogen analog. Rosa26R $^{flox(LacZ)/+}$ mice [52] were also mated with Osx-CreERT2 mice to optimize a Tamoxifen regimen sufficient to activate Osx-driven Cre recombination in bones of adult mice and to examine the lineage specificity and efficiency of recombination. Both alleles were generous gift of Dr. Henry Kronenberg, Harvard University). All the mouse lines used in this project were developed in a mixed C57BL/BalbC background and littermates were used as controls. Mice were fed regular chow ad libitum and housed in a room maintained at constant temperature (25°C) on a 12 hours of light and 12 hours of dark schedule. All procedures were approved by the Animal Studies Committee of Washington University in St Louis. Genotyping was performed by PCR on genomic DNA extracted from mouse tails using the HotSHOT method [53]. The following primers were used for genotyping: Smad4: Forward 5'-TTCAGTGGCTATTGATTTGGGCAGCGTAGC-3', Reverse 5'-AAAGACCGCGTGGTCACTAAGGCACCTGAC-3', ROSA26: R1295, 5′-GCGAAGAGTTTGTCCTCAACC-3′, R26F2, 5′-AAAGTCGCTCTGAGTTGTTAT-3′, R523, 5′-GGAGCGGGAGAAATGGATATG-3′ [54]. The Osx-CreERT2 allele was detected using a pair of primers specific for both Cre and the ERalpha coding regions: Forward 5'-GAAGCAACTCATCGATTG-3', and Osx-CreERT2 R 5'-TGGTCAGTAAGCCCATC-3'.

In Vivo Analysis of Rosa26 $^{flox(LacZ)}$ Recombination Intact bones were fixed in 10% neutral buffered formalin for 1 hr, decalcified in 14% EDTA and stained for LacZ overnight at 30°C with the addition of 100mM galactose to the staining solution to quench non-specific staining. Stained bones were post-fixed overnight at 4°C and embedded paraffin for histology. Sections were counterstained with Eosin or Safranin O.

Dkk1 Neutralizing Antibody Rat monoclonal anti-mouse Dkk1 (clone 11H10, Lot 14073109) was a kind gift of W Richards (Amgen; Thousand Oaks, CA), was prepared in sterile saline and given to 8 week old mice (20 mg/kg/day, i.p.) for 5 consecutive days and on day 7.

In Vivo Analysis of Proliferation Bromodeoxyuridine was administered to mice 2 hr prior to sacrifice. Bones were fixed in 10% neutral buffered formalin, decalcified in 14% EDTA, and embedded paraffin for histological sectioning. BrdU+ cells were detected in deparaffanized and rehydrated slides using the BrdU Staining Kit (Invitrogen; Carlsbad, CA). Fluorescein-conjugated strepavidin (#RPN 1232 Amersham, Buckinghamshire, England) was substituted for the DAB secondary detection reagents provided in the kit. Sections were counterstained with DAPI and mounted with coverslips in Vectashield. Ablation of Smad4 in Osterix+ cells caused widespread proliferation throughout the bone marrow compartment. Thus, to facilitate visualization of BrdU incorporation in bone-adherent cells, the images in Fig. 2D were captured in the trochanter, which displayed very high efficiency of recombination as well as a replacement of marrow cells with fat.

In Vitro Proliferation Bone Marrow Stromal Cells: The entire marrow cavity of the shafts (femora and tibiae) of 2 month old mice was flushed by removing one of the epiphyses and centrifuging the bone at 9,000 rpm for 10 sec. After hemolysis in a red blood cells lysis buffer, the material was resuspended in αMEM (Mediatech Inc., Herndon, VA), filtered through a 70 μm cell strainer, and pelleted by centrifugation. Cells were resuspended in αMEM containing 20% fetal calf serum (FCS) and antibiotics plus osteogenic cocktail of 10mM b-glycerophosphate and 50 mg/ml ascorbic acid and seeded in black-sided 96-well tissue culture plates at 30,000 cells per well. After 4 days of differentiation, cells were treated with 10uM tamoxifen (Sigma; St. Louis, MO). Twenty four hours later, BMSC were labeled with BrdU and incorporation was quantified using a chemiluminescent Cell Proliferation ELISA kit as per manufactures instructions (Roche, Mannheim, Germany). C3H10T1/2 cells: Cells were transfected with indicated combinations of siRNA and expression plasmids. After 48 hours, they were deprived of serum overnight. Media with serum was added back along with labeling solution and proliferation was assessed as above.

Materials Purified recombinant human BMP-2 (R&D Systems, Minneapolis, MN). Tcf/Lef-luc is pTopFlash (Promega, Madison, WI) and consists of the luciferase open reading frame preceded by 6 tandemly-arranged Tcf/Lef binding elements. p12X-SBE-Luc (SBE-luc) was a kind gift from Dr. Di Chen (University of Texas Health Science Center) and consists of luciferase ORF preceded by an osteocalcin minimal promoter and 12 tandem Smad binding elements. CCND1-luciferase [19] was a kind gift from Dr. Fanxin Long (Washington University in St. Louis). β-catenin cDNAs were previously described [22,29,30,31] . Wild type murine Smad4 with an N-terminal HA-tag was a kind gift from V. Rosen (Harvard School of Dental Medicine). We used a previously described method [55] to generate in-frame deletion mutants and one point mutant. Primers—Sigma-Aldrich (St. Louis, MO). Smad4 and control siRNA—Ambion (Austin, TX). Unless otherwise indicated, all other chemicals and reagents were purchased from Sigma.

Cell Culture C3H10T1/2 murine embryonic fibroblast cells (ATCC, Manassas, VA) were maintained in basal medium of Eagle (BME; Gibco; Carlsbad, CA) containing 10% fetal bovine serum (Atlas Biologicals; Fort Collins, CO), 40mM L-glutamine, 100U/ml penicillin-G, and 100mg/ml streptomycin, and incubated at 37°C in a humidified atmosphere with 5% CO_2. MC3T3 immortalized mouse calvaria cells were maintained in ascorbic acid free αMEM (Invitrogen; Carlsbad, CA) containing 10% fetal bovine serum (Atlas Biologicals; Fort Collins, CO), 40mM L-glutamine, 100U/ml penicillin-G, and 100mg/ml streptomycin, and incubated at 37°C in a humidified atmosphere with 5% CO_2.

Luciferase Activity Cells ($4x10^4$ cells per well of a 24-well plate) were transfected with plasmids and/or siRNAs using Lipofectamine2000 (Invitrogen; Carlsbad, CA) per manufacturer's instructions. Each well was transfected with indicated combinations of luciferase reporter (0.4ug/well), expression plasmid (0.4, 0.2, or 0.1 μg/well), or siRNAs (75, 50, or 25 nM). Transfection media was replaced the following day with complete media plus additional treatments as indicated. Luciferase activity was quantified 72hr after transfection using Bright-Glo luciferase substrate according to manufacturer instructions (Promega). Since we have found that Renilla reporters, commonly used for normalization of transfection efficiency, were

significantly modulated by some treatments used in this study, Firefly activity is expressed as fold change relative to the control group. Assays were repeated at least 3 times.

Immunofluorescence Cell layers grown on chamber slides were rinsed with once with PBS and fixed in freshly prepared 4% paraformaldehyde for 15 min at room temperature, permeabilized and blocked in PBS + 0.25% Triton-X-100 and 5% normal goat serum for 30 min at room temperature. Primary antibody (#9581, Cell Signaling; Danvers, MA) was prepared in PBS + 0.25% Triton-X-100 and incubated for 1 hr at 37°C in a humidified chamber. Goat anti-Rabbit AlexaFluor 488 and DAPI were used for visualization of β-catenin and nuclei.

Immunoprecipitation and Immunoblotting Whole cell protein extracts were collected in RIPA lysis buffer containing 150nm NaCl, 10mM Tris at pH 7.2, 0.1% SDS, 1.0% Triton X-100, 1% Deoxycholate, and 5 mM EDTA. Subcellular protein fractions were prepared as previously described [48]. Protein from primary marrow-free bone tissue was prepared as previously described [56]. Proteins were separated by SDS-PAGE, and transferred to PDVF membranes (Millipore; Billerica, MA). Membranes were blocked in TBS containing 0.05% Tween-20 and 5% non-fat dry milk, and then probed overnight at 4°C with primary antibody in buffers recommended by the manufacturers. Antigen-antibody complexes were visualized by horseradish peroxidase-conjugated secondary antibody and HRP-detection reagent (Millipore; Billerica, MA). Non-denatured proteins for co-immunoprecipitation were collected in NP-40 buffer containing 150 nM NaCl, 20 mM Tris at pH 7.5, 1% NP40, and 5 mM EDTA. Lysates were incubated with primary antibody overnight, under agitation, at 4°C. Immune complexes were precipated using isotype-matched Dynabeads (Invitrogen; Carlsbad, CA). Extraction buffers were supplemented with Halt protease inhibitor cocktail kit (Pierce; Rockford, IL), 2 mM sodium vanadate, 10 mM sodium fluoride, and PMSF. Protein concentrations were determined by BCA kit (Pierce; Rockford, IL). Antibodies are as follows: β-catenin (#610154, BD Transduction Laboratories); HA-tag (#11867423001, Roche; Indianapolis, IN); Smad4 (#7966, #7154, Santa Cruz; Santa Cruz, CA); TCF4 (#05-512, Millipore; Billerica, MA); β-actin (#A5316, Sigma; St. Louis, MO); phosphorylated Lrp5/6 (#2568S, Cell Signaling; Danvers, MA); total GSK3β (#05-412, Millipore; Billerica, MA);

phosphorylated GSK3β (#9336, Cell Signaling; Danvers, MA); and HA-tag (#11-867-423-001, Roche; Indianapolis, IN).

Oligo Pulldowns Single stranded oligos encoding complementary Smad4 binding elements (SBEs) and a 5'-biotin modification were resuspended in water and mixed in equal molar ratios. SBE forward 5'-AGTATGTCTAGACTGA-3'. SBE antisense 5' TCAGTCTAGACATACT-3'. Single stranded oligos were annealed into double stranded DNA in SCC buffer by heating to 95°C and then cooling down slowly to 25°C. Biotinylated oligos were bound to Streptavidin-coated magnetic beads (Pierce; Rockford, IL) and blocked with BSA and poly dIdC. Blocked beads were incubated with 10ug of nuclear extracts for 45 mins at 4°C under agitation. Nucleoprotein complexes were pulled down on a magnetic rack (Dynal, Carlsbad, CA) and washed extensively prior to eluting precipitates in 1X Laemli loading buffer.

RNA Isolation and RT-PCR Total RNA from cells was isolated using RNeasy kit (Qiagen; Valencia, CA) per manufacturer's instructions. MessagerRNA was prepared from marrow free bone tissue or duodenum was prepared as previously described (Watkins 2011). One µg RNA was reverse transcribed using Superscript II reverse transcriptase and oligo(dT)15 primers. Taqman® Gene expression assays (Applied Biosystems, Foster City, CA) were used per manufacturer's instructions to measure Ccnd1, Dkk1 and Gapdh. The same primers sequences were used for RT-PCR.

Statistics analysis All data are expressed as the mean ± standard deviation. Group means were compared by two-tailed student's t-test; n=3.

3.4 RESULTS

3.4.1 BMP2 Stimulates the Formation of a Smad4/β-catenin Transcription Complex In the first set of experiments, we determined whether BMP-2 can alter β-catenin cellular distribution and transcriptional activity and. First, an EGFP::β-catenin fusion protein was transfected in C3H10T1/2. Transfected, serum-starved cells were treated with Lithium Chloride (LiCl, a GSK3β inhibitor and known activator of β-catenin nuclear translocation), BMP2, or both. Fluorescent

microscopy on live cells showed EGFP::β-catenin diffusely distributed throughout the cytoplasm in serum-starved cells, with little if any fluorescence at the cell membrane, possibly because cells were subconfluent (Fig. 1A, left). Addition of 40 mM LiCl (a GSK3 inhibitor and activator of β-catenin nuclear translocation) triggered nuclear accumulation of EGFP::β-catenin, with distinct punctuate condensations (Fig. 1A, center). BMP2 also caused EGFP::β-catenin nuclear accumulation, although some diffuse cytoplasmic signal remained (Fig. 1A, right). To corroborate these findings, we also monitored cellular distribution of endogenous β-catenin in MC3T3 cells. In subconfluent cells in serum-free conditions, most β-catenin specific signal was found at cell boundaries, presumably at adhesion complexes (Fig. 1B, left). Exposure to 50 ng/mL of Wnt3a for 90 minutes resulted in increased β-catenin accumulation in the nucleus and a decrease in proximity of the cell membrane (Fig. 1B, center). BMP2 treatment (200 ng/mL) also induced β-catenin nuclear accumulation, but there was also a detectable diffuse cytoplasmic staining, and a large amount of specific staining remained at the cell membrane (Fig. 1B, right). To determine whether β-catenin nuclear translocation was associated with increased transcriptional activity, C3H10T1/2 cells were transfected with a Tcf/Lef reporter construct (TopFlash). Exposure to BMP-2 did not activate Tcf/Lef promoter activity, and in fact it inhibited LiCl activation of Tcf/Lef transcriptional activity (Fig. 1C), suggesting that BMP-2 recruits β-catenin away from the canonical Tcf/Lef transcriptional machinery. Next, we used two approaches to test whether Smad4 and β-catenin physically interact. First, Smad4 was immunoprecipitated from non-denaturing cell lysates from serum starved C3H10T1/2 cells treated with BMP-2 for 10 minutes. Immunoblot analysis confirmed that the amount of Smad4 recovered from each treatment group was similar. β-catenin was also detected by immunoblot in the Smad4 pellets, and the intensity of this band was greatly enhanced after BMP2 treatment (Fig. 1D). Second, we used short biotinylated DNA oligos comprised of tandem Smad-binding elements (SBE) to pull down nuclear Smad-based protein complexes and determine if β-catenin was associated. Cytosolic and nuclear extracts were separated from confluent MC3T3 cells treated with BMP2 (200ng/ml, 40 min) and analyzed by immunoblot prior to oligo pull-down. Nuclear extracts were deficient of Gapdh, as expected, and enriched for TCF3, TCF4, and Smad4. In contrast to subconfluent

cells, β-catenin was present in both cytosolic and nuclear fractions, even in the absence of exogenous BMP2. However, assessement of phosphorylated R-Smads 1/5/8 indicate that confluent cells had active BMP signaling occurring even prior to addition of exogenous BMP2, which was not surprising given that we previously demonstrated that pre-osteoblasts begin to express endogenous BMP4 upon confluence [22]. When mixed with nuclear extracts, SBE oligos pulled down a protein complex containing Smad4, β-catenin, and TCF4. Treatment with BMP2 enhanced the abundance of the complex and further recruited phosphorylated (activated) Smad1/5/8 (all Fig. 1E). Thus, BMP2 stimulates physical interaction of β-catenin with Smad4 and recruitment of β-catenin to DNA binding, nuclear complexes that also contain TCF4. To test whether β-catenin can modulate Smad-dependent transcription activity, as results from the pull down assay suggest, we monitored Smad-dependent luciferase activity (SBE-luc) in C3H10T1/2 cells co-transfected with either EGFP, dominant-negative β-catenin (mutGSKΔC) [22,29,30], or constitutively active β-catenin (mutGSK) [22,31]. Loss-of-function and gain-of-function mutations to β-catenin reciprocally regulated the Smad-dependent luciferase reporter in the absence and presence of exogenous BMP2 (Fig. 1F). Importantly, loss-of-function mutation to β-catenin was not sufficient to abrogate a BMP2 transcriptional response, indicating β-catenin activity is sufficient to modulate, but not necessary for Smad-dependent transcription.

3.4.2 Smad4 Expression Inversely Correlates with Tcf/Lef-dependent Transcription and Proliferation

In support of our initial hypothesis, the evidence provided in Fig. 1 demonstrates that BMP2 treatment stimulates recruitment of β–catenin and TCF4 to DNA sequences encoding Smad-binding elements. Thus, a series of experiments were conducted to evaluate whether this recruitment of β–catenin and TCF4 correlated with a decrease in Tcf/Lef dependent transcriptional activity. We manipulated expression levels of Smad4 in C3H10T1/2 cells, mouse embryonic fibroblasts capable of producing osteoblasts, by transient transfection of either small-interfering RNAs (siRNAs) targeted to murine Smad4 or an expression plasmid encoding HA-tagged wild type murine Smad4. Confirming efficiency and specificity of Smad4

knockdown, RT-PCR analysis revealed dose-dependent (0-75nM) decreased expression of endogenous Smad4 mRNA, while levels of Gapdh and the closely related transcript of Smad5 remained unchanged (Fig. 2A). By contrast, transfection of Smad4-encoding plasmid resulted in dose-dependent increases abundance of HA-Smad4 protein, relative to stable levels of α-tubulin (Fig. 2B). To measure the effects of Smad4 silencing or over-expression on transcription, C3H10T1/2 cells were co-transfected with either the SBE-luc or the Tcf/Lef-luc constructs and either siRNAs or the HA-Smad4 expression construct. As expected, HA-Smad4 enhanced SBE-luc activity by >200% and silencing of endogenous Smad4 with siRNAs diminished SBE-luc activity by over 90% (Fig. 2C). By contrast, Smad4 over expression reduced TopFlash activity by >80%, while Smad4 silencing enhanced TopFlash activity almost 100% (Fig. 2D). Thus, Smad4 abundance directly and positively regulates Smad-dependent transcription but inversely correlates with Tcf/Lef-dependent transcription. To test this finding on a natural promoter, we transfected C3H10T1/2 cells with a luciferase reporter driven by the human CYCLIN-D1 promoter (CCND1-luc). The CCND1 promoter contains Tcf/Lef binding elements and is a known β-catenin target [19]. Consistent with increased Tcf/Lef activity on an empirical promoter, co-transfection with Smad4 siRNA increased CCND1-luc activity 14.9-fold, thus, to a significantly larger extent than up-regulation by expression of a constitutively active β-catenin (mutGSK3) or Wnt3a (4.1- and 7.5-fold, respectively). Importantly, expression of active β-catenin or Wnt3a in Smad4 depleted cells synergistically activated transcription on the human CCND1 promoter, producing 43.9- and 55-fold higher luciferase activity than in cells expressing EGFP and control non-coding siRNAs (Fig. 2E). Corroborating these findings, real-time PCR analysis for Ccnd1 mRNA showed that compared to cells expressing EGFP alone, expression of active β-catenin or Smad4 silencing produced similar increases in abundance of Ccnd1 mRNA (1.3- and 1.4-fold) and expression of active β-catenin in a Smad4-depleted background had an additive effect on Ccnd1 mRNA abundance, which was approximately double of that in control EGFP-expressing cells (Fig. 2F). Consistent with these changes in Ccdn1 expression, BrdU incorporation was approximately

doubled by expression of Wnt3a, tripled by depletion of Smad4, and quadrupled by concomitant expression of Wnt3a and Smad4 silencing, relative to cells expressing EGFP alone (Fig. 2G).

3.4.3 Smad4 Antagonizes Transcriptional Activity on the Human CCND1 Promoter via DNA-binding Activity but not Smad-Dependent Transcription

To generate mechanistic information concerning how Smad4 antagonizes CCND1 promoter activity in osteoblasts, we conducted a structure/function analysis of murine Smad4 in MC3T3 cells, which are immortalized mouse calvaria cells. A library of Smad4 mutants were cloned based on the wild type HA-Smad4 parental vector. Five protein domains were individually targeted for deletion (Fig. 3A). Loss of the DNA-binding (DBD) or the MH1 domain disrupts DNA-binding activity and thus transcriptional activity of Smad4. We specifically designed the MH1 mutant to spare the integrity of a nuclear export signal (NES), which begins within the 3' region of the MH1 domain. The NES was targeted separately. A central linker region of Smad4 contains a variety of amino residues targeted for post-translational modifications [32]. The MH2 domain contains specific amino acids shown to be involved in direct protein-protein interactions with other Smads. Finally, we generated a sixth Smad4 mutant, also shown in Fig. 3A, bearing an R100T point mutation. Smad4-R100T is an allele discovered in human colorectal tumors [33]. The R100T point mutation in the N-terminal MH1 domain lies outside of the proper DNA binding motif but causes conformational changes rendering the protein defective in DNA-binding activity [34].

We first assessed the ability to over express each Smad4 construct. MC3T3 cells were transiently transfected with equal amounts plasmid encoding each Smad4 mutant. Protein lysates were collected 48 hours after transient transfection and analyzed by immunoblot for the N-terminal HA-tag of each Smad4 construct. As expected, deletion constructs generated proteins that migrated appropriately faster during electrophoresis than wild type and R100T Smad4, which encode full-length proteins. Deletion of the MH1 domain generates a protein that appeared to be more stable than other Smad4 variants. By contrast, deletion of the MH2 domain appeared to cause instability of either Smad4 mRNA or protein--despite screening three unique and fully-

sequenced ΔMH2 clones by anti-HA immunoblot, we were unable to detect expression of an intact ΔMH2 Smad4 protein (Fig. 3B). Thus, structure/function analysis was conducted on wtSmad4, one point mutant (R100T), and 4 deletion mutants (ΔDBD, ΔNES, ΔMH1, and ΔLinker). MC3T3 cells in which no ectopic Smad4 protein was expressed (ΔMH2) provided an internal negative control for further analysis by western blot. We examined the possibility that Smad4 regulates or Tcf/Lef-dependent transcription by altering the activation or integrity of the canonical Wnt pathway. To determine if such a mechanism was at play, we examined abundance and/or phosphorylation of critical Wnt signaling molecules in protein lysates from MC3T3 cells over expressing Smad4. Fig. 3C illustrates that no appreciable differences in the abundance of Tcf4, β-catenin, or GSK3β were detected in response to increased expression of either wild type or mutant Smad4. Phosphorylation of Lrp5, Lrp6, and GSK3β were also normal. These data suggest Smad4 does not alter expression of or signaling through essential components of the canonical Wnt pathway in MC3T3, eliminating the possibility of an autocrine or paracrine mode of antagonism.

In C3H10T1/2 cells, decreased Smad4 expression significantly upregulates promoter activity on TopFlash and CCND1-luciferase reporters (Figs. 1D-E), while elevated Smad4 expression has the opposite effect and attenuates Tcf/Lef- and CCND-luciferase activity. To determine if this mechanism is operative in additional cell types, MC3T3 cells were co-transfected with CCND1-luciferase and wild type Smad4. Wild type Smad4 diminished CCND1-luciferase activity in MC3T3 cells by approximately 70% compared to control cells receiving an empty expression plasmid (Fig. 3D). This suppressive effect was not dependent on the nuclear export signal or the linker domain of Smad4, as ΔNES and ΔLinker Smad4 mutants reduced CCND1-luciferase by a magnitude comparable to the effect of wild type Smad4. Compared to the 66% reduction of CCND1-luciferase activity induced by wildtype Smad4, ΔMH1, ΔDBD, and R100T reduced this activity by approximately 27%, 41%, and 33%. The ability of Smad4 to suppress CCND1-promoter activity at least partially depends on a function of the DNA-binding motif.

Since DNA-binding activity is required for Smad4 to operate as a transcription factor, we next determined whether Smad-dependent transcription was necessary for Smad4 to suppress CCND1. MC3T3 calvaria cells were co-transfected with SBE-luc and wild type or mutant Smad4. There was a fair amount of basal SBE-luc activity in cells transfected with an empty expression plasmid, corroborating the presence of phosphorylated Smads1/5/8 in untreated cell lysates (Fig. 1E). However, we have previously demonstrated this basal activity is dependent on endogenous production of BMP2/4 production [22] as well as expression of endogenous Smad4 (Fig. 3E). Basal SBE-luc activity was increased to about 200% in BMP2 treated cells, 500% in cells over expressing wild type Smad4, and 800% in BMP2 treated cells over expressing wildtype Smad4. ΔNES is as transcriptionally active as wildtype Smad4, but is insensitive to BMP2. This is expected since BMP signals enhance Smad signaling via kinase reactions in the cytoplasmic compartment and loss of the nuclear export signal should maintain ΔNES in the nucleus [35]. Deletion of the MH1, DBD, Linker domains all resulted in loss of canonical Smad4 function as none of these mutants increased SBE-luciferase activity above baseline. In fact, ΔMH1 and ΔDBD were slighty inhibitory on basal SBE-luc activity, indicating these mutants may be dominant-negative as well as loss-of-function. Additionally, ΔMH1, ΔDBD, and ΔLinker were all rendered insensitive to BMP2 stimulation in MC3T3 cells. An R100T point mutation similarly resulted in loss of function which was insensitive to BMP2. Since loss of the Linker domain renders Smad4 transcriptionally dead and insensitive to BMP2 stimulation but maintains its ability to suppress CCND1 promoter activity, these results suggest that Smad4-dependent transcription is not required for the ability of Smad4 to antagonize canonical Wnt signaling.

3.4.4 Acute Postnatal Ablation of Smad4 in Osterix+ Cells Enhances Proliferation in Bone

β-catenin acts through Tcf/Lef proteins to stimulate proliferation in many cell types of the body. In keeping with this model, conditional activation of β-catenin in Osterix+ cells using Osx1-GFP::Cre stimulates proliferation of osteogenic cells in bone [2]. Based on our preliminary data, we hypothesized that loss of Smad4 in Osterix+ cells should also stimulate proliferation of

osteogenic cells in bone. The Osx1-GFP::Cre allele used by Rodda and MacMahon to activate β-catenin is first expressed at stage E14.5 during development. Since osteoblasts can survive very long periods of time as osteocytes (decades in humans [36]), we considered whether the Osx1-GFP::Cre model was appropriate to test our hypothesis. An abundance of in vitro and genetic studies indicate a paramount role for the BMP and greater TGFβ signaling pathway in osteoblast biology. Since Smad4 is a canonical mediator of BMP/TGFβ signaling, long term deficiency of Smad4 might result in an accumulation of Tcf/Lef-independent signaling defects that could negatively impact the competency of an osteogenic cell in an adult mouse to respond to a pro-mitotic stimulus. Thus, to study the effect of Smad4 ablation on proliferation in bone, we induced acute ablation of floxed Smad4 alleles [37] in otherwise normal, healthy osteoblasts of adult mice using the Tamoxifen-dependent Osterix-CreERT2 allele [38].

To optimize a Tamoxifen treatment regimen sufficient to activate CreERT2-dependent gene recombination, and to evaluate the lineage specificity of Osterix-CreERT2 in adult bone, we first generated ROSA26$^{fl(LacZ)/+}$; Osterix-CreET2 mice. In this model, Tamoxifen-dependent and Cre-mediated recombination activates expression of a β-galactosidase reporter gene which is preceded by a floxed stop codon. Thus, LacZ expression should be activated only in Tamoxifen-exposed cells expressing the osteogenic transcription factor, Osterix. Whole tissue analysis of LacZ activity in bones from these mice indicates that five consecutive doses of Tamoxifen (100mg/kg/day, Fig. 4A) are sufficient to induce substantial Cre-mediated recombination in the femurs (Fig. 4B-D) and tibia (Fig. 4E-F). Histological examination of these bones revealed strong β-galactosidase activity in a high percentage of cells lining the cortical and trabecular bone surfaces. Rarely, LacZ expression was present in clonal populations of chondrocytes (data not shown). We did not find evidence that any cells in the bone marrow space had been recombined (Fig. 4C). The Osterix-CreERT2 allele represents an effective genetic model to achieve post-natal gene recombination in bone with high specificity for the osteoblast lineage.

We administered the optimized Tamoxifen treatment regimen to Smad4$^{flox/flox}$; Osx-CreERT2 mice (Fig 4A). Since Tamoxifen is an analog of estrogen, the study was restricted to 6

week old male mice. Tamoxifen can exert anti-proliferative activity on some cells. However, this agent has a short half-life in mice. Thus, to circumvent any potential anti-proliferative effects of Tamoxifen treatment, mice were allowed metabolize any residual Tamoxifen for 3 days after the last dose. Following this recovery period, actively dividing cells were labeled in vivo by giving mice a single injection of BrdU 2 hours prior to sacrifice (Fig. 4A). To visualize changes in proliferation in bone following conditional ablation of Smad4 in osteoblasts, we performed anti-BrdU immunofluoresence on paraffin-embedded sections of the femur and counterstained each section with DAPI. Examination of stained sections by fluorescence microscopy revealed that the abundance of BrdU+ cells in Tamoxifen treated Smad4$^{flox/flox}$; Osx-CreER^{T2} mice (Fig. 4G, right) was vastly increased in comparison to Tamoxifen-treated Smad4$^{flox/flox}$ mice (Fig. 4G, left). Importantly, the abundance of BrdU+ cells in femurs from Tamoxifen-treated Smad4$^{flox/+}$; Osx-CreER^{T2} mice (Fig. 4G, center) was less than in cKOs but still greater than in cWTs. Changes in osteoblast proliferation following ablation of Smad4 in Osterix+ cells, depicted in Fig. 4G, are representative of reproducible results from 5 independent experiments. The pro-mitotic effect of Smad4 ablation was particulary evident in cells sitting directly on the trabecular bone surfaces of the primary and secondary spongiosa. These data directly support our hypothesis that Smad4 antagonizes proliferation in the osteogenic lineage. Moreover, the anti-proliferative effect of Smad4 is sensitive to loss of a single allele, indicating that the concentration-dependent effect of Smad4 siRNAs in cell culture translates into a gene-dosage dependent effect in vivo.

3.4.5 Postnatal Ablation of Smad4 in Osterix+ cells Enhances Osteoblast Proliferation more than Inhibition of Dkk1

Our in vitro studies provide evidence that loss of Smad4 is equally, if not more potent, than Wnt3a/β-catenin signals in stimulating proliferation of osteoprogenitors. We used the Smad4$^{flox/flox}$; Osx-CreER^{T2} mouse model to compare the pro-mitotic effect of Smad4 ablation versus canonical Wnt/β-catenin signaling. To activate canonical Wnt signaling in vivo, we used an antibody to neutralize the Wnt receptor antagonist, Dkk1 [39]. The secreted Wnt antagonist, Dkk1, is highly expressed in bone and attenuates endogenous Wnt

signaling by forming a heteromeric complex with Kremen proteins and the canonical Wnt receptors, Lrp5 and 6 [40]. This complex undergoes clathrin-mediated endocytosis, thereby downregulating the abundance of cell surface Lrp5/6 receptors available for activation by Wnt ligands [41]. Lrp5 activity can affect bone indirectly through the enterochromaffin cells in the duodenum [42] or directly through osteoblasts in bone. However, RT-PCR (Fig. 5A) and qPCR on primary tissues from Smad4$^{flox/flox}$ mice (Fig. 5B) indicate that expression of the pharmacologic target of anti-Dkk1 is high in bone and below detection in the duodenum. Thus, contribution by endocrine signaling from the GI to bone is probably minimal in this model. Since anti-Dkk1 antibody is administered systemically, we performed basic molecular pharmacology to determine if it can drive activation of β-catenin locally in bone. Immunoblot on marrow-free femoral bone tissue demonstrates that a single dose of anti-Dkk1 dramatically upregulates Lrp5 and β-catenin protein levels in bone, an effect seen within 15 and 30 minutes of a single injection. Administration of anti-Dkk1 is associated with the appearance of high molecular weight species of β-catenin not usually seen in cell cultures with the same antibody, suggesting extensive and rapid post-translational modifications in primary bone tissue (Fig. 5C-D). To examine the mitotic effect of Wnt pathway activation on osteoblasts in vivo, Smad4$^{flox/flox}$ and Smad4$^{flox/flox}$; Osx-CreER^{T2} mice were given 5 consecutive daily doses of Tamoxifen, either alone or in combination with Dkk1 neutralizing antibody (Figure 5F). Three days after the last dose of Tamoxifen, mitotic cells were labeled with a single dose of BrdU 2 hours prior to sacrifice. Immunofluorescence was used to detect mitotic BrdU+ cells in histologic sections of the tibia. Osteoblast proliferation was analyzed in the primary spongiosa based on the substantial amount of ROSA26$^{fl(LacZ)/+}$; Osterix-CreET2 recombination below the growth plate where osteoblasts are easily distinguished from growth plate chondrocytes and other constituent cells of the bone marrow (Figs. 4E-F). Antibody-mediated inhibition of Dkk1 produced a 55% increase in osteoblast proliferation compared to controls (Fig. 4G). By contrast, ablation of Smad4 increased proliferating cells by 213%, an effect more than 4-fold higher than that of anti-Dkk1. Treatment of Smad4-ablated mice with anti-Dkk1 did not have an additional effect on proliferation, (Fig. 4G, 193% vs. Tam-treated controls). We

also monitored proliferation of primary bone marrow stromal cells (BMSC), a source of osteoblast progenitors, following Tamoxifen-induced ablation of Smad4 and treatment with Wnt3a. Confluent BMSC were differentiated in ascorbic acid for 3 days, treated overnight with Tamoxifen (10uM in media), and labeled with BrdU to measure proliferation by luminescence. Proliferation of BMSC was enhanced 68% by Wnt3a, 55% by treatment with Tamoxifen, and 205% by combined treatment. These results demonstrate that loss of Smad4 is a mitotic stimulus to primary osteoblasts, providing equal or stronger proliferative cues that canonical Wnt signaling.

3.5 DISCUSSION

Our studies illuminate a novel role for Smad4, a transcription factor of the greater TGFβ superfamily, in modulating pro-mitotic canonical Wnt signals and proliferation in the osteogenic lineage. A post-natal analysis of proliferation in bone demonstrates that Osterix+ cells residing on the endocortical bone surface are generally not mitotic, but retain a proliferative capacity that can be reactivated by acute genetic ablation of Smad4. Mechanistic in vitro studies reveal that Smad4 attenuates expression of the pro-mitotic gene, Cyclin-D1, by antagonizing canonical Wnt/β-catenin signaling at the level of Tcf/Lef-dependent transcription. Antagonism of CCCN-D1 promoter activity by Smad4 requires a function of the Smad4 DNA-binding motif, but not Smad-dependent transcription. We propose that β-catenin and Smad4 play opposing roles to control proliferation of osteoprogenitors.

A fundamental objective of our work is to examine how the BMP and canonical Wnt/β-catenin pathways interact on a genetic and molecular level to regulate the formation and function of osteoblasts. Importantly, machinery for canonical Wnt and BMP signaling is expressed at many, if not all, stages of the osteoblast lifecycle including cell fate specification, progenitor proliferation, exit from cell-cycle, acquisition of mineralizing function, and programmed cell death. It is only reasonable to expect that the mechanism of interaction between these two pillar pathways must be multi-faceted in order to provide stage-specific information. For example, we previously demonstrated that during cell fate specification, β–catenin operates downstream of BMP signals to promote osteoblast and suppress adipocyte cell fate. While, the C-terminal

transactivation domain of β-catenin was required to inhibit adipogenesis, it was dispensible for stimulating osteoblastogenesis [22]. Here, we have utilized genetic and molecular methods to manipulate Smad4 expression in cells of the osteogenic lineage to characterize how BMP and canonical Wnt/β-catenin signals interact to define the boundary between proliferative and post-mitotic phases of osteoblast formation.

Tcf/Lef-dependent transcription and expression of Cyclin-D1 inversely correlate with Smad4 levels We demonstrate using two independent cell lines that ectopic expression of wildtype Smad4 diminishes transcriptional activity on empirical and natural promoters containing Tcf/Lef-binding elements. The opposite result was obtained by reducing endogenous Smad4 levels, which was sufficient to stimulate Tcf/Lef-dependent transcriptional activity and synergistically enhanced the response to ectopically expressed Wnt3a or constitutively activated β-catenin. We conducted studies to understand the mechanism of action for antagonism of Wnt signaling by Smad4. Results show that essential Wnt signaling components are expressed normally, and the abundance of β-catenin, phosphorylated Lrp5/6 and phosphorylated GSK3β remain unchanged 48 hours after introduction of Smad4. Thus, antagonism of Tcf/Lef activity by Smad4 does not likely involve changes in the abundance of a secreted molecule which can negatively regulate the canonical Wnt pathway via action at the plasma membrane. These data instead suggested an intracellular mechanism of action. Thus, we performed a structure /function analysis on Smad4. We were not able to evaluate the contribution of the MH2 domain to suppressive activity of Smad4 due to inability to achieve expression of this mutant in our cell model. However, these experiments did reveal that while the nuclear export signal and linker domains are dispensible, the MH1 and DNA-binding motif are necessary for full suppressive effect. An R100T point mutation that disrupts the tertiary protein structure of Smad4 necessary for DNA-binding activity also disrupted Smad4 suppressive effect. Since DNA-binding activity is necessary for Smad4-dependent transcription, we considered the possibility that Smad4 induced expression of an intracellular Wnt antagonist. However, loss of the Smad4 linker region and the R100T mutation were both sufficient to abrogate canonical Smad4 transcriptional activity and yet

each mutant was still able to antagonize CCND1 promoter activity. Thus, the role for Smad4-dependent expression any kind of Wnt regulatory molecule is unlikely. Nevertheless, the finding that expression of $Smad4^{R100T}$ on a wild type Smad4 background was sufficient to block BMP transcriptional response and also reduce the ability of Smad4 to downregulate CCND1 means its' biological activity is dominant over wildtype protein. Smad4 is a tumor suppressor, although it is still not clear exactly how this function is fulfilled. The presence of a single copy of $Smad4^{R100T}$ can cause tissue hyperplasia, particularly in the digestive tract where loss or mutation to Smad4 causes Juvenile Polyposis Syndrome (JPS). JPS is a rare, hereditary autosomal dominant condition characterized by pathobiologic growth of polyps and an elevated risk of gastrointestinal adenocarninomas. It is intriguing to consider that one manner Smad4 may function as a tumor suppressor could in fact be related to how β-catenin functions as a proto-oncogene—loss of BMP/Smad4 signaling and activation of Wnt/β-catenin pathway can both upregulate Tcf/Lef transcriptional activity. Therefore, our finding that Smad4 antagonizes proliferation and pro-mitotic Wnt/β-catenin signaling in osteoblasts may have broader implications if the same mechanism is operative in other tissues where BMP and Wnt pathways interact to control proliferation and differentiation.

Post-natal Ablation of Smad4 Reactivates Proliferation in Differentiating Osteoblasts Because in vitro loss of Smad4 altered expression of the Tcf/Lef target gene Cyclin-D1, a fundamental gene involved in coordination of cell cycle, we conducted an in vivo analysis to examine the role of Smad4 in controlling proliferation in osteoblasts. Genetic activation of β-catenin stimulates proliferation of differentiating and mostly non-mitotic Osterix+ cells in bones of growing mice [2]. Therefore, though mostly non-mitotic, Osterix+ cells in bone retain the machinery required to re-enter cell cycle and provide an ideal model to evaluate the role of Smad4 in osteoblast proliferation. Using the Osx-$CreER^{T2}$ mouse model [38], we demonstrate that acute loss of a single allele of Smad4 in Osterix+ cells activates proliferation of cells sitting directly on the endocortical bone surface, an effect which was enhanced by loss of both copies of

Smad4. Importantly, we demonstrate in C3H10T1/2 cells and in mice that loss of Smad4 provides an equal and often more powerful mitotic stimulus that activation of the Wnt pathway alone. Importantly, we further show that loss of Smad4 has a synergistic effect on Tcf/Lef-dependent transcription and can enhance Wnt-mediated proliferation. Given the abundance of data implicating Smad4 as a tumor suppressor and β-catenin a proto-oncogene, this interaction may be operative in other tissues and suggests that cell types under high levels of Wnt activity may be more susceptible to hyperplasia or oncogenic events following loss of Smad4.

The Osx-CreER^{T2} mouse model represents a relatively new method of conducting genetic studies in bone [38,43]. We show that administration of Tamoxifen activates substantial and acute post-natal gene recombination with a high degree of specificity for cells on the endocortical surfaces of the femur and tibia. Osterix expression persists in terminally differentiated osteocytes (Zhou 2010 PNAS). However, we detected very little evidence of LacZ expression in matrix-embedded cells. Since we do see recombination of the ROSA26$^{fl(LacZ)}$ allele in matrix-embedded osteocytes using a related CreLox model, Osx1-GFP::Cre, the lack recombination by Osx-CreER^{T2} in osteocytes might be due to low bioavailability of Tamoxifen in the bone matrix. Osterix is expressed at very low levels in mature chondrocytes, so recombination in clonal populations of chondrocytes was expected, but was minimal and did not affect the objectives of our study. LacZ analysis produced no evidence of recombination in the bone marrow. Accumulating evidence indicates that osteoblasts can exert non cell-autonomous control over other cells types in bone. Thus, it was quite intriguing to find that Tamoxifen-induced deletion of Smad4 in osteoblasts reproducibly triggered a massive burst of proliferation in the bone marrow compartment (data not shown). Our preliminary data suggest that expression of Smad4 specifically in Osterix+ cells controls the proliferative capacity of the bone marrow, although these studies were beyond the scope of this work.

A Competitive Recruitment Model Our data demonstrate that BMP2 stimulation causes a rapid increase in the abundance of nuclear β-catenin. Titrating the dose of BMP2 did not change the abundance of responding cells (Fig. 4E) but rather increased abundance of β-catenin

present throughout the cell, particularly at areas of dense cell-cell contact (data not shown). Importantly we and others have shown that even 48 hours of BMP2 stimulation does not increase Tcf/Lef-dependent luciferase activity. BMP2 treatment resulted in a cellular distribution pattern of endogenous β-catenin that was distinct from that found in either serum-deprived or Wnt3a-stimulated cells. This unique cellular distribution may be related to the ability of BMP2 to induce rapid physical interaction between β-catenin and Smad4. Since Smad4 is a DNA-binding protein, recruitment of β-catenin to Smad4-binding elements is expected to decrease the abundance of β-catenin available to bind to Tcf/Lefs. This model implies that Smad4 antagonizes Tcf/Lef-dependent transcription through its ability to interact with β-catenin and bind to DNA. Thus, we propose that increased expression of Smad4 reduces the abundance of β-catenin available to bind at Tcf/Lef gene targets. And conversely, loss of Smad4 or loss of Smad4 DNA-binding activity alleviates antagonism at Tcf/Lef-dependent promoters by liberating a pool of β-catenin found in DNA-associated Smad4 complexes. In this model, β-catenin becomes a rate-limited transcription factor. This model accommodates the ability of Smad4, β-catenin, and Tcf/Lefs to integrate and synergize on promoters containing both Smad and Tcf/Lef binding sites. Hence, in addition to the existence of gene targets which are synergistically regulated by Wnt and BMP, such c-Myc, there should also a category of competitive gene targets, such as CCND1.

Mitotic versus Osteoanabolic Canonical Wnt/β-catenin Signaling In this work we have focused on the pro-mitotic function of canonical Wnt signaling. However, it is essential to discuss two issues. First, expression of β-catenin is maintained through mitotic, bone-forming, and post-mitotic stages of the osteoblast lifecycle. Second, canonical Wnt/β-catenin signaling can be potently osteoanabolic [2]. In fact, knowledge of a biologic role for Wnts in bone arose from the discovery that loss- and gain-of-function mutations to the Wnt co-receptor, Lrp5, manifest clinically as low and high bone mass syndromes in humans [44,45,46]. And, antibody-mediated neutralization Wnt of antagonists, like Sclerostin and Dikkhopf-1, represents the currently emerging clinical therapies for treatment of osteoporosis [47]. So an intriguing question is how Wnt/β-catenin signals are refined into mitotic versus osteoanabolic cues. Given the

fundamental role for BMP signaling in osteoblasts, we hypothesize that BMP/Smad4 activity attenuates mitotic β-catenin cues to promote exit from cell cycle while enhancing anabolic β-catenin cues to facilitate maturation and function of osteoblasts. Indeed, we have previously shown that enhanced expression of β-catenin synergizes with BMP2 to promote osteoblastogenesis and new bone formation [22,48]. Our model implies that integrity of BMP/Smad4 transduction pathway signaling is necessary for canonical Wnt/β-catenin signaling to manifest an osteoanabolic response. This remains to be tested, and clearly further investigation is needed to define the genetic requirement for various components of the BMP signaling pathway in osteoblasts. Several studies using transgenic expression of BMP antagonists or mutant BMP receptors have provided some early information on the role of pathway in vivo [5,6,7,8,9,10,11,12]. However, phenotypic analysis using a systematic gene ablation approach remains to be assembled, much in the way multiple labs have collectively conducted genetic analysis of the Wnt pathway in bone. BMP signaling is complex, but a specific role for Smad4 in osteoblast function is emerging as deficiency of Smad4 in fully differentiated Osteocalcin+ osteoblasts significantly impedes post-natal growth, regulates bone resorption, and leads to generalized osteopenia in mice [49]. As was shown with genetic analysis of β-catenin in bone, timing of genetic ablation is critical for understanding the multifaceted role a single molecule at discrete stages of the osteoblast lifecycle. Thus, it will be interesting to see whether BMP/Smad4 signaling also exerts stage-specific effects on bone formation, post-natal skeletal homeostasis, and response to osteoanabolic Wnt signaling.

3.6 BIBLIOGRAPHY

1. Otto F, Thornell AP, Crompton T, Denzel A, Gilmour KC, et al. (1997) Cbfa1, a candidate gene for cleidocranial dysplasia syndrome, is essential for osteoblast differentiation and bone development [see comments]. Cell 89: 765-771.
2. Rodda SJ, McMahon AP (2006) Distinct roles for Hedgehog and canonical Wnt signaling in specification, differentiation and maintenance of osteoblast progenitors. Development 133: 3231-3244.
3. Aubin JE (2008) Principles of Bone Biology; Bilezikian JP, Raisz LG, Martin TJ, editors. San Diego, CA: Elsevier Inc. 954 p.
4. Tatsumi S, Ishii K, Amizuka N, Li M, Kobayashi T, et al. (2007) Targeted ablation of osteocytes induces osteoporosis with defective mechanotransduction. Cell Metab 5: 464-475.
5. Devlin RD, Du Z, Pereira RC, Kimble RB, Economides AN, et al. (2003) Skeletal overexpression of noggin results in osteopenia and reduced bone formation. Endocrinology 144: 1972-1978.
6. Bandyopadhyay A, Tsuji K, Cox K, Harfe BD, Rosen V, et al. (2006) Genetic analysis of the roles of BMP2, BMP4, and BMP7 in limb patterning and skeletogenesis. PLoS Genet 2: e216.
7. Gazzerro E, Pereira RC, Jorgetti V, Olson S, Economides AN, et al. (2005) Skeletal overexpression of gremlin impairs bone formation and causes osteopenia. Endocrinology 146: 655-665.
8. Wu XB, Li Y, Schneider A, Yu W, Rajendren G, et al. (2003) Impaired osteoblastic differentiation, reduced bone formation, and severe osteoporosis in noggin-overexpressing mice. Journal of Clinical Investigation 112: 924-934.
9. Mishina Y, Starbuck MW, Gentile MA, Fukuda T, Kasparcova V, et al. (2004) Bone morphogenetic protein type IA receptor signaling regulates postnatal osteoblast function and bone remodeling. Journal of Biological Chemistry 279: 27560-27566.
10. Zhao M, Harris SE, Horn D, Geng Z, Nishimura R, et al. (2002) Bone morphogenetic protein receptor signaling is necessary for normal murine postnatal bone formation. Journal of Cell Biology 157: 1049-1060.
11. Kamiya N, Ye L, Kobayashi T, Lucas DJ, Mochida Y, et al. (2008) Disruption of BMP signaling in osteoblasts through type IA receptor (BMPRIA) increases bone mass. J Bone Miner Res 23: 2007-2017.
12. Kamiya N, Ye L, Kobayashi T, Mochida Y, Yamauchi M, et al. (2008) BMP signaling negatively regulates bone mass through sclerostin by inhibiting the canonical Wnt pathway. Development 135: 3801-3811.
13. Shi Y, Massague J (2003) Mechanisms of TGF-beta signaling from cell membrane to the nucleus. Cell 113: 685-700.
14. Javed A, Afzal F, Bae JS, Gutierrez S, Zaidi K, et al. (2009) Specific residues of RUNX2 are obligatory for formation of BMP2-induced RUNX2-SMAD complex to promote osteoblast differentiation. Cells Tissues Organs 189: 133-137.
15. Chi XZ, Yang JO, Lee KY, Ito K, Sakakura C, et al. (2005) RUNX3 suppresses gastric epithelial cell growth by inducing p21(WAF1/Cip1) expression in cooperation with transforming growth factor {beta}-activated SMAD. Mol Cell Biol 25: 8097-8107.
16. Kobielak K, Pasolli HA, Alonso L, Polak L, Fuchs E (2003) Defining BMP functions in the hair follicle by conditional ablation of BMP receptor IA. J Cell Biol 163: 609-623.

17. Mira H, Andreu Z, Suh H, Lie DC, Jessberger S, et al. Signaling through BMPR-IA regulates quiescence and long-term activity of neural stem cells in the adult hippocampus. Cell Stem Cell 7: 78-89.
18. Takaesu NT, Herbig E, Zhitomersky D, O'Connor MB, Newfeld SJ (2005) DNA-binding domain mutations in SMAD genes yield dominant-negative proteins or a neomorphic protein that can activate WG target genes in Drosophila. Development 132: 4883-4894.
19. Tetsu O, McCormick F (1999) β-catenin regulates expression of cyclin D1 in colon carcinoma cells. Nature 398: 422-426.
20. Hill TP, Spater D, Taketo MM, Birchmeier W, Hartmann C (2005) Canonical Wnt/β-catenin signaling prevents osteoblasts from differentiating into chondrocytes. Developmental Cell 8: 727-738.
21. Day TF, Guo X, Garrett-Beal L, Yang Y (2005) Wnt/β-catenin signaling in mesenchymal progenitors controls osteoblast and chondrocyte differentiation during vertebrate skeletogenesis. Developmental Cell 8: 739-750.
22. Salazar VS, Mbalaviele G, Civitelli R (2008) The pro-osteogenic action of β-catenin requires interaction with BMP signaling, but not Tcf/Lef transcriptional activity. Journal of Cellular Biochemistry 104: 942-952.
23. Lei S, Dubeykovskiy A, Chakladar A, Wojtukiewicz L, Wang TC (2004) The murine gastrin promoter is synergistically activated by transforming growth factor-β/Smad and Wnt signaling pathways. Journal of Biological Chemistry 279: 42492-42502.
24. Hu MC, Rosenblum ND (2005) Smad1, β-catenin and Tcf4 associate in a molecular complex with the Myc promoter in dysplastic renal tissue and cooperate to control Myc transcription. Development 132: 215-225.
25. Nishita M, Hashimoto MK, Ogata S, Laurent MN, Ueno N, et al. (2000) Interaction between Wnt and TGF-beta signalling pathways during formation of Spemann's organizer. Nature 403: 781-785.
26. Hussein SM, Duff EK, Sirard C (2003) Smad4 and β-catenin coactivators functionally interact with LEF1 to regulate graded expression of Msx2. Journal of Biological Chemistry 278: 48805-48814.
27. Fuentealba LC, Eivers E, Ikeda A, Hurtado C, Kuroda H, et al. (2007) Integrating Patterning Signals: Wnt/GSK3 Regulates the Duration of the BMP/Smad1 Signal. Cell 131: 980-993.
28. Liu Z, Tang Y, Qiu T, Cao X, Clemens TL (2006) A dishevelled-1/Smad1 interaction couples WNT and bone morphogenetic protein signaling pathways in uncommitted bone marrow stromal cells. Journal of Biological Chemistry 281: 17156-17163.
29. Cong F, Schweizer L, Chamorro M, Varmus H (2003) Requirement for a nuclear function of beta-catenin in Wnt signaling. MolCell Biol 23: 8462-8470.
30. Barth AI, Pollack AL, Altschuler Y, Mostov KE, Nelson WJ (1997) NH2-terminal deletion of β-catenin results in stable colocalization of mutant β-catenin with adenomatous polyposis coli protein and altered MDCK cell adhesion Journal of Cell Biology 136: 693-706.
31. Barth AI, Stewart DB, Nelson WJ (1999) T cell factor-activated transcription is not sufficient to induce anchorage-independent growth of epithelial cells expressing mutant beta-catenin. Proc Natl Acad Sci U S A 96: 4947-4952.
32. Verheyen EM (2007) Opposing effects of Wnt and MAPK on BMP/Smad signal duration. Dev Cell 13: 755-756.
33. Schutte M, Hruban RH, Hedrick L, Cho KR, Nadasdy GM, et al. (1996) DPC4 gene in various tumor types. Cancer Res 56: 2527-2530.

34. Shi Y, Wang YF, Jayaraman L, Yang H, Massague J, et al. (1998) Crystal structure of a Smad MH1 domain bound to DNA: insights on DNA binding in TGF-beta signaling. Cell 94: 585-594.
35. Xiao Z, Watson N, Rodriguez C, Lodish HF (2001) Nucleocytoplasmic shuttling of Smad1 conferred by its nuclear localization and nuclear export signals. Journal of Biological Chemistry 276: 39404-39410.
36. Bonewald LF (2011) The amazing osteocyte. J Bone Miner Res 26: 229-238.
37. Yang X, Li C, Herrera PL, Deng CX (2002) Generation of Smad4/Dpc4 conditional knockout mice. Genesis 32: 80-81.
38. Maes C, Kobayashi T, Kronenberg HM (2007) A novel transgenic mouse model to study the osteoblast lineage in vivo. Ann N Y Acad Sci 1116: 149-164.
39. Diarra D, Stolina M, Polzer K, Zwerina J, Ominsky MS, et al. (2007) Dickkopf-1 is a master regulator of joint remodeling. Nature Medicine 13: 156-163.
40. Mao B, Wu W, Davidson G, Marhold J, Li M, et al. (2002) Kremen proteins are Dickkopf receptors that regulate Wnt/beta-catenin signalling. Nature 417: 664-667.
41. Yamamoto H, Sakane H, Michiue T, Kikuchi A (2008) Wnt3a and Dkk1 regulate distinct internalization pathways of LRP6 to tune the activation of beta-catenin signaling. Dev Cell 15: 37-48.
42. Yadav VK, Ryu JH, Suda N, Tanaka KF, Gingrich JA, et al. (2008) Lrp5 controls bone formation by inhibiting serotonin synthesis in the duodenum. Cell 135: 825-837.
43. Maes C, Kobayashi T, Paruch J, Kronenberg HM (2006) Characterization of the osteoblast lineage in vivo during early bone development. Journal of Bone and Mineral Research 21: S3.
44. Gong Y, Slee RB, Fukai N, Rawadi G, Roman-Roman S, et al. (2001) LDL receptor-related protein 5 (LRP5) affects bone accrual and eye development. Cell 107: 513-523.
45. Ellies DL, Viviano B, McCarthy J, Rey JP, Itasaki N, et al. (2006) Bone density ligand, Sclerostin, directly interacts with LRP5 but not LRP5G171V to modulate Wnt activity. Journal of Bone and Mineral Research 21: 1738-1749.
46. Brunkow ME, Gardner JC, Van Ness J, Paeper BW, Kovacevich BR, et al. (2001) Bone dysplasia sclerosteosis results from loss of the SOST gene product, a novel cystine knot-containing protein. American journal of human genetics 68: 577-589.
47. Rachner TD, Khosla S, Hofbauer LC Osteoporosis: now and the future. Lancet 377: 1276-1287.
48. Mbalaviele G, Sheikh S, Stains JP, Salazar VS, Cheng SL, et al. (2005) β-catenin and BMP-2 synergize to promote osteoblast differentiation and new bone formation. Journal of Cellular Biochemistry 94: 403-418.
49. Tan X, Weng T, Zhang J, Wang J, Li W, et al. (2007) Smad4 is required for maintaining normal murine postnatal bone homeostasis. Journal of Cell Science 120: 2162-2170.
50. Theis M, de Wit C, Schlaeger TM, Eckardt D, Kruger O, et al. (2001) Endothelium-specific replacement of the connexin43 coding region by a lacZ reporter gene. Genesis 29: 1-13.
51. Yu K, Xu J, Liu Z, Sosic D, Shao J, et al. (2003) Conditional inactivation of FGF receptor 2 reveals an essential role for FGF signaling in the regulation of osteoblast function and bone growth. Development 130: 3063-3074.
52. Soriano P (1999) Generalized lacZ expression with the ROSA26 Cre reporter strain. NatGenet 21: 70-71.

53. Truett GE, Heeger P, Mynatt RL, Truett AA, Walker JA, et al. (2000) Preparation of PCR-quality mouse genomic DNA with hot sodium hydroxide and tris (HotSHOT). Biotechniques 29: 52, 54.
54. Mao X, Fujiwara Y, Orkin SH (1999) Improved reporter strain for monitoring Cre recombinase-mediated DNA excisions in mice. Proc Natl Acad Sci U S A 96: 5037-5042.
55. Byrappa S, Gavin DK, Gupta KC (1995) A highly efficient procedure for site-specific mutagenesis of full-length plasmids using Vent DNA polymerase. Genome Res 5: 404-407.
56. Watkins M, Grimston SK, Norris JY, Guillotin B, Shaw A, et al. (2011) Osteoblast connexin43 modulates skeletal architecture by regulating both arms of bone remodeling. Mol Biol Cell 22: 1240-1251.

3.7 FIGURE LEGENDS

Figure 3.1 β-catenin translocates to the nucleus and physically associates with Smad4 to modulate the transcriptional response to BMP2. (A) Fluorescence microscopy monitoring subcellular distribution of a chimeric EGFP::β-catenin protein expressed in C3H10T1/2 cells by transient transfection. (B) Subconfluent MC3T3 cells were serum starved, treated 3h with Wnt3a or BMP2. Endogenous β-catenin was localized by immunofluoresence. (C) Tcf/Lef-dependent luciferase activity in C3H10T1/2 cells in response to lithium chloride, BMP2, or both. $p<0.05$ vs. (*) Control or (#) Lithium. (D) Smad4 was immunoprecipitated from non-denatured protein lysates of serum-starved or BMP2 treated C3H10T1/2 cells and immunoblotted for Smad4 or β-catenin. (E) Cytosolic and nuclear proteins from confluent MC3T3 cells were analyzed by immunoblot to characterize distribution and abundance of various Wnt and BMP transcription factors after 40 mins of BMP2 treatment. Biotinylated oligos encoding Smad-binding sequences were used to pull down DNA-binding protein complexes from nuclear extracts. (F) Smad-dependent luciferase was quantified after BMP2 treament in C3H10T1/2 cells expressing EGFP, constitutively active, or dominant-negative β–catenin. $p<0.05$ vs. (*) EGFP or (#) EGFP + BMP2.

Figure 3.2 Smad4 expression inversely correlates with Tcf/Lef-dependent transcription. (A) C3H10T1/2 cells were transfected with non-targeted control or Smad4-specific small interfering RNAs and assessed for specificity and efficiency of Smad4 knockdown by RT-PCR. (B) Alternatively, C3H10T1/2 cells were transfected with expression plasmids encoding wildtype HA-Smad4, then assessed by immublot for transgene expression. Cells expressing increasing amounts of HA-Smad4 (black solid lines) were transfected with luciferase reporters to assess Smad-dependent transcriptional activity (C) or Tcf/Lef-dependent transcriptional activity (D). Effects of empty pcDNA3 are expressed as black hatched lines. Cells with dose-dependent knockdown of Smad4 (grey solid lines) were tranfected with luciferase reporters to measure Smad-dependent (C) or Tcf/Lef-dependent (D) transcriptional activity. Effects of control siRNAs are expressed as grey hatched lines. $p<0.05$ vs. (*) Control siRNA or (#) pcDNA3. Luciferase

activity driven by the human CYCLIN-D1 promoter was monitored in C3H10T1/2 cells in response to expression of EGFP, constitutively activated β-catenin, or Wnt3a either in the presence (grey bars) or absence (black bars) of Smad4. $p<0.05$ vs. (*) Control or (#) Smad4 siRNA. (F) Real time PCR was used to measure expression of endogenous Cyclin-D1 mRNA in C3H10T1/2 in response to expression of EGFP or constitutively activated β-catenin in the presence (grey bars) or absence (black bars) of Smad4. $p<0.05$ vs. (*) Control or (#) Smad4 siRNA. (G) Proliferation of C3H10T1/2 cells, as a function of BrdU incorportation, was monitored in response to expression of EGFP (grey bars) or Wnt3a (black bars). $p<0.05$ vs. (*) EGFP + Control siRNA, Wnt3a + control siRNA, or ## EGFP + Smad4 siRNA.

Figure 3.3 Antagonism of CCND1 promoter activity is partially dependent on Smad4 DNA-binding activity, but independent of Smad transcriptional activity or autocrine regulation of canonical Lrp5/6 pathway. (A) Structure of wild type Smad4 and mutagenesis strategy targeting the MH1, linker, and MH2 domains, the nuclear export signal and motifs critical for DNA-binding activity. (B) Anti-HA immunoblot analysis for expression of HA-Smad4 mutants in MC3T3 cells following transient transfection of expression plasmids. (C) Immunoblot analysis on MC3T3 cells to examine the abundance and phospho-regulation of critical components of the canonical Lrp5/6 pathway. MC3T3 cells expressing the Smad4 mutants were transfected with a luciferase reporter to examine which domains of Smad4 are required to either (D) attenuate transcription on the human CCND1 promoter or (E) enhance BMP2 response on an empirical Smad-dependent promoter. (D) $p<0.05$ vs. (*) pcDNA3, or (#) wild type Smad4. (E) $p<0.05$ vs. (*) pcDNA3 + vehicle control or (#) pcDNA3 + BMP2.

Figure 3.4 Post-natal tamoxifen-dependent ablation of Smad4 in Osterix+ cells activates proliferation of osteoblasts. (A) Treatment Schema—Five consecutive daily injections of tamoxifen (100 mg/kg i.p). Mitotic cells were labeled with BrdU 2 hours prior to sacrifice on day 8. (B) After treatment with Tamoxifen or vehicle, intact femurs from $Rosa26^{flox(LacZ)/+}$; Osterix-CreERT2 mice were stained to detect recombination-dependent expression of β-galactosidase.

LacZ staining was further evaluated by histology to determine efficiency and specificity of tamoxifen-dependent recombination in osteoblasts. Eosin counterstain shows Osx-CreERT2 activates the LacZ reporter in endocortical osteoblasts of the diaphysis (C), trabecular osteoblasts in primary ossification centers (D-E), but not in the bone marrow compartment (C and D). Eosin (E) and Safranin O (F) counterstain of the proximal tibia demonstrates that OsxERT2- mediated recombination is efficiently restricted to osteoblasts in the primary spongiosa (PS) and generally excluded from chondrocytes in the growth plate (GP). Hatched black brackets demarcate the representative anatomical location used for analysis in Figure 5E-G. (G) $Smad4^{+/+}$, $Smad4^{flox/+}$; Osterix-CreERT2, and $Smad4^{flox/flox}$; Osterix-CreERT2 mice were treated with tamoxifen and BrdU as indicated in Fig4A. Mitotic cells in bone were visualized by BrdU immunofluorescence and DAPI. Fluourescence microscopy was used to capture images of BrdU+ cells in the proximal femur.

Figure 3.5 The mitotic response to ablation of Smad4 in Osterix+ cells is stronger than the response to inhibition of Dkk1 (A) Reverse-transcription PCR to examine Dkk1 expression in marrow-free bone or duodenum. (B) Quantitative PCR to compare Dkk1 levels in bone and duodenum. (C) Treatment schema to examine acute effects of anti-Dkk1 on bone-specific signaling. (D) Western blot analysis on marrow-free bone tissue from mice given a single injection of Dkk1 neutralizing antibody (20 mg/kg, i.p.). (C) Treatment Schema. Five consecutive daily injections of tamoxifen (100 mg/kg i.p) and 6 consective doses of Dkk1 neutralizing antibody (20 mg/kg i.p). (E) Mitotic cells in the trabecular compartment of the primary spongiosa were visualized by BrdU immunofluorescence. (F) Treatment schema to compare proliferative effects of anti-Dkk1 and Smad4 ablation. (G) BrdU+ cells in the trabecular compartment between the growth plate and the medullary cavity were counted. Acute post-natal loss of Smad4 provides a stronger mitotic stimulus than anti-Dkk1 treatment. (H) Adherent bone marrow stromal cells from $Smad4^{flox/flox}$; $Rosa26^{flox(LacZ)/+}$; Osterix-CreERT2 mice were seeded to confluence and allowed to differentiate for 3 days prior to treatment with Tamoxifen (10uM) and subsequently rWnt3a (5ng/ml). (I) Mitotic cells were labeled with BrdU to quantify proliferation by luminescence.

3.8 FIGURES

Figure 3.1

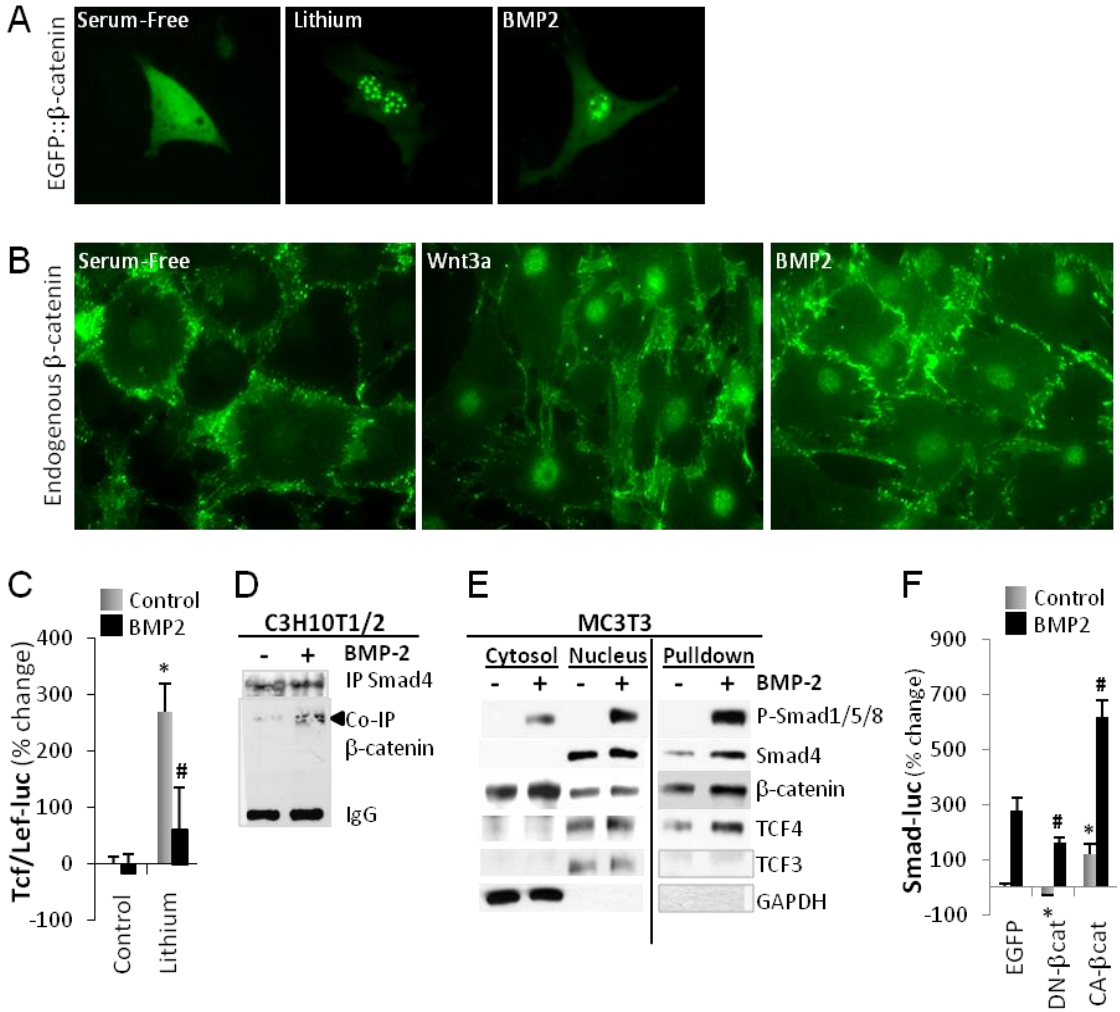

Figure 3.2

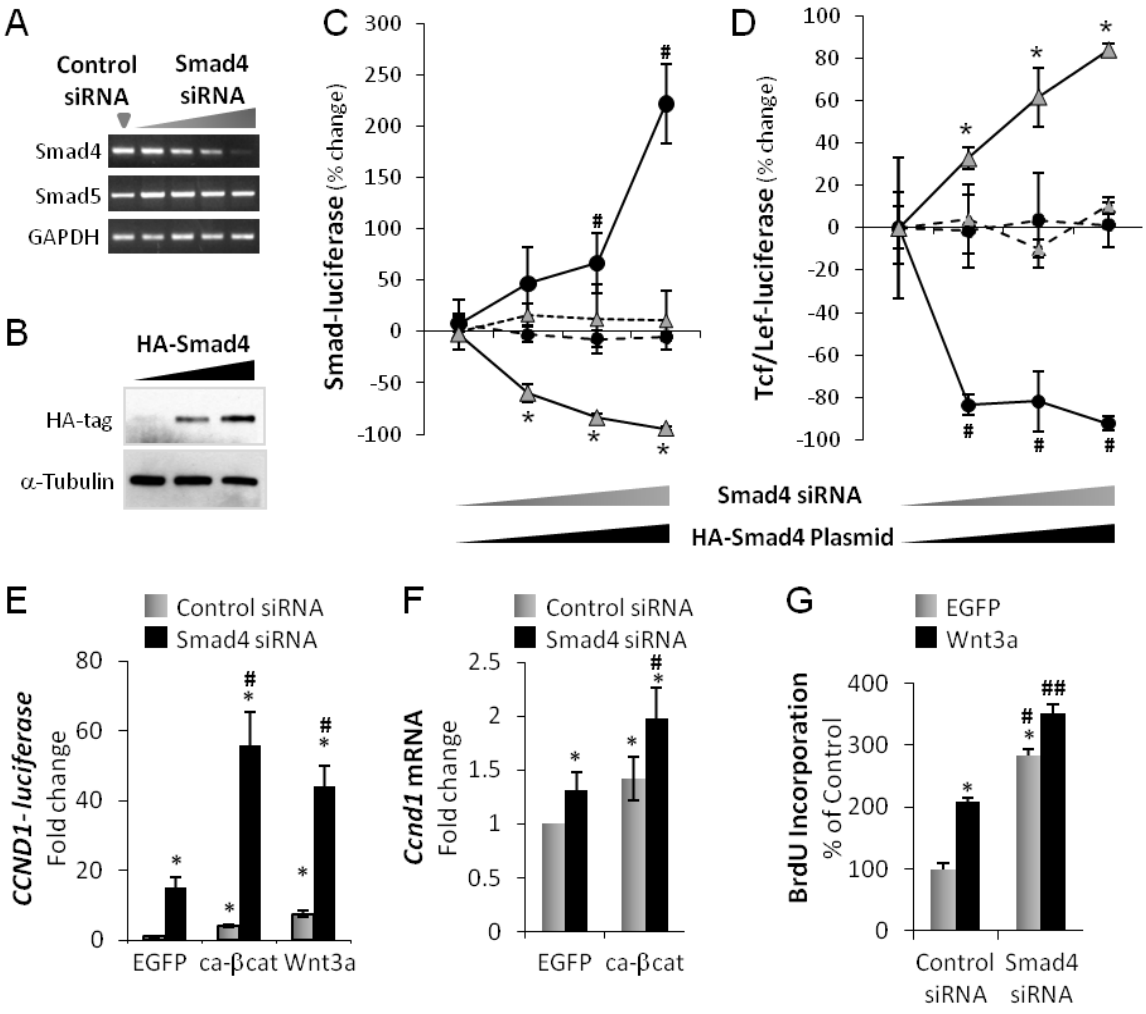
A
Control siRNA
Smad4 siRNA
Smad4
Smad5
GAPDH
B
HA-Smad4
HA-tag
α-Tubulin
C
Smad-luciferase (% change)
300
250
200
150
100
50
0
-50
-100
D
Tcf/Lef-luciferase (% change)
100
80
60
40
20
0
-20
-40
-60
-80
-100
Smad4 siRNA
HA-Smad4 Plasmid
E
Control siRNA
Smad4 siRNA
CCND1-luciferase
Fold change
80
60
40
20
0
EGFP
ca-βcat
Wnt3a
F
Control siRNA
Smad4 siRNA
Ccnd1 mRNA
Fold change
2.5
2
1.5
1
0.5
0
EGFP
ca-βcat
G
EGFP
Wnt3a
BrdU Incorporation
% of Control
400
300
200
100
0
Control siRNA
Smad4 siRNA

Figure 3.3

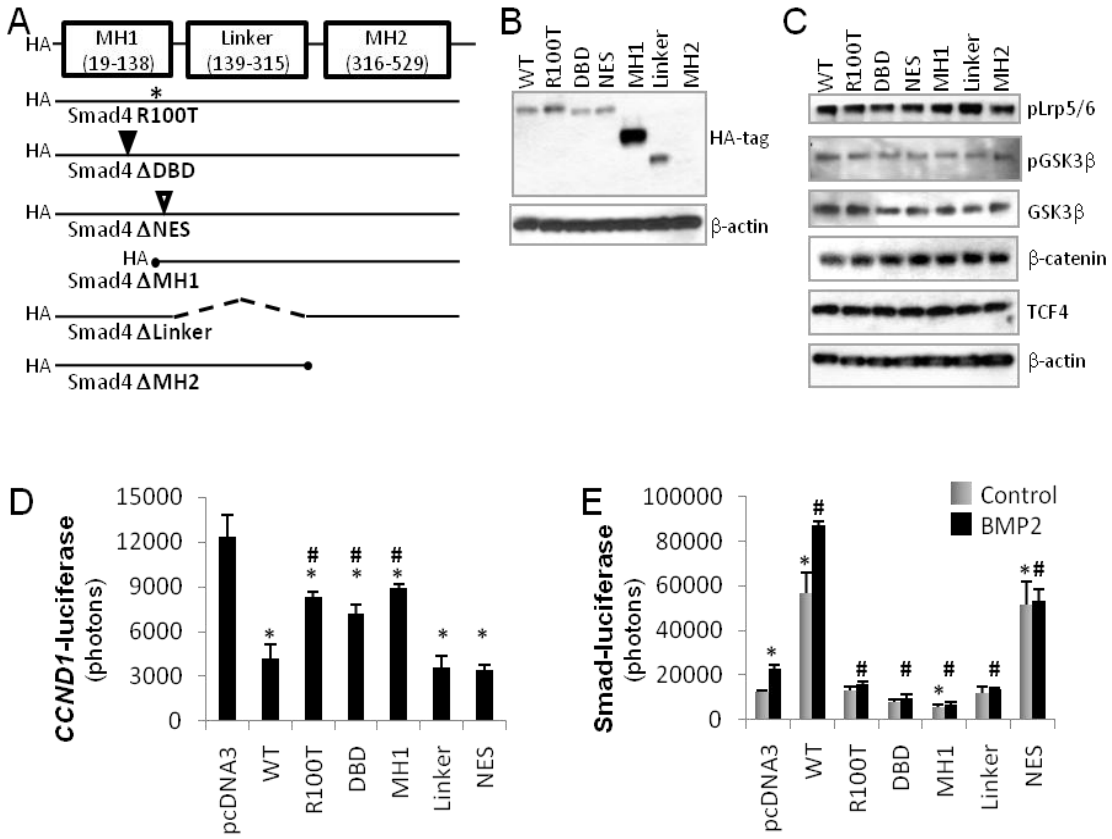
A
HA
MH1 (19-138)
Linker (139-315)
MH2 (316-529)
Smad4 R100T
Smad4 ΔDBD
Smad4 ΔNES
Smad4 ΔMH1
Smad4 ΔLinker
Smad4 ΔMH2
B
WT
R100T
DBD
NES
MH1
Linker
MH2
HA-tag
β-actin
C
pLrp5/6
pGSK3β
GSK3β
β-catenin
TCF4
β-actin
D
CCND1-luciferase (photons)
15000
12000
9000
6000
3000
0
pcDNA3
WT
R100T
DBD
MH1
Linker
NES
E
Smad-luciferase (photons)
100000
80000
60000
40000
20000
0
Control
BMP2

Figure 3.4

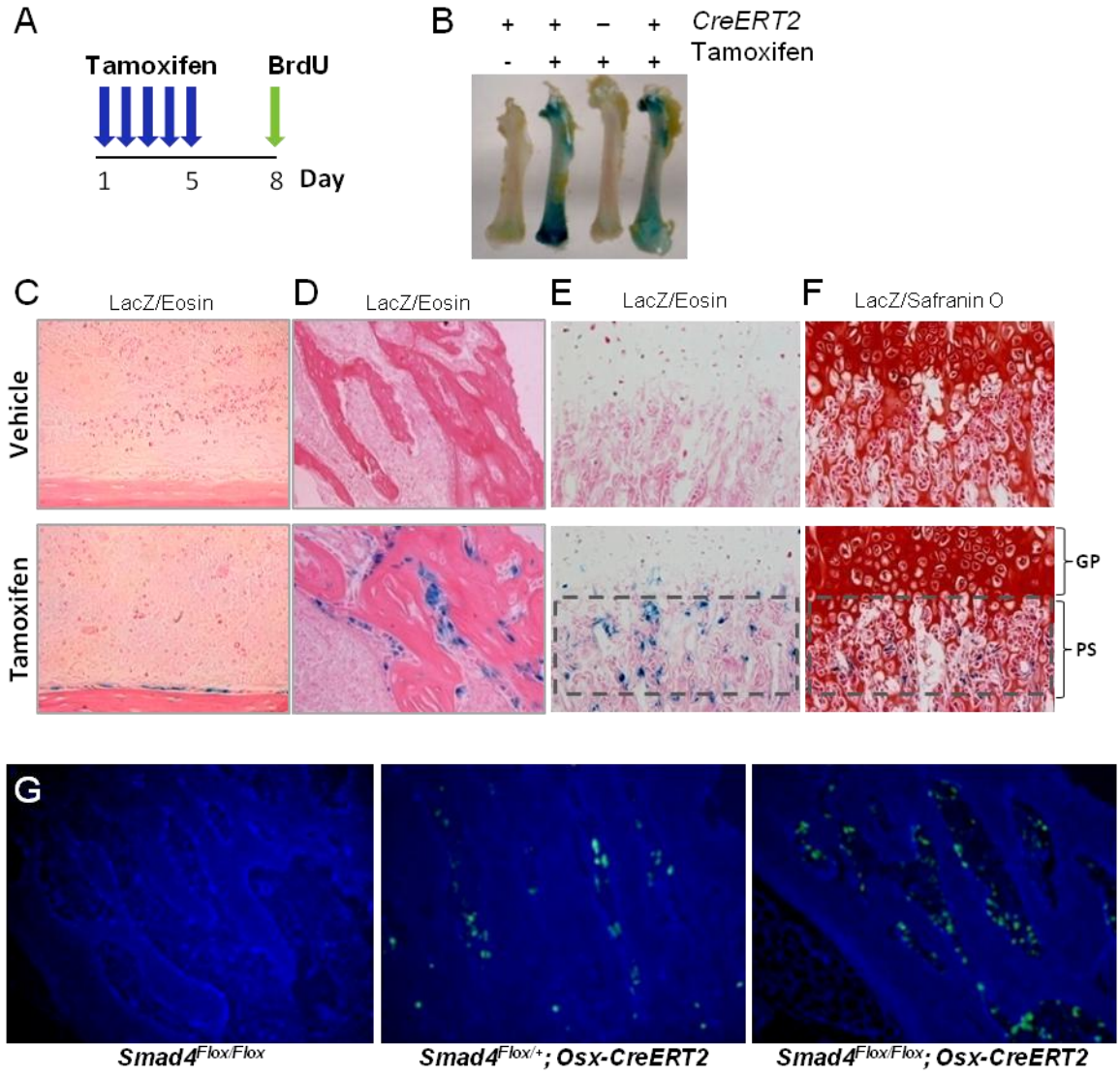
A
Tamoxifen
BrdU
1
5
8
Day
B
+ + – +
CreERT2
- + + +
Tamoxifen
C
LacZ/Eosin
D
LacZ/Eosin
E
LacZ/Eosin
F
LacZ/Safranin O
Vehicle
Tamoxifen
GP
PS
G
Smad4Flox/Flox
Smad4Flox/+; Osx-CreERT2
Smad4Flox/Flox; Osx-CreERT2

Figure 3.5

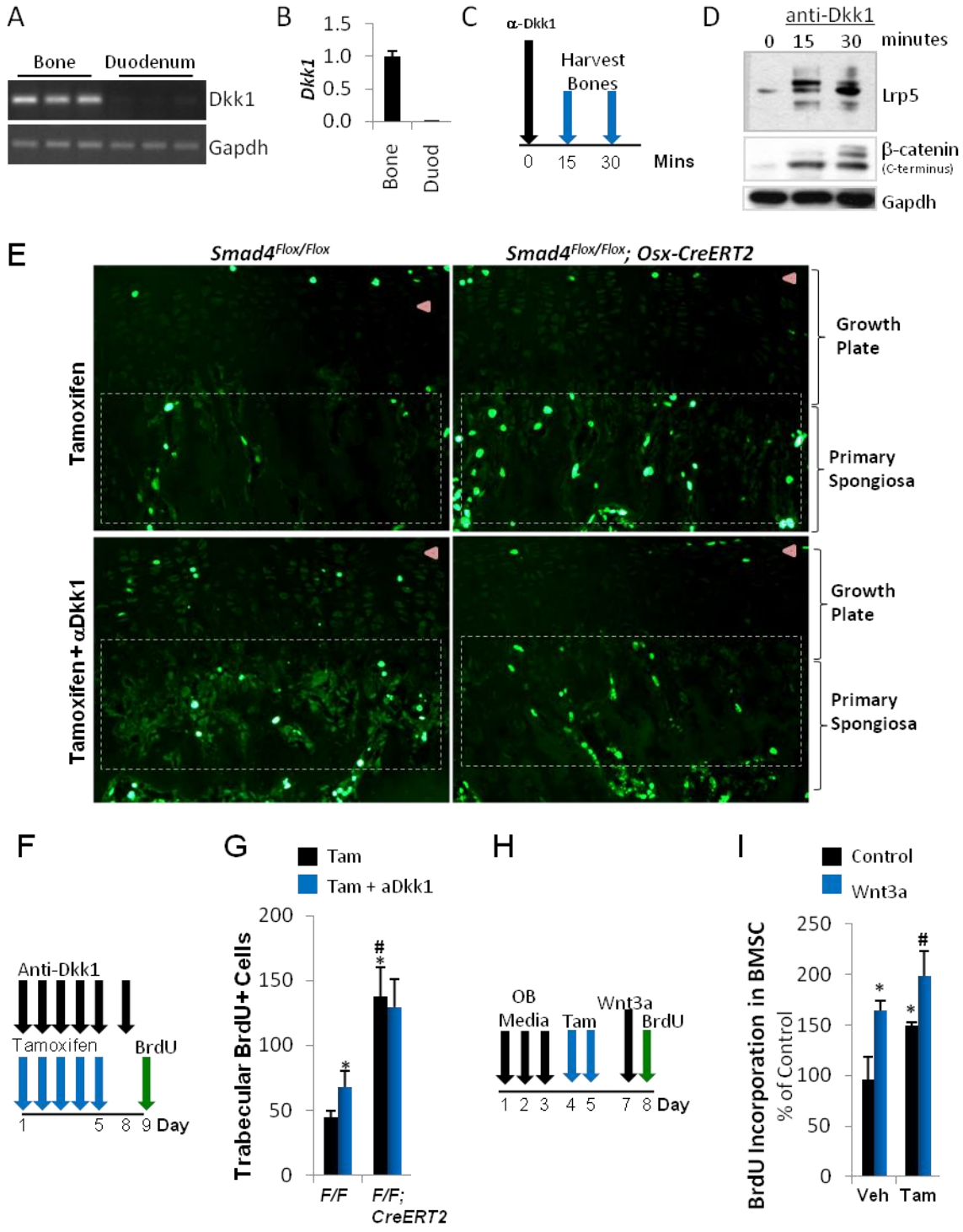
A
Bone
Duodenum
Dkk1
Gapdh
B
Dkk1
1.5
1.0
0.5
0.0
Bone
Duod
C
α-Dkk1
Harvest
Bones
0
15
30
Mins
D
anti-Dkk1
0
15
30
minutes
Lrp5
β-catenin
(C-terminus)
Gapdh
E
Smad4Flox/Flox
Smad4Flox/Flox; Osx-CreERT2
Tamoxifen
Tamoxifen+αDkk1
Growth Plate
Primary Spongiosa
Growth Plate
Primary Spongiosa
F
Anti-Dkk1
Tamoxifen
BrdU
1
5
8
9 Day
G
Tam
Tam + aDkk1
Trabecular BrdU+ Cells
200
150
100
50
0
F/F
F/F; CreERT2
H
OB Media
Tam
Wnt3a
BrdU
1 2 3 4 5 7 8 Day
I
Control
Wnt3a
BrdU Incorporation in BMSC
% of Control
250
200
150
100
50
0
Veh
Tam

CHAPTER 4

Smad4 Coordinates R-Smad and p38 Signaling in Osteoblasts and is Required for Bone Anabolic Response to Canonical Wnt Signaling

4.1 ABSTRACT

β-catenin and BMP signaling synergize to promote osteoblast differentiation and bone formation. To examine the molecular mechanisms underlying this cooperative interaction, we tested whether canonical Wnt signaling can generate bone anabolic cues in mice and cells with osteoblast-specific ablation of Smad4, a key mediator of the BMP and greater TGF-beta pathway. $Smad4^{Flox/Flox}$; Osx1-Cre mice exhibit a lethal post-natal skeletal phenotype characterized by stunted growth, dramatic hypomineralization of skeletal and dental structures, a persistence of medullary trabeculation, and clavicle hypoplasia. Mechanistically, Smad4 links R-Smad and p38 MAPK pathways in bone to regulate collagen biochemistry and protect osteoblasts from Caspase-3 associated cleavage of β-catenin. Accordingly, Smad4–deficient osteoblasts do not mineralize in response to BMP2 or Wnt3a. And conditional Smad4-deficient mice fail to form new bone following in vivo administration of Dkk1-neutralizing antibody. In summary, Smad4 regulates collagen processing, promotes osteoblast survival, and is necessary, indirectly, for manifestation of osteoanabolic Wnt cues.

4.2 INTRODUCTION

During endochondral bone development, chondrocytes construct an avascular cartilage template which is converted to a mineralized skeletal structure by the orchestrated invasion of blood vessels, cartilage-resorbing cells of the monocyte lineage known as osteoclasts, and mesodermally derived bone-forming cells called osteoblasts (Maes et al.). The skeleton undergoes constant remodeling by osteoblasts and osteoclasts throughout post-natal life. Two pillar pathways contributing to skeletal developmental and postnatal skeletal homeostasis are the Bone Morphogenetic Protein (BMP) and the canonical Wnt (cWnt) signaling systems.

BMP2 and BMP4, members of the TGF-β superfamily, are together necessary (Bandyopadhyay et al., 2006) and each sufficient (Kang et al., 2004; Wozney et al., 1988) to drive de novo bone formation. Accordingly, bone formation is diminished by transgenic expression of the BMP2/4/7 antagonists Noggin and Gremlin (Devlin et al., 2003; Gazzerro et al., 2005) in bone; and mice with Bmpr1a or Smad4 ablation in mature Col1A1- or Bglap-expressing osteoblasts display low bone formation with decreased resorption (Kamiya et al., 2008a; Kamiya et al., 2008b; Mishina et al., 2004; Tan et al., 2007), underscoring direct action by BMPs on osteoblasts in vivo. Further in vivo work is needed to characterize the roles and molecular mechanisms of action for BMP receptors, Smads1/5/8, and Smad4 in early osteoblasts. BMP receptors activate canonical Smad and non-canonical kinase pathways, which by historic models are believed to act independently (Moustakas and Heldin, 2009; Zhang, 2009). Studies in condrocytes instead provide compelling evidence that BMP signals unify R-Smads1/5/8, p38 MAPK, and TAK1 MAPKKK activity in cartilage (Greenblatt et al., ; Gunnell et al., 2010; Retting et al., 2009; Shim et al., 2009; Zhang et al., 2005). Mice with genetic ablation of any of these molecules display strikingly similar phenotypes of dwarfism secondary to reduced proliferation and increased apoptosis of chondrocytes, as well as delayed vascular invasion and resorption of cartilage from the medullary cavities. One study suggests R-Smad and TAK1/p38 pathways are linked in osteoblasts as in chondrocytes (Greenblatt et al.), warranting additional genetic studies and representing a potential need for adjustments to BMP signaling paradigms in connective tissue types.

Wnt ligands signal through a Frizzled and Lrp5/6 heteromeric receptor complex to release β-catenin from negative regulation of GSK3 and permit its nuclear accumulation where it co-activates Tcf/Lef-dependent gene expression. Gain- and loss-of-function mutations to the Wnt co-receptor, LRP5, are the underlying cause of high and low bone mass phenotypes in humans (Boyden et al., 2002; Gong et al., 2001; Gong et al., 1996; Little et al., 2002); and two high bone mass syndromes, van Buchem's disease and Sclerosteosis, are linked to loss-of-function mutations of SOST, a gene encoding the Lrp5/6 antagonist Sclerostin (Balemans et al., 2002; Loots et al., 2005). Neutralizing antibodies targeting SOST and DKK1, another Lrp5/6 antagonist, are currently being evaluated as therapeutic agents designed to increase bone mass in osteoporotic patients (Rachner et al.)).

Complex and sometimes seemingly contradictory interactions between BMP and Wnt signaling occur in the skeletal system. For example, osteogenic effects of BMP-2 require β-catenin (Chen et al., 2007; Hill et al., 2005), supporting the notion that Wnt signaling through β-catenin operates downstream of BMP (Bain et al., 2003; Rawadi et al., 2003). However, BMPR1a signaling suppresses cWnt activity via Sost and Dkk1 (Kamiya et al., 2008a; Kamiya et al., 2008b), and in vitro neutralization of BMPs blocks Wnt/β-catenin-induced osteoblast differentiation, suggesting instead that Wnt is upstream of BMPs (Salazar et al., 2008; Winkler et al., 2005). Because simple epistatic models do not satisfactorily explain the BMP and Wnt/β-catenin relationship in bone, it is more likely that the two pathways work together.

In this work, we use mice with conditional ablation of Smad4 in Osx1+ osteoblasts to test whether bone anabolic response to cWnt signaling requires integrity of the BMP pathway. In first characterizing the baseline phenotype of these mice, we uncover novel mechanistic details about the role of Smad4 in skeletal homeostasis, collagen biosynthesis, and osteoblast survival. We furthermore demonstrate that cWnt signaling is not sufficient to stimulate bone anabolism in the absence of Smad4.

4.3 METHODS

Materials

Rat monoclonal anti-mouse Dkk1 (αDkk1, clone 11H10, Lot 14073109), a kind gift of Dr. William Richards, Amgen, Inc. (Thousand Oaks, CA), was prepared in sterile saline and administered at 20 mg/kg/day via i.p. injections, 3 times a week for 4 weeks. All other chemicals and reagents, unless specified otherwise, were obtained from Sigma Aldrich.

Mouse Models

Osx1-GFP::Cre (Osx1-Cre) transgenic mice express a Tet-off regulated GFP::Cre fusion protein under control of the Osx1 promoter (Rodda and McMahon, 2006). Rosa26R$^{flox(LacZ)}$ reporter alleles (R26R^{F}) are activated by Cre-mediated excision of a floxed stop codon upstream of a beta-galactosidase cassette (Soriano, 1999). Conditional Smad4 alleles (Smad4^{F}) are ablated by Cre-mediated excision of a floxed exon 8 (Yang et al., 2002). We examined β-galactosidase activity in bones of Osx1-Cre; R26R$^{F/+}$ mice to monitor efficiency and lineage specificity of the Osx1-Cre. To ablate Smad4 in differentiating osteoblasts, we generated Osx1-Cre; Smad4$^{Flox/Flox}$ (Smad4$^{\Delta/\Delta}$, conditional knockout) along with Osx1-Cre; Smad4$^{Flox/+}$ (Smad4$^{F/\Delta}$, conditional heterozygous), and Smad4$^{Flox/Flox}$ (Smad4$^{F/F}$, conditional wildtype) mice. Mice were in a mixed C57BL/6-C129/J background, fed regular chow ad libitum, and housed at 25°C with 12 hour light/dark cycles. Genotyping was done with a HotSHOT method (Truett et al., 2000) and originally described primers. Studies approved by Animal Studies Committee of Washington University in St Louis.

Histology

We have described decalcification, and preparation of bones for paraffin or methyl-methacrylate embedding and sectioning and whole mount staining (Chung et al., 2006). Calcein Injections were given 11 and 3 days before euthanasia (15 mg/kg i.p.). LacZ Non-specific β-galactosidase staining on decalcified bones was prevented by supplementing stain solution (Chung et al., 2006) with 100mM galactose and developing at 30°C. TUNEL Apoptotic cells were detected in paraffin embedded sections of tibia with In Situ Cell Death Detection Kit (Roche). Brightfield and

fluorescence microscopy were captured with a Nikon Eclipse E600, picrosirius red with polarized light microscope (Olympus BX51P), and whole mounts with a digital camera.

MicroCT

Bones, embedded in 2.0% agarose, were scanned post-mortem with a high resolution computed tomography system (μCT40; Scanco Medical AG) using 45 EkVp of radiation energy at standard resolution (20μm). In vivo, we used a VivaμCT40; Scanco Medical AG set to 70kVPs and 110μA. The first 30 slices below the growth plate of the proximal tibia were analyzed. Data are expressed as Mean±STD and were compared by t-test for unpaired samples, $n \geq 4$.

Immunoblot

Protein from marrow-free bones (N≥3 per genotype) or cells was prepared in RIPA buffer and separated by SDS-PAGE electrophoresis (Watkins et al., 2011). Antibodies are listed in **Table 1.**

Real-Time Quantitative PCR (QPCR)

Messenger RNA was prepared from marrow free bones (N≥3 per genotype) or cells, converted into cDNA, and analyzed as described (Watkins et al., 2011). Data were normalized to Cyclophilin and calculated as a ratio to the average of $Smad4^{F/F}$ samples. Taqman® Gene expression assays (Applied Biosystems) were used for Dmp1, Lox, Plod and P3ha4. Other primers available upon request. Data are expressed as the Mean±STD and were compared by t-test for unpaired samples.

Cell Culture

All cultures were incubated at 37°C in a humidified atmosphere with 5% CO_2 in basic media (ascorbic acid free α-MEM (Invitrogen) with 40mM L-glutamine, 100U/ml penicillin-G, and 100mg/ml streptomycin) plus osteogenic cocktail (50 μM ascorbic acid, and 10 μM β-glycerophosphate) as indicated. Calvaria organ cultures Sagittal halves of neonatal mouse calvaria were cultured 9 days basic media (no FBS) plus osteogenic cocktail ± 100 or 200 □g/ml Dkk1 neutralizing antibody. New tissue was labeled on day 10 with 20 □M xylenol orange in culture media (Wang et al., 2005). MC3T3 immortalized mouse calvaria cells were maintained in basic media plus 10% FBS. Osteoblasts were differentiated by plating to confluence (Day 0) in media plus osteogenic cocktail ± 200 ng/ml rhBMP2 and/or 10 □M SB203580. RNA was

harvested with an RNeasy Plus kit (Qiagen) and protein as prepared in RIPA buffer as described (Salazar et al., 2008). Bone marrow stromal cells (BMSC) and macrophages (MΦ) were isolated by removing the distal epiphyses, centrifuging the bone at 9,000 rpm for 10 sec, then processing for culture as described (Watkins et al., 2011). For mineralization, BMSC were seeded 40,000 cells per well (96-well plate) and cultured 21 days in media with 10% FBS, osteogenic cocktail ± 200 ng/ml rhBMP2 or 50 ng/ml rmWnt3a (R&D Systems) prior to alizarin red and alkaline phosphatase staining (Salazar et al., 2008). Osteoclasts were differentiated from MCSF-primed MΦ plus MCSF and RANKL or BMSC, vitamin D3 and dexamethosone, as described (Watkins et al., 2011).

4.4 RESULTS

4.4.1 Progressive Skeletal Phenotype in Mice with Deficiency of Smad4 in Osx1+ Osteoblasts

In histologic sections of femurs from Osx1-Cre; $R26R^{F/+}$ mice, LacZ activity is evident in osteoblasts and osteocytes, but not in chondrocytes in articular cartilage of the epiphysis, or other bone marrow cells (Figure 4.1A). Compared to $Smad4^{F/F}$ mice, Smad4 protein is nearly undetectable by immunoblot on marrow-free bone tissue from Osx1-Cre; $Smad4^{F/F}$ ($Smad4^{\Delta/\Delta}$) mice (Figure 4.1B). Thus, Osx1-Cre mediates osteoblast-specific ablation of Smad4. Since Osx1-Cre is first expressed at E13.5 (Rodda and McMahon, 2006), we performed whole mount staining to determine if skeletal anomalies manifest before birth. In $Smad4^{\Delta/\Delta}$ mice, the nasal arch is narrow and the frontal, parietal, and interparietal bones (Figure 4.1C) are hypominerilized. The xyphisternum is short, with dysmorphisms of the xyphoid process and ventral costal cartilage of the false ribs. Ventral costal cartilage on true ribs is fully mineralized (Figure 4.1D). Clavicles are hypoplastic with only a lateral rudiment (Figure 4.1E).

Most $Smad4^{\Delta/\Delta}$ mice die before weaning. About 50% die by P14, another 25% by 5 weeks, and almost none survive to 8 weeks of age, even if provided access to soft, paste-based nutrition (Nutri-Cal). Despite nearly normal body size at birth (Figure 4.1F), $Smad4^{\Delta/\Delta}$ mice are

severely runted and osteopenic compared to littermates at weaning (Figure 4.1G). Both Smad4$^{F/\Delta}$ and Smad4$^{\Delta/\Delta}$ develop oral malocclusion, a feature linked to the Osx1-Cre transgene (http://jaxmice.jax.org/strain/006361.html). However, only Smad4$^{\Delta/\Delta}$ mice exhibit enamel hypoplasia and brittle teeth (Figure 4.1H), a feature confirmed by computerized 3-D reconstruction using µCT of skeletal structures in 4 week old littermates (Figures 4.1I-L). Lower incisors appear to be missing in Smad4$^{\Delta/\Delta}$ mice. There is severe hypomineralization of the cranial vault, mandible, scapulae, and vertebral column (Figure 4.1K, red arrows). Dorsal segments of the ribs lack curvature, forming a restricted thoracic cavity (Figures 4.1K-L). The sternal segment of the clavicle remains hypoplastic and fails to reach the sternum (Figure 4.1L). Ribs of Smad4$^{\Delta/\Delta}$ mice show new and old fractures with callus formation at 4 and 8 weeks of age (Figures 4.1K, M, blue arrows).

Computerized 3-D reconstructions show that tibiae of Smad4$^{\Delta/\Delta}$ mice are morphologically normal although smaller than Smad4$^{F/F}$ (Figure 4.2A). Trabecular structures, normally restricted to the metaphysis, populate the entire length of Smad4$^{\Delta/\Delta}$ bones and fill the secondary ossification center (Figures 4.2A, red arrows). While growth plate cartilage of all genotypes is Safranin O+ and Fast Green- (Figure 4.2B), these trabeculae in the diaphysis of Smad4$^{\Delta/\Delta}$ mice are Safranin O- and Fast Green+ (Figure 4.2C), indicating they are boney tissue as opposed to unresorbed cartilage islands left behind during formation of the medullary cavity. Trabeculation of the diaphysis is also evident by Goldner Trichrome staining, which further reveals that Smad4$^{\Delta/\Delta}$ bones exhibit a prevalence of marrow fat and a high density of osteocytes (Figures 4.2D-E).

Quantitative analysis at the proximal metaphysis indicates that although trabecular tissue volume and bone volume are significantly lower in Smad4$^{\Delta/\Delta}$ relative to either Smad4$^{F/F}$ or Smad4$^{F/\Delta}$ mice (Figures 4.2F-G), trabecular BV/TV is not different across genotypes (Figure 4.2H). Thus, trabecular bone in Smad4$^{\Delta/\Delta}$ mice is appropriate for reduced bone size, a finding corroborated by BMC/TV at the metaphysis (Figure 4.2I). Trabecular number, thickness, and spacing are not statistically different in any Smad4 genotype (Supplemental Figures 4.2A-C). At the mid-diaphysis, total cross-sectional tissue area (Figure 4.2J) and cortical thickness (Figure

4.2K) are statistically decreased in Smad4$^{\Delta/\Delta}$ mice by 43±1.3% and 51±4.5%, respectively, relative to Smad4$^{F/F}$ or Smad4$^{F/\Delta}$. Bone mineral content as a function of bone volume (BMC/BV) is 8.2±2.8% lower in trabecular compartment and 20±3.8% lower in the cortical compartment of Smad4$^{\Delta/\Delta}$ relative to Smad4$^{F/F}$ mice (Figures 4.2L-M), consistent with hypomineralization of the skull, spine, and scapulae (Figures 4.1K-L). Dynamic indices of bone formation were not quantitated due to early lethality. Since bone mass and architecture are essentially the same in Smad4$^{F/F}$ or Smad4$^{F/\Delta}$, 3-D reconstructions and histologic images are shown only for Smad4$^{F/F}$ and Smad4$^{\Delta/\Delta}$ mice.

The increased trabeculation of the diaphyses in Smad4$^{\Delta/\Delta}$ mice could be the result of either over-active osteoblasts or diminished osteoclast bone resorption. Considering the generalized, severe hypomineralization of Smad4$^{\Delta/\Delta}$ mice mice, the former hypothesis seems highly unlikely. Thus, we examined osteoclast activity in tibia sections. TRAP-positive osteoclasts are abundant at the growth plate in all genotypes but sparse on endocortical or periosteal surfaces of Smad4$^{\Delta/\Delta}$ (Figure 4.3A). In vitro, bone marrow macrophages from Smad4$^{F/F}$ and Smad4$^{\Delta/\Delta}$ mice form similar numbers of TRAP+ multinucleated osteoclasts in the presence and RANKL and MCSF (Figures 4.3B-C). However, Smad4$^{\Delta/\Delta}$ osteoblasts generate 60% fewer osteoclasts from macrophages of Smad4$^{F/F}$ mice than do Smad4$^{F/F}$ osteoblasts (Figures 4.3D-E), demonstrating a non-cell autonomous osteoclast defect. QPCR on marrow-free bone tissue reveals that MCSF and RANKL are constant in all genotypes while Opg was statistically decreased in Smad4$^{\Delta/\Delta}$, a finding confirmed by immublot on bone (Figures 4.3F-G).

4.4.2 Loss of Smad4 impairs R-Smad and p38 MAPK Pathways in Osteoblasts

To create a context to test bone anabolic Wnt signaling in Smad4$^{\Delta/\Delta}$ mice, we investigated the osteoblast defect by using QPCR on bone extracts to profile genes expressed in the osteogenic lineage. High EGFP and Cre levels in Smad4$^{F/\Delta}$ and Smad4$^{\Delta/\Delta}$, but not in Smad4$^{F/F}$ samples, confirmed our sample processing enriches mRNAs from cells expressing the Osx1-Cre transgene. Surprisingly, considering our striking phenotype and previous findings on a

related model (Tan et al., 2007), expression of Cbfa1, Osx, Dmp1, and Phex are not statistically different in Smad4$^{\Delta/\Delta}$ compared to Smad4$^{F/F}$ or Smad4$^{F/\Delta}$ samples (Figure 4.4A). Expression of non-collagen components of the skeletal extracellular matrix, such as BSP, Opn and Ocn are modestly but not statistically decreased in Smad4$^{\Delta/\Delta}$ bone relative to the other genotypes (Figure 4.4B). Importantly, abundance of Col1α1, the major organic component of bone matrix, is only decreased about 20% in Smad4$^{\Delta/\Delta}$ bones (Figure 4.4C). By contrast, deletion of one or two Smad4 alleles leads to gene-dosage dependent down-regulation of procollagen lysyl hydroxylase (Plod), prolyl 3-hydroxylase (P3HA4), and lysyl oxidase (Lox) mRNA (Figure 4.4C), enzymes required for assembly and crosslinking of collagen fibrils (Trackman, 2005). We thus examined histologic sections of tibiae under polarized light following picrosirius red staining. A red/yellow color display in Smad4$^{\Delta/\Delta}$ compared to primarily green on Smad4$^{F/F}$ sections (Figure 4.4D) confirmed that collagen extracellular matrix formation is defective in Smad4$^{\Delta/\Delta}$ bones and is likely characterized by abnormal thickness or packing density of fibers (Dayan et al., 1989).

Immunoblot on bone confirmed that Osx is expressed in Smad4$^{\Delta/\Delta}$ bones, though the abundance of high molecular weight Osx bands is sharply diminished (Figure 4.5A). Notably, electrophoretic patterns of Osx and other proteins are more complex in bone samples than cell extracts, suggesting extensive post-translational modifications occurring in primary tissue. Relative to Osx and β-actin, Lox is almost undetectable (Figure 4.5A), corroborating QPCR. Lox is regulated by BMP2 in a Smad4- and p38- dependent manner during formation of adipoctyes (Huang et al., 2009), which share a common progenitor as osteoblasts. Lox mRNA (Figure 4.5B) and Lox protein (Figure 4.5C) are similarly up regulated during BMP2-mediated osteoblast differentiation and are sensitive to p38 inhibition by SB203508. In vivo, immunoblots reveal that loss of Smad4 sharply diminishes phospho-p38 in bone without affecting p38 abundance (Figure 4.5D). TGFβ can regulate p38 MAPK activation of TAK1 or expression Gadd45β (Miyake et al., 2007; Takekawa et al., 2002; Yoo et al., 2003). While TAK1 mRNA is expressed normally Smad4$^{\Delta/\Delta}$ bones (Figure 4.5J), the immunoblot band of TAK1 shown to be targeted by TAK1 siRNA (Figure 4.5D, red asterix) is low in mutant bones, while the faster-migrating, non-specific

band (black asterix) is unaffected (van der Heide et al., 2011). Downstream, there is reduced CREB, ATF1, and ATF2 phosphorylation and decreased expression of Bcl-2, an anti-apoptotic molecule and transcriptional target of CREB and ATF (Ma et al., 2007) (Figure 4.5D). Overall, this p38 pathway is increasingly disrupted by loss of each Smad4 allele. By contrast, phosphorylation of Akt and downstream Akt substrates is similar in all genotypes, despite that total Akt is low in $Smad4^{\Delta/\Delta}$ bone (Figure 4.5E). Abundance and phosphorylation of ERK or JNK are unchanged by loss of Smad4 (Figure 4.5F), as is GADD45β, an alternative link from Smad4 to p38/CREB (van der Heide et al., 2011), (Figures 4.5G and J). Loss of both Smad4 alleles is however associated with low abundance of phosphorylated Smads1/5/8 and phosphorylated Smad2 (Figures 4.5H). Smad3 phosphorylation is below detection in all genotypes, and is not shown. Total Smad1 and Smad2, but not Smad3 or Smad5 proteins, are sharply reduced in $Smad4^{\Delta/\Delta}$ bones (Figure 4.5I), despite normal steady-state mRNA levels (Figure 4.5J). Thus, loss of Smad4 in Osx1+ osteoblasts profoundly impairs TGFβ/BMP signaling through R-Smads and p38, thereby providing an excellent model to test whether integrity of the BMP pathway is necessary for a bone anabolic response to cWnt signaling.

4.4.3 Bone Anabolic Responses to cWnt Signaling Require Smad4 in Osteoblasts

We manipulated cWnt signaling with αDkk1, an antibody that neutralizes the Wnt antagonist, Dkk1, and induces bone formation when given systemically to mice with rheumatoid arthritis (Diarra et al., 2007). In our hands, a single dose of αDkk1 dramatically upregulates Lrp5 and β-catenin proteins in bone within 15 minutes of injection (unpublished data). Accordingly, incubation of ex vivo intact calvaria culture with αDkk1 dose-dependently increases calvarial thickness and xylenol orange incorporation, two indicators of new bone deposition (Figure 4.6A). With respect to lingering controversy as to whether cWnt signaling stimulates bone formation by direct action on osteoblasts (Cui et al., 2011) or indirectly, via an endocrine loop (Yadav et al., 2008), we find that αDkk1 activates cWnt signaling and stimulates new bone deposition, at least in part, by direct action on bone. Wild type C57B6 male mice treated for 4 weeks with αDkk1 (20 mg/kg/day, 3 times/week) exhibited a 48% increase in mineral apposition rate at the proximal tibia

(Figure 4.6B), with no effect on bone resorption, as determined by circulating CTX collagen fragments (Figure 4.6C). Male Smad4$^{F/F}$ and Smad4$^{F/\Delta}$ mice treated with αDkk1 had significantly increased bone volume/trabecular tissue volume (BV/TV) at the proximal tibia (60% and 59% vs. pre-treatment, Figures 4.6D-E). Early lethality impeded a statistical analysis of the effect of αDkk1 on age and sex-matched Smad4$^{\Delta/\Delta}$ mice. Nevertheless, whereas BV/TV at the metaphysis was normal in Smad4$^{\Delta/\Delta}$ mice at 1 month (Figure 4.2H), a Smad4$^{\Delta/\Delta}$ female that survived to 3 months exhibited a BV/TV that was 56% lower than age-matched Smad4$^{F/F}$ females and did not accrue trabecular bone in response to αDkk1 treatment compared to 39% and 49% increases in BV/TV of female Smad4$^{F/F}$ and Smad4$^{\Delta/\Delta}$ mice (Figure 4.6F). While abundant and wide-spaced double calcein labels were present in Smad4$^{F/F}$ female tibia after αDkk1 treatment (Figures 4.6G and H), the Smad4$^{\Delta/\Delta}$ female had very few labeled surfaces and a distinct absence of double labels (Figures 4.6K and L). Also, areas of unmineralized osteoid persisted in Smad4$^{\Delta/\Delta}$ cortical bone after αDkk1 treatment (Figures 4.6I and M). To confirm an osteoblast defect, primary bone marrow stromal cells (BMSC) from Smad4$^{F/F}$ and Smad4$^{\Delta/\Delta}$ mice were differentiated under osteogenic conditions. While Smad4$^{F/F}$ cultures formed alizarin red-positive mineralized nodules, particularly when exposed to BMP-2 or Wnt3a, Smad4$^{\Delta/\Delta}$ cultures failed to mineralize, even in the presence of these stimulators (Figure 4.6N). Furthermore, alkaline phosphatase+ cells were not observed in Smad4$^{\Delta/\Delta}$ cultures, even in the presence of BMP-2 or Wnt3a, in contrast to abundant alkaline phosphatase+ cells and mineralization in Smad4$^{F/F}$ cultures (Figure 4.6O).

Wnt pathway components were profiled to investigate why Smad4$^{\Delta/\Delta}$ mice and cells do not respond to αDkk1 or Wnt3a. Dkk1 and Sost mRNAs are sharply decreased by loss of each Smad4 allele (Figure 4.7A) while Lrp5, Lrp6, and GSK3β protein levels are normal in all genotypes. In contrast to a previous study where loss of Bmpr1A augmented cWnt signaling via decreased expression of Sost and Dkk1 (Kamiya et al., 2008a), phosphorylation of GSK3β and GSK3β target residues on β-catenin is unaffected by loss of Smad4 (Figure 4.7B). More

importantly, immunoblots on bone with an antibody to the N-terminus of β-catenin reveal that the bands between 82-115 kDa in Smad4$^{F/F}$ and Smad4$^{F/\Delta}$ bones are substantially fainter in the Smad4$^{\Delta/\Delta}$ (Figure 4.7C, upper panel). And bands between 82-115 kDa produced by an antibody to the C-terminus of β-catenin are nearly below detection, with increased abundance of a band at about 70 kDa in the Smad4$^{\Delta/\Delta}$ sample (Figure 4.7C, middle panel), suggesting β-catenin cleavage in mutant mice. GSK3β–independent proteolysis of β-catenin can be accomplished via direct cleavage by Caspase-3 at specific sites (Figure 4.7D) (Brancolini et al., 1997; Hunter et al., 2001; Steinhusen et al., 2000). Indeed, Smad4$^{\Delta/\Delta}$ mice exhibit activated Caspases-9 and -3 and cleaved PARP in bone (Figure 4.7E), as well as focal aggregates of TUNEL+ apoptotic osteoblasts on cortical and trabecular surfaces in the diaphysis (Figure 4.7G). Critically, C-terminal cleavage of β-catenin (Figure 4.7C, middle) can remove its transcriptional activity (Cong et al., 2003). Indeed, mRNA of two β-catenin target genes, Ccnd1 (Tetsu and McCormick, 1999) and EphB4 (Batlle et al., 2002) are downregulated ~50% in Smad4$^{\Delta/\Delta}$ bone (Figure 4.7F, and not shown).

In summary (Figure 4.7H), Smad4$^{\Delta/\Delta}$ osteoblasts do not properly utilize the p38 MAPK pathway to drive collagen biosynthesis and protect against apoptosis. This cell autonomous signaling defect renders Smad4$^{\Delta/\Delta}$ osteoblasts insensitive to BMP2, and causes a secondary depletion of β-catenin making them also resistant to cWnt signaling. In this model, Smad4 and cWnt/β-catenin signaling act cooperatively, not sequentially, to orchestrate the osteoblast differentiation and control post-natal bone homeostasis.

4.5 DISCUSSION

The key finding of this work is that Smad4 is required for bone forming responses to cWnt signaling in vitro and in vivo. Intriguingly, expression of Dkk1 in osteoblasts is regulated by Bmpr1a signaling through Smad4, while Sost is regulated by Bmpr1a signaling through p38 (Kamiya et al., 2008a; Kamiya et al., 2008b). We find that loss of Smad4 abrogates expression of both Dkk1 and Sost, implying Smad4 is upstream of p38 in the BMP signal cascade. Thus, if cWnt is indeed sufficient downstream of Smad4 to induce new bone formation, then $Smad4^{\Delta/\Delta}$ mice should display an osteosclerotic phenotype owing to increased osteoblast activity, as predicted by the high bone mass syndromes caused by activating LRP5 mutations (Boyden et al., 2002; Ellies et al., 2006) and loss-of-function SOST mutations (Balemans et al., 2002; Brunkow et al., 2001). Furthermore, $Smad4^{\Delta/\Delta}$ mice should respond more aggressively to Dkk1 therapy since less antibody would be required to saturate the target. And $Smad4^{\Delta/\Delta}$ primary osteoblasts should mineralize better in response to purified Wnt3a. To the contrary, we show that $Smad4^{\Delta/\Delta}$ mice have small, poorly mineralized bones; and $Smad4^{\Delta/\Delta}$ cells do not mineralize in response to Wnt3a. Further, a $Smad4^{\Delta/\Delta}$ mouse that survived beyond 6 weeks completely failed to mount an osteoanabolic response to αDkk1 treatment. Thus, loss of Smad4 in osteoblasts results in a resistance to anabolic Wnt signaling in bone. Importantly, diminished bone formation was also reported in mice with selective ablation of Bmpr1a in differentiated osteoblasts despite reduced expression of Dkk1 and Sost (Kamiya et al.), indicating loss of Smad4 phenocopies loss of Bmpr1a, and thus that disruption of BMP signaling through Smad4 in osteoblasts impairs anabolic responses to cWnt.

While loss of Smad4 does not prevent Osx+ osteoblasts from progressing to a Dmp1+/Phex+ stage of maturation, it does render these cells unable to mineralize their matrix. $Smad4^{\Delta/\Delta}$ osteoblasts are also unable to support normal osteoclastogenesis, a non-cell autonomous defect unexplained by changes to the RANKL/OPG ratio. Osteoblast-specific deficiency of BMP2 and 4 (Bandyopadhyay et al., 2006), Bmpr1a (Mishina et al., 2004), or Smad4 (Tan et al., 2007) cause very similar phenotypes with low bone turnover and a

persistence of osteochondral tissues in the medullary cavity, suggesting defects in Smad4$^{\Delta/\Delta}$ osteoblasts are largely attributable to disruption of BMP, not TGFβ, signaling. Also, our Smad4$^{\Delta/\Delta}$ mice exhibit skeletal and dental features remindful of cleidocranial dysplasia, or haploinsufficiency of Runx2 (Camilleri and McDonald, 2006; Fukuta et al., 2001; Otto et al., 1997; Yamamoto et al., 1989). Such features are not reported in TGFβ mutant mice, but are caused by osteoblast-specific ablation of BMP2/4 (Bandyopadhyay et al., 2006) or TAK1/p38 (Greenblatt et al.), implying that BMP2/4, Smad4, TAK1/p38 and Runx2 are components of a common pathway.

We provide evidence that resistance to cWnt signaling in Smad4$^{\Delta/\Delta}$ mice is associated with activation of the Caspase-9/-3 pathway and GSK3β-independent cleavage of β-catenin in bone. N-terminal cleavages of β-catenin by Caspase-3 are typically activating, even oncogenic, modifications that promote extrusion of a cell from the epithelium via enhanced disassembly of adherens junctions (Kessler and Muller, 2009). By contrast, C-terminal cleavage removes the transcriptional activation domain thereby deactivating the transcription factor function of β-catenin (Brancolini et al., 1997; Cong and Varmus, 2004; Hunter et al., 2001; Steinhusen et al., 2000). β-catenin is a critical downstream mediator of the cWnt cascade. It is both necessary and sufficient in Osx+ cells for controlling skeletal mineralization (Rodda and McMahon, 2006). Thus, the impaired mineralizing function of Smad4$^{\Delta/\Delta}$ osteoblasts and their inability to respond to extracellular cWnt activation (i.e. αDkk1 and Wnt3a) can most likely be reconciled by a secondary depletion of β-catenin. We further show that Smad4 is required for expression of collagen biosynthetic enzymes in bone. Collagen synthesizing defects are not reported in β-catenin mutant mice. Thus, β-catenin depletion probably causes, or exacerbates, the mineralizing defect in Smad4$^{\Delta/\Delta}$ mice, whereas altered production of the organic bone matrix, failed expression of Dkk1 and Sost and apoptosis are all linked to defective p38 MAPK signaling.

This illuminates a second, equally important, finding of this work. Smad4, canonical R-Smads, and non-canonical TAK1/p38 MAPK pathways are tightly networked in bone, not independent. In comparison to chondrocytes, where TAK1 coordinates only with BMP-specific R-Smads (Gunnell et al., 2010; Shim et al., 2009), TAK1 in osteoblasts coordinates with both BMP-

and TGFβ-specific R-Smads. Mechanistically, loss of Smad4 disrupts not only phosphorylation of p38, but also phosphorylation of the downstream p38 targets CREB, ATF1, and ATF2. However, ERK, JNK, and Akt pathways are not affected, indicating, as a recent in vitro study proposed (van der Heide et al., 2011), that Smad4 is linked specifically to p38/CREB/ATF cascade but not to MAPK pathways in general. This mechanism may be operative in other tissues (Xu et al., 2008). The p38 pathway is typically considered to be pro-apoptotic (van der Heide et al., 2011; Wagner and Nebreda, 2009). But accumulating evidence indicates TAK1/p38 signals generate pro-survival effects in bone and cartilage synthesizing cells (Gunnell et al., 2010; Shim et al., 2009; Yoon et al., 2005). In cartilage, pro-survival p38 signals appear to be mediated by CREB- and ATF2-dependent expression of Bcl-2 (Ma et al., 2007). In bone, we find diminished Bcl-2 expression and low CREB and ATF2 phosphorylation are similarly associated with defective p38 signaling. Importantly, these are all downstream of Smad4 ablation. Thus, we propose that the central mediator in this signaling network is Smad4, not TAK1/p38.

To conclude, Smad4 in Osx1+ osteoblasts regulates collagen synthesis and osteoblast survival, each of which are at least partly modulated by a BMP signaling network involving Smad4, R-Smads, and TAK1/p38. Moreover, Smad4 is required, indirectly via suppression of apoptosis, to maintain adequate levels of β-catenin required for bone anabolic responses to cWnt signaling.

4.6 BIBLIOGRAPHY

Bain, G., Muller, T., Wang, X., and Papkoff, J. (2003). Activated b-catenin induces osteoblast differentiation of C3H10T1/2 cells and participates in BMP2 mediated signal transduction. Biochem Biophys Res Com 301, 84-91.

Balemans, W., Patel, N., Ebeling, M., Van Hul, E., Wuyts, W., Lacza, C., Dioszegi, M., Dikkers, F.G., Hildering, P., Willems, P.J., Verheij, J.B.G.M., Lindpaintner, K., Vickery, B., Foernzler, D., and Van Hul, W. (2002). Identification of a 52 kb deletion downstream of the SOST gene in patients with van Buchem disease. Journal of medical genetics 39, 91-97.

Bandyopadhyay, A., Tsuji, K., Cox, K., Harfe, B.D., Rosen, V., and Tabin, C.J. (2006). Genetic analysis of the roles of BMP2, BMP4, and BMP7 in limb patterning and skeletogenesis. PLoS Genet 2, e216.

Batlle, E., Henderson, J.T., Beghtel, H., van den Born, M.M., Sancho, E., Huls, G., Meeldijk, J., Robertson, J., van de, W.M., Pawson, T., and Clevers, H. (2002). b-catenin and TCF mediate cell positioning in the intestinal epithelium by controlling the expression of EphB/ephrinB. Cell 111, 251-263.

Boyden, L.M., Mao, J., Belsky, J., Mitzner, L., Farhi, A., Mitnick, M.A., Wu, D., Insogna, K., and Lifton, R.P. (2002). High bone density due to a mutation in LDL-receptor-related protein 5. N Eng J Med 346, 1513-1521.

Brancolini, C., Lazarevic, D., Rodriguez, J., and Schneider, C. (1997). Dismantling cell-cell contacts during apoptosis is coupled to a caspase-dependent proteolytic cleavage of beta-catenin. J Cell Biol 139, 759-771.

Brunkow, M.E., Gardner, J.C., Van Ness, J., Paeper, B.W., Kovacevich, B.R., Proll, S., Skonier, J.E., Zhao, L., Sabo, P.J., Fu, Y., Alisch, R.S., Gillett, L., Colbert, T., Tacconi, P., Galas, D., Hamersma, H., Beighton, P., and Mulligan, J. (2001). Bone dysplasia sclerosteosis results from loss of the SOST gene product, a novel cystine knot-containing protein. Am. J Hum Genet 68, 577-589.

Camilleri, S., and McDonald, F. (2006). Runx2 and dental development. Eur J Oral Sci 114, 361-373.

Chen, Y., Whetstone, H.C., Youn, A., Nadesan, P., Chow, E.C., Lin, A.C., and Alman, B.A. (2007). b-catenin signaling pathway is crucial for bone morphogenetic protein 2 to induce new bone formation. J Biol Chem 282, 526-533.

Chung, D.J., Castro, C.H., Watkins, M., Stains, J.P., Chung, M.Y., Szejnfeld, V.L., Willecke, K., Theis, M., and Civitelli, R. (2006). Low peak bone mass and attenuated anabolic response to parathyroid hormone in mice with an osteoblast-specific deletion of connexin43. J Cell Sci 119, 4187-4198.

Cong, F., Schweizer, L., Chamorro, M., and Varmus, H. (2003). Requirement for a nuclear function of beta-catenin in Wnt signaling. Mol.Cell Biol. 23, 8462-8470.

Cong, F., and Varmus, H. (2004). Nuclear-cytoplasmic shuttling of Axin regulates subcellular localization of beta-catenin. Proc.Natl.Acad.Sci.U.S.A 101, 2882-2887.

Cui, Y., Niziolek, P.J., Macdonald, B.T., Zylstra, C.R., Alenina, N., Robinson, D.R., Zhong, Z., Matthes, S., Jacobsen, C.M., Conlon, R.A., Brommage, R., Liu, Q., Mseeh, F., Powell, D.R., Yang, Q.M., Zambrowicz, B., Gerrits, H., Gossen, J.A., He, X., Bader, M., Williams, B.O., Warman, M.L., and Robling, A.G. (2011). Lrp5 functions in bone to regulate bone mass. Nat Med 17, 684-691.

Dayan, D., Hiss, Y., Hirshberg, A., Bubis, J.J., and Wolman, M. (1989). Are the polarization colors of picrosirius red-stained collagen determined only by the diameter of the fibers? Histochemistry 93, 27-29.

Devlin, R.D., Du, Z., Pereira, R.C., Kimble, R.B., Economides, A.N., Jorgetti, V., and Canalis, E. (2003). Skeletal overexpression of noggin results in osteopenia and reduced bone formation. Endocrinology 144, 1972-1978.

Diarra, D., Stolina, M., Polzer, K., Zwerina, J., Ominsky, M.S., Dwyer, D., Korb, A., Smolen, J., Hoffmann, M., Scheinecker, C., van der, H.D., Landewe, R., Lacey, D., Richards, W.G., and Schett, G. (2007). Dickkopf-1 is a master regulator of joint remodeling. Nat Med 13, 156-163.

Ellies, D.L., Viviano, B., McCarthy, J., Rey, J.P., Itasaki, N., Saunders, S., and Krumlauf, R. (2006). Bone density ligand, Sclerostin, directly interacts with LRP5 but not LRP5G171V to modulate Wnt activity. J Bone Miner Res 21, 1738-1749.

Fukuta, Y., Totsuka, M., Takeda, Y., Yoshida, Y., Niitsu, J., and Yamamoto, H. (2001). Histological and analytical studies of a tooth in a patient with cleidocranial dysostosis. J Oral Sci 43, 85-89.

Gazzerro, E., Pereira, R.C., Jorgetti, V., Olson, S., Economides, A.N., and Canalis, E. (2005). Skeletal overexpression of gremlin impairs bone formation and causes osteopenia. Endocrinology 146, 655-665.

Gong, Y., Slee, R.B., Fukai, N., Rawadi, G., Roman-Roman, S., Reginato, A.M., Wang, H., Cundy, T., Glorieux, F.H., Lev, D., Zacharin, M., Oexle, K., Marcelino, J., Suwairi, W., Heeger, S., Sabatakos, G., Apte, S., Adkins, W.N., Allgrove, J., Arslan-Kirchner, M., Batch, J.A., Beighton, P., Black, G.C., Boles, R.G., Boon, L.M., Borrone, C., Brunner, H.G., Carle, G.F., Dallapiccola, B., De Paepe, A., Floege, B., Halfhide, M.L., Hall, B., Hennekam, R.C., Hirose, T., Jans, A., Juppner, H., Kim, C.A., Keppler-Noreuil, K., Kohlschuetter, A., LaCombe, D., Lambert, M., Lemyre, E., Letteboer, T., Peltonen, L., Ramesar, R.S., Romanengo, M., Somer, H., Steichen-Gersdorf, E., Steinmann, B., Sullivan, B., Superti-Furga, A., Swoboda, W., van den Boogaard, M.J., Van Hul, W., Vikkula, M., Votruba, M., Zabel, B., Garcia, T., Baron, R., Olsen, B.R., and Warman, M.L. (2001). LDL receptor-related protein 5 (LRP5) affects bone accrual and eye development. Cell 107, 513-523.

Gong, Y., Vikkula, M., Boon, L., Liu, J., Beighton, P., Ramesar, R., Peltonen, L., Somer, H., Hirose, T., Dallapiccola, B., De Paepe, A., Swoboda, W., Zabel, B., Superti-Furga, A., Steinmann, B., Brunner, H.G., Jans, A., Boles, R.G., Adkins, W., van den Boogaard, M.J., Olsen, B.R., and Warman, M.L. (1996). Osteoporosis-pseudoglioma syndrome, a disorder affecting skeletal strength and vision, is assigned to chromosome region 11q12-13. Am.J.Hum.Genet. 59, 146-151.

Greenblatt, M.B., Shim, J.H., Zou, W., Sitara, D., Schweitzer, M., Hu, D., Lotinun, S., Sano, Y., Baron, R., Park, J.M., Arthur, S., Xie, M., Schneider, M.D., Zhai, B., Gygi, S., Davis, R., and Glimcher, L.H. The p38 MAPK pathway is essential for skeletogenesis and bone homeostasis in mice. J Clin Invest 120, 2457-2473.

Gunnell, L.M., Jonason, J.H., Loiselle, A.E., Kohn, A., Schwarz, E.M., Hilton, M.J., and O'Keefe, R.J. (2010). TAK1 regulates cartilage and joint development via the MAPK and BMP signaling pathways. J Bone Miner Res 25, 1784-1797.

Hill, T.P., Spater, D., Taketo, M.M., Birchmeier, W., and Hartmann, C. (2005). Canonical Wnt/b-catenin signaling prevents osteoblasts from differentiating into chondrocytes. Dev Cell 8, 727-738.

Huang, H., Song, T.J., Li, X., Hu, L., He, Q., Liu, M., Lane, M.D., and Tang, Q.Q. (2009). BMP signaling pathway is required for commitment of C3H10T1/2 pluripotent stem cells to the adipocyte lineage. Proc Natl Acad Sci U S A 106, 12670-12675.

Hunter, I., McGregor, D., and Robins, S.P. (2001). Caspase-dependent cleavage of cadherins and catenins during osteoblast apoptosis. J Bone Miner Res 16, 466-477.

Kamiya, N., Kobayashi, T., Mochida, Y., Yu, P.B., Yamauchi, M., Kronenberg, H.M., and Mishina, Y. Wnt inhibitors Dkk1 and Sost are downstream targets of BMP signaling through the type IA receptor (BMPRIA) in osteoblasts. J Bone Miner Res 25, 200-210.

Kamiya, N., Ye, L., Kobayashi, T., Lucas, D.J., Mochida, Y., Yamauchi, M., Kronenberg, H.M., Feng, J.Q., and Mishina, Y. (2008a). Disruption of BMP signaling in osteoblasts through type IA receptor (BMPRIA) increases bone mass. J Bone Miner Res 23, 2007-2017.

Kamiya, N., Ye, L., Kobayashi, T., Mochida, Y., Yamauchi, M., Kronenberg, H.M., Feng, J.Q., and Mishina, Y. (2008b). BMP signaling negatively regulates bone mass through sclerostin by inhibiting the canonical Wnt pathway. Development 135, 3801-3811.

Kang, Q., Sun, M.H., Cheng, H., Peng, Y., Montag, A.G., Deyrup, A.T., Jiang, W., Luu, H.H., Luo, J., Szatkowski, J.P., Vanichakarn, P., Park, J.Y., Li, Y., Haydon, R.C., and He, T.C. (2004). Characterization of the distinct orthotopic bone-forming activity of 14 BMPs using recombinant adenovirus-mediated gene delivery. Gene Ther. 11, 1312-1320.

Kessler, T., and Muller, H.A. (2009). Cleavage of Armadillo/beta-catenin by the caspase DrICE in Drosophila apoptotic epithelial cells. BMC Dev Biol 9, 15.

Little, R.D., Carulli, J.P., Del Mastro, R.G., Dupuis, J., Osborne, M., Folz, C., Manning, S.P., Swain, P.M., Zhao, S.C., Eustace, B., Lappe, M.M., Spitzer, L., Zweier, S., Braunschweiger, K.,

Benchekroun, Y., Hu, X., Adair, R., Chee, L., FitzGerald, M.G., Tulig, C., Caruso, A., Tzellas, N., Bawa, A., Franklin, B., McGuire, S., Nogues, X., Gong, G., Allen, K.M., Anisowicz, A., Morales, A.J., Lomedico, P.T., Recker, S.M., Van Eerdewegh, P., Recker, R.R., and Johnson, M.L. (2002). A mutation in the LDL receptor-related protein 5 gene results in the autosomal dominant high-bone-mass trait. Am. J Hum Genet 70, 11-19.

Loots, G.G., Kneissel, M., Keller, H., Baptist, M., Chang, J., Collette, N.M., Ovcharenko, D., Plajzer-Frick, I., and Rubin, E.M. (2005). Genomic deletion of a long-range bone enhancer misregulates sclerostin in Van Buchem disease. Genome Res 15, 928-935.

Ma, Q., Li, X., Vale-Cruz, D., Brown, M.L., Beier, F., and LuValle, P. (2007). Activating transcription factor 2 controls Bcl-2 promoter activity in growth plate chondrocytes. J Cell Biochem 101, 477-487.

Maes, C., Kobayashi, T., Selig, M.K., Torrekens, S., Roth, S.I., Mackem, S., Carmeliet, G., and Kronenberg, H.M. Osteoblast precursors, but not mature osteoblasts, move into developing and fractured bones along with invading blood vessels. Dev Cell 19, 329-344.

Mishina, Y., Starbuck, M.W., Gentile, M.A., Fukuda, T., Kasparcova, V., Seedor, J.G., Hanks, M.C., Amling, M., Pinero, G.J., Harada, S., and Behringer, R.R. (2004). Bone morphogenetic protein type IA receptor signaling regulates postnatal osteoblast function and bone remodeling. J Biol Chem 279, 27560-27566.

Miyake, Z., Takekawa, M., Ge, Q., and Saito, H. (2007). Activation of MTK1/MEKK4 by GADD45 through induced N-C dissociation and dimerization-mediated trans autophosphorylation of the MTK1 kinase domain. Mol Cell Biol 27, 2765-2776.

Moustakas, A., and Heldin, C.H. (2009). The regulation of TGFbeta signal transduction. Development 136, 3699-3714.

Otto, F., Thornell, A.P., Crompton, T., Denzel, A., Gilmour, K.C., Rosewell, I.R., Stamp, G.W., Beddington, R.S., Mundlos, S., Olsen, B.R., Selby, P.B., and Owen, M.J. (1997). Cbfa1, a candidate gene for cleidocranial dysplasia syndrome, is essential for osteoblast differentiation and bone development [see comments]. Cell 89, 765-771.

Rachner, T.D., Khosla, S., and Hofbauer, L.C. Osteoporosis: now and the future. Lancet 377, 1276-1287.

Rawadi, G., Vayssiere, B., Dunn, F., Baron, R., and Roman-Roman, S. (2003). BMP-2 controls alkaline phosphatase expression and osteoblast mineralization by a Wnt autocrine loop. J Bone Miner Res 18, 1842-1853.

Retting, K.N., Song, B., Yoon, B.S., and Lyons, K.M. (2009). BMP canonical Smad signaling through Smad1 and Smad5 is required for endochondral bone formation. Development 136, 1093-1104.

Rodda, S.J., and McMahon, A.P. (2006). Distinct roles for Hedgehog and canonical Wnt signaling in specification, differentiation and maintenance of osteoblast progenitors. Development 133, 3231-3244.

Salazar, V.S., Mbalaviele, G., and Civitelli, R. (2008). The pro-osteogenic action of b-catenin requires interaction with BMP signaling, but not Tcf/Lef transcriptional activity. J Cell Biochem 104, 942-952.

Shim, J.H., Greenblatt, M.B., Xie, M., Schneider, M.D., Zou, W., Zhai, B., Gygi, S., and Glimcher, L.H. (2009). TAK1 is an essential regulator of BMP signalling in cartilage. EMBO J 28, 2028-2041.

Soriano, P. (1999). Generalized lacZ expression with the ROSA26 Cre reporter strain. Nat.Genet. 21, 70-71.

Steinhusen, U., Badock, V., Bauer, A., Behrens, J., Wittman-Liebold, B., Dorken, B., and Bommert, K. (2000). Apoptosis-induced cleavage of beta-catenin by caspase-3 results in proteolytic fragments with reduced transactivation potential. J Biol Chem 275, 16345-16353.

Takekawa, M., Tatebayashi, K., Itoh, F., Adachi, M., Imai, K., and Saito, H. (2002). Smad-dependent GADD45beta expression mediates delayed activation of p38 MAP kinase by TGF-beta. EMBO J 21, 6473-6482.

Tan, X., Weng, T., Zhang, J., Wang, J., Li, W., Wan, H., Lan, Y., Cheng, X., Hou, N., Liu, H., Ding, J., Lin, F., Yang, R., Gao, X., Chen, D., and Yang, X. (2007). Smad4 is required for maintaining normal murine postnatal bone homeostasis. J Cell Sci 120, 2162-2170.

Tetsu, O., and McCormick, F. (1999). b-catenin regulates expression of cyclin D1 in colon carcinoma cells. Nature 398, 422-426.

Trackman, P.C. (2005). Diverse biological functions of extracellular collagen processing enzymes. J Cell Biochem 96, 927-937.

Truett, G.E., Heeger, P., Mynatt, R.L., Truett, A.A., Walker, J.A., and Warman, M.L. (2000). Preparation of PCR-quality mouse genomic DNA with hot sodium hydroxide and tris (HotSHOT). Biotechniques 29, 52, 54.

van der Heide, L.P., van Dinther, M., Moustakas, A., and ten Dijke, P. (2011). TGFbeta activates mitogen- and stress-activated protein kinase-1 (MSK1) to attenuate cell death. J Biol Chem 286, 5003-5011.

Wagner, E.F., and Nebreda, A.R. (2009). Signal integration by JNK and p38 MAPK pathways in cancer development. Nat Rev Cancer 9, 537-549.

Wang, Y.H., Liu, Y., Buhl, K., and Rowe, D.W. (2005). Comparison of the action of transient and continuous PTH on primary osteoblast cultures expressing differentiation stage-specific GFP. J Bone Miner Res 20, 5-14.

Watkins, M., Grimston, S.K., Norris, J.Y., Guillotin, B., Shaw, A., Beniash, E., and Civitelli, R. (2011). Osteoblast connexin43 modulates skeletal architecture by regulating both arms of bone remodeling. Mol Biol Cell 22, 1240-1251.

Winkler, D.G., Sutherland, M.S., Ojala, E., Turcott, E., Geoghegan, J.C., Shpektor, D., Skonier, J.E., Yu, C., and Latham, J.A. (2005). Sclerostin inhibition of Wnt-3a-induced C3H10T1/2 cell differentiation is indirect and mediated by bone morphogenetic proteins. J Biol Chem 280, 2498-2502.

Wozney, J.M., Rosen, V., Celeste, A.J., Mitsock, L.M., Whitters, M.J., Kriz, R.W., Hewick, R.M., and Wang, E.A. (1988). Novel regulators of bone formation: molecular clones and activities. Science 242, 1528-1534.

Xu, X., Han, J., Ito, Y., Bringas, P., Jr., Deng, C., and Chai, Y. (2008). Ectodermal Smad4 and p38 MAPK are functionally redundant in mediating TGF-beta/BMP signaling during tooth and palate development. Dev Cell 15, 322-329.

Yadav, V.K., Ryu, J.H., Suda, N., Tanaka, K.F., Gingrich, J.A., Schutz, G., Glorieux, F.H., Chiang, C.Y., Zajac, J.D., Insogna, K.L., Mann, J.J., Hen, R., Ducy, P., and Karsenty, G. (2008). Lrp5 controls bone formation by inhibiting serotonin synthesis in the duodenum. Cell 135, 825-837.

Yamamoto, H., Sakae, T., and Davies, J.E. (1989). Cleidocranial dysplasia: a light microscope, electron microscope, and crystallographic study. Oral Surg Oral Med Oral Pathol 68, 195-200.

Yang, X., Li, C., Herrera, P.L., and Deng, C.X. (2002). Generation of Smad4/Dpc4 conditional knockout mice. Genesis 32, 80-81.

Yoo, J., Ghiassi, M., Jirmanova, L., Balliet, A.G., Hoffman, B., Fornace, A.J., Jr., Liebermann, D.A., Bottinger, E.P., and Roberts, A.B. (2003). Transforming growth factor-beta-induced apoptosis is mediated by Smad-dependent expression of GADD45b through p38 activation. J Biol Chem 278, 43001-43007.

Yoon, B.S., Ovchinnikov, D.A., Yoshii, I., Mishina, Y., Behringer, R.R., and Lyons, K.M. (2005). Bmpr1a and Bmpr1b have overlapping functions and are essential for chondrogenesis in vivo. Proc Natl Acad Sci USA 102, 5062-5067.

Zhang, J., Tan, X., Li, W., Wang, Y., Wang, J., Cheng, X., and Yang, X. (2005). Smad4 is required for the normal organization of the cartilage growth plate. Dev Biol 284, 311-322.

Zhang, Y.E. (2009). Non-Smad pathways in TGF-b signaling. Cell Res 19, 128-139.

4.7 Figure Legends

Figure 4.1 Progressive Skeletal Phenotype in Smad4$^{F/F}$; Osx1-Cre Mice

(A) Eosin and LacZ stain on histologic sections of the femur (40X)

(B) Immunoblot on marrow-free bone tissue

(C-E) Alizarin red and alcian blue skeletal preparations. Shown to scale, bar indicates 1mm.

(F-G) Contract radiograph, littermates

(H) Malocclusion and enamel hypoplasia of the inscisors

(I-L) 3-D microCT (μCT) reconstructions of skeletal structures in 4 week old littermates. Not shown to scale, bars indicate 5 mm.

(M) Contact radiograph, 8 week old Smad4$^{\Delta/\Delta}$ mouse.

Figure 4.2 Abnormal Architecture and Quality of Long Bones in Smad4$^{F/F}$; Osx1-Cre Mice

(A) 3-D μCT reconstructions of tibias in 4 week-old littermates, shown to scale.

(B-C) Safranin O staining on the tibia. Top, 10X. Bottom, 15X.

(D-E) Goldner trichrome stain on the tibia. Top, 4X. Bottom, 40X.

(F-I) Quantitative μCT analysis of trabecular bone at the proximal tibia

(J-K) Quantitative μCT analysis of cortical bone in the mid-diaphysis

(L-M) Mineral content per unit volume of trabecular bone (L) or cortical bone (M). Note different y-axis. All μCT data are expressed as Mean±STD. p*<0.05 and p$^{\#}$<0.02 vs. Smad4$^{F/F}$.

Figure 4.3 Non-cell autonomous regulation of osteoclastogenesis by Smad4 in Osx1+ cells is not explained by the RANK ligand to Osteoprotegerin ratio.

(A) TRAP stain on mid-sagittal sections of the tibia from 4 week old mice. Left, ventral, 10X. Center, 4X. Right, dorsal, 10X.

(B) MCSF-primed bone marrow macrophages (MΦ), cultured in the presence of RANKL and MCSF, were stained for TRAP to monitor osteoclastogenesis. Genotype of donor mouse is specified.

(C) Quantitation of Figure S2B, osteoclasts derived from 2500 bone marrow macrophages.

(D) MCSF-primed bone marrow macrophages (MΦ) were cultured with equal numbers of bone marrow osteoblasts (Ob), vitamin D3, and dexamethasone, then stained for TRAP to monitor osteoclastogenesis. Genotype of donor mouse for macrophages and osteoblasts is specified.

(E) Quantitation of Figure S2D, osteoclasts derived from 47,000 macrophages.

(F) QPCR on marrow-free bone tissue

(G) Immunoblot on marrow-free bone tissue

Numerical data are expressed as Mean±STD. $p^{*}<0.05$ and $p^{\#}<0.01$ vs. $Smad4^{F/F}$.

Figure 4.4 Smad4 is Required in Osx1+ Cells for Expression of Collagen-Processing Enzymes

(A-C) QPCR on marrow-free bone tissue. (A) Osteoblast differentiation markers. (B) Non-collagen extracellular matrix components. (C) Collagen synthesizing enzymes. $p^{*}<0.05$ vs. $Smad4^{F/F}$.

(D) Picrosirius red stain and polarized light microscopy on mid-sagittal sections of the tibia. Top, 4X. Middle, 20X, Bottom, 40X.

Figure 4.5 Smad4 Integrates with p38 MAPK to Regulate Lysyl Oxidase and Bcl-2

(A, D-I) Immunoblot on marrow-free bone tissue

(B-C) QPCR (B) and immunoblot (C) analysis on MC3T3 osteoblast cultures treated with BMP2 (200 ng/ml) ± p38 inhibitor SB203580 (10 μM).

(J) QPCR on marrow-free bone. Expressed as Mean±STD. $p^{*}<0.05$ vs. $Smad4^{F/F}$.

Figure 4.6 Loss of Smad4 Abrogates Osteoanabolic Responses to Canonical Wnt Signaling

(A) Calvaria cultured ex vivo with Dkk1-neutralizing antibody. (Ai-iii) Fluorescence microscopy (20X). New tissue labeled with xylenol orange. (Aiv) Goldner Trichrome showing Aiii in brightfield (20X). New osteoid (pink), pre-existing bone (blue).

(B) Effect of αDkk1 therapy on mineral apposition rate on the endocortical surface of the proximal tibia (20 mg/kg/day, i.p. 3 times/week, 4 weeks). $p^{*}<0.05$ vs. $Smad4^{F/F}$.

(C) Effect of αDkk1 therapy on bone resorption, measure by serum RatLaps elisa.

(D) Effect of αDkk1 therapy on trabecular bone mass at the proximal tibia of male mice, assessed pre and post therapy by in vivo μCT, and compared to normal growth in untreated 3mo old mice. Data are expressed as Mean±STD. P values compare one genotype pre and post-treatment.

(E) 3-D reconstructions of the proximal tibia by μCT illustrating representative changes in bone architecture in one $Smad4^{F/F}$ mouse given αDkk1 therapy

(F) Effect of αDkk1 therapy on trabecular bone mass at the proximal tibia of female mice, assessed pre/post treatment by in vivo μCT. Data are expressed as Mean±STD. P values compare one genotype pre and post-treatment.

(G-M) Histologic sections of tibias from $Smad4^{F/F}$ (top) or $Smad4^{\Delta/\Delta}$ (bottom) mice after 4-weeks αDkk1. (G, K) Calcein, 4X. (H, L) Calcein, 20X, boxed areas in G and K. Blue arrowhead, endocortical surface. Black arrowhead, periosteum. (L) Note lack of double labels in $Smad4^{\Delta/\Delta}$. (I, M) Görömi Trichrome (20X) showing the persistence of sporadic osteomalacia after treatment.

(N) Alizarin red stain on calcium deposits in osteoblast cultures of primary bone marrow stromal cells

(O) Alizarin red counterstained for alkaline phosphatase activity (4X)

Figure 4.7 Smad4 Protects Osteoblasts from Apoptosis and Deactivating Cleavage of β-catenin

(A) QPCR on marrow-free bone tissue. Expressed as Mean±STD. *p<0.05, *p<0.01 vs. $Smad4^{F/F}$

(B-C) Immunoblot analysis of Wnt signaling in marrow-free bone tissue

(D) Schematic of β-catenin showing relative positions of antibody epitopes and Caspase-3 cleavage sites

(E) Immunoblot analysis of Wnt signaling in marrow-free bone tissue

(F) QPCR on marrow-free bone tissue. Expressed as Mean±STD. *$p<0.05$, vs. $Smad4^{F/F}$

(G) Immunofluorescence for TUNEL+ cells in the tibia. Open arrows (endosteum) and closed arrows (periosteum) in 40X magnified images, shown to scale.

(H) Anabolic signaling by Smad4 and Canonical Wnt Pathways in Osteoblasts

4.8 FIGURES

Figure 4.1

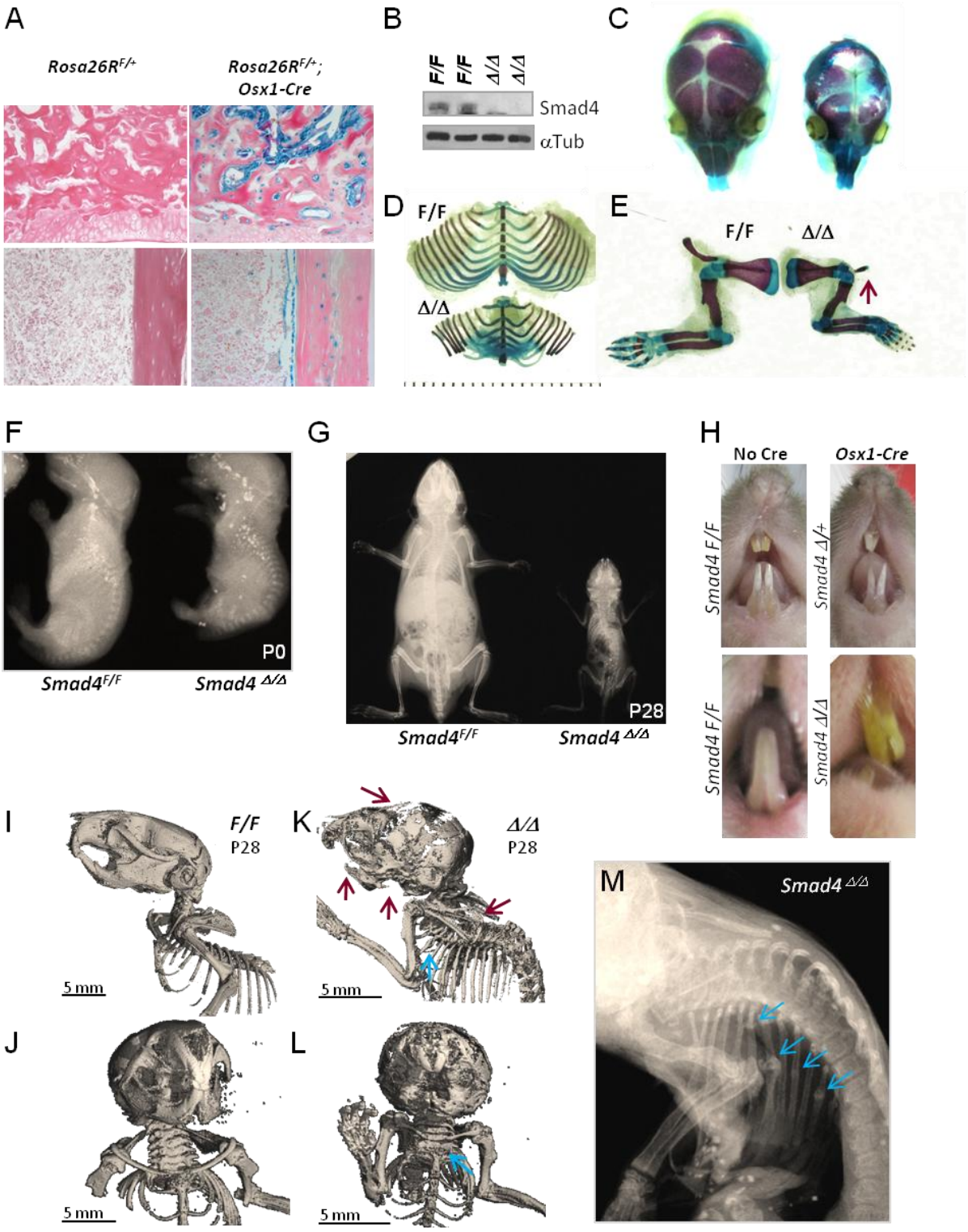

Figure 4.2

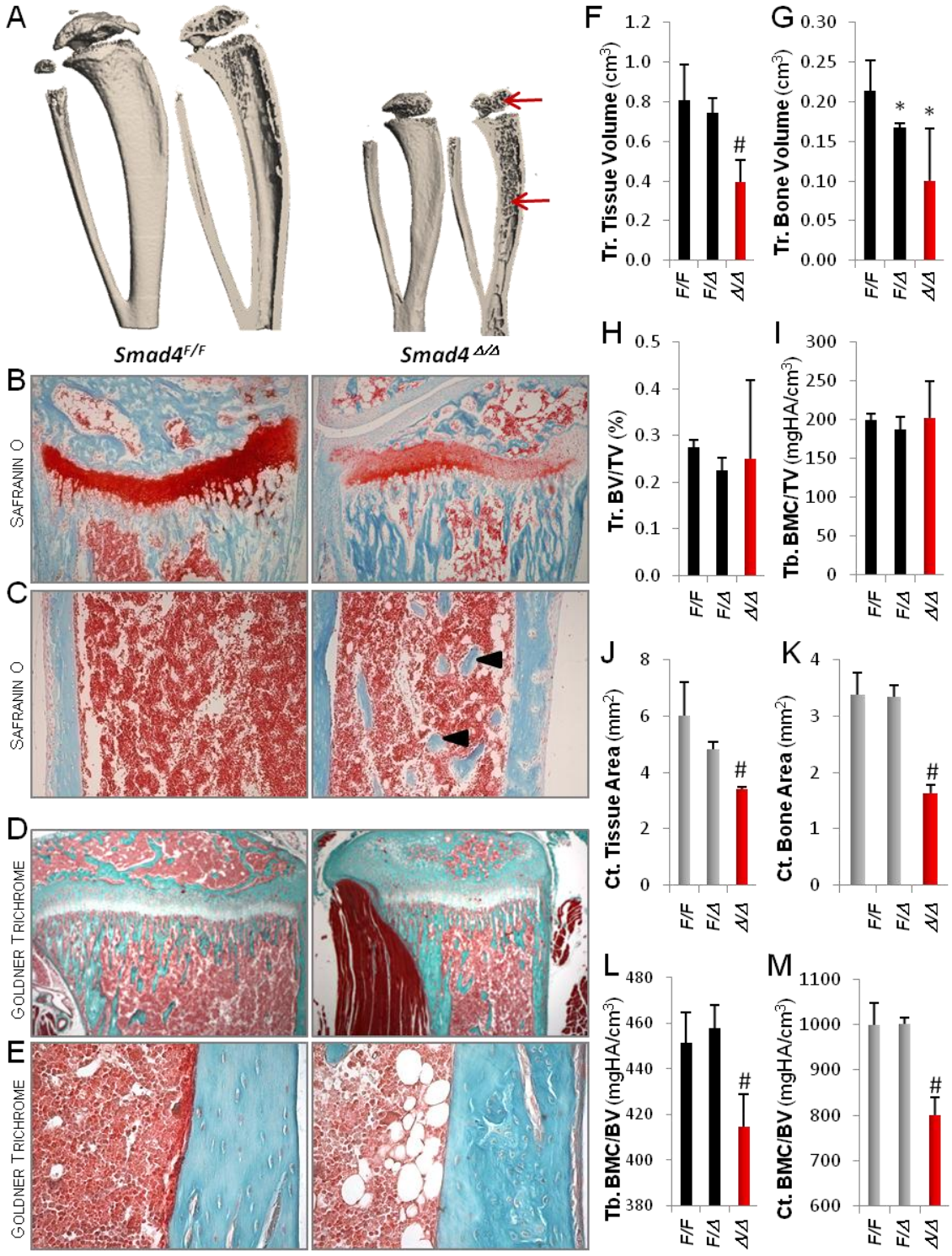
A
Smad4F/F
Smad4Δ/Δ
B
SAFRANIN O
C
SAFRANIN O
D
GOLDNER TRICHROME
E
GOLDNER TRICHROME
F
Tr. Tissue Volume (cm3)
G
Tr. Bone Volume (cm3)
H
Tr. BV/TV (%)
I
Tb. BMC/TV (mgHA/cm3)
J
Ct. Tissue Area (mm2)
K
Ct. Bone Area (mm2)
L
Tb. BMC/BV (mgHA/cm3)
M
Ct. BMC/BV (mgHA/cm3)
F/F
F/Δ
Δ/Δ

Figure 4.2 (Supplemental)

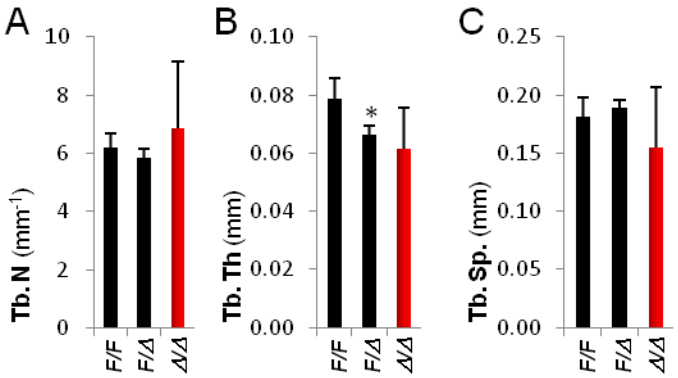

Figure 4.3

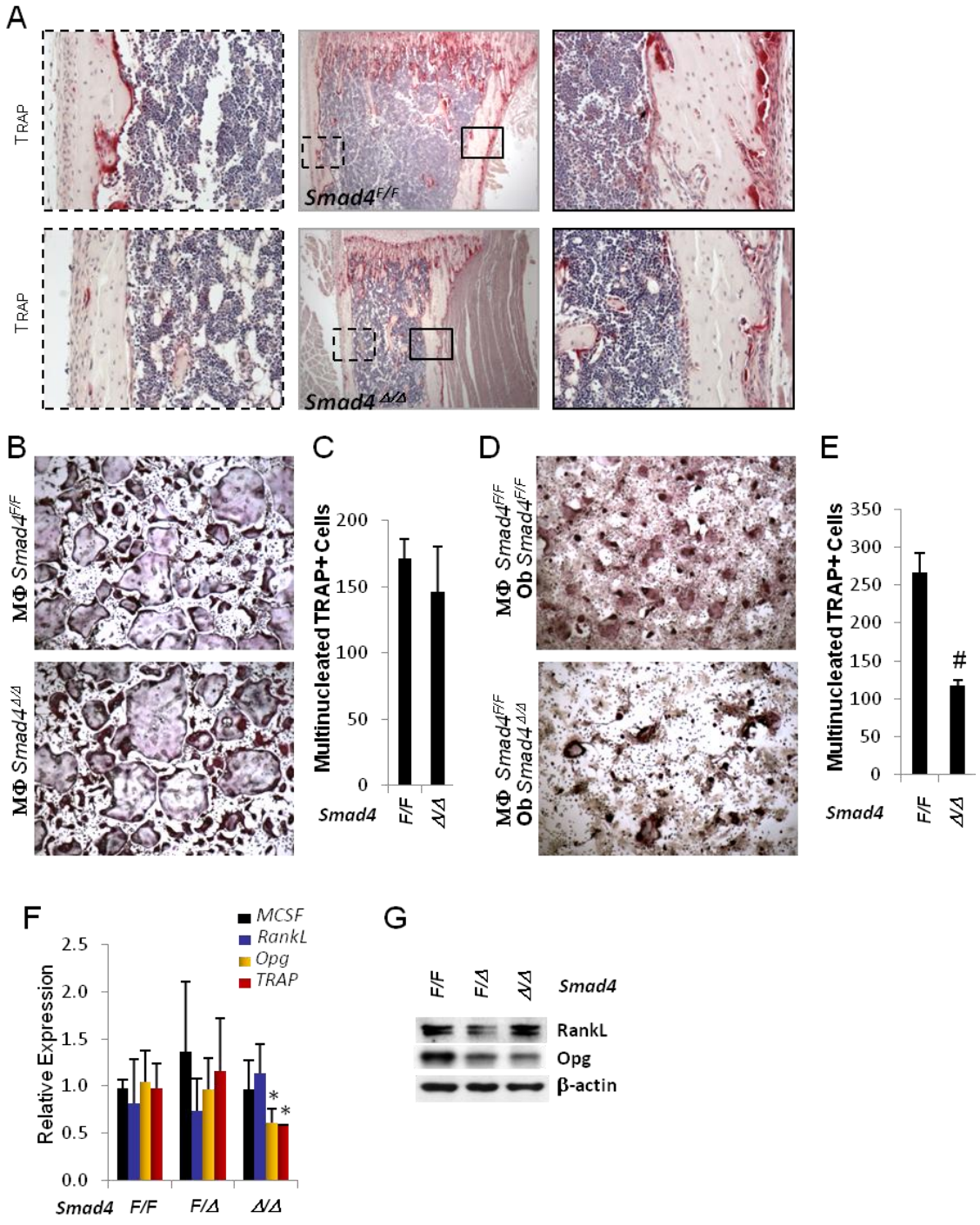
A
TRAP
TRAP
Smad4F/F
Smad4Δ/Δ
B
MΦ Smad4F/F
MΦ Smad4Δ/Δ
C
Multinucleated TRAP+ Cells
200
150
100
50
0
Smad4
F/F
Δ/Δ
D
MΦ Smad4F/F
Ob Smad4F/F
MΦ Smad4F/F
Ob Smad4Δ/Δ
E
Multinucleated TRAP+ Cells
350
300
250
200
150
100
50
0
#
Smad4
F/F
Δ/Δ
F
MCSF
RankL
Opg
TRAP
Relative Expression
2.5
2.0
1.5
1.0
0.5
0.0
*
*
Smad4
F/F
F/Δ
Δ/Δ
G
F/F
F/Δ
Δ/Δ
Smad4
RankL
Opg
β-actin

Figure 4.4

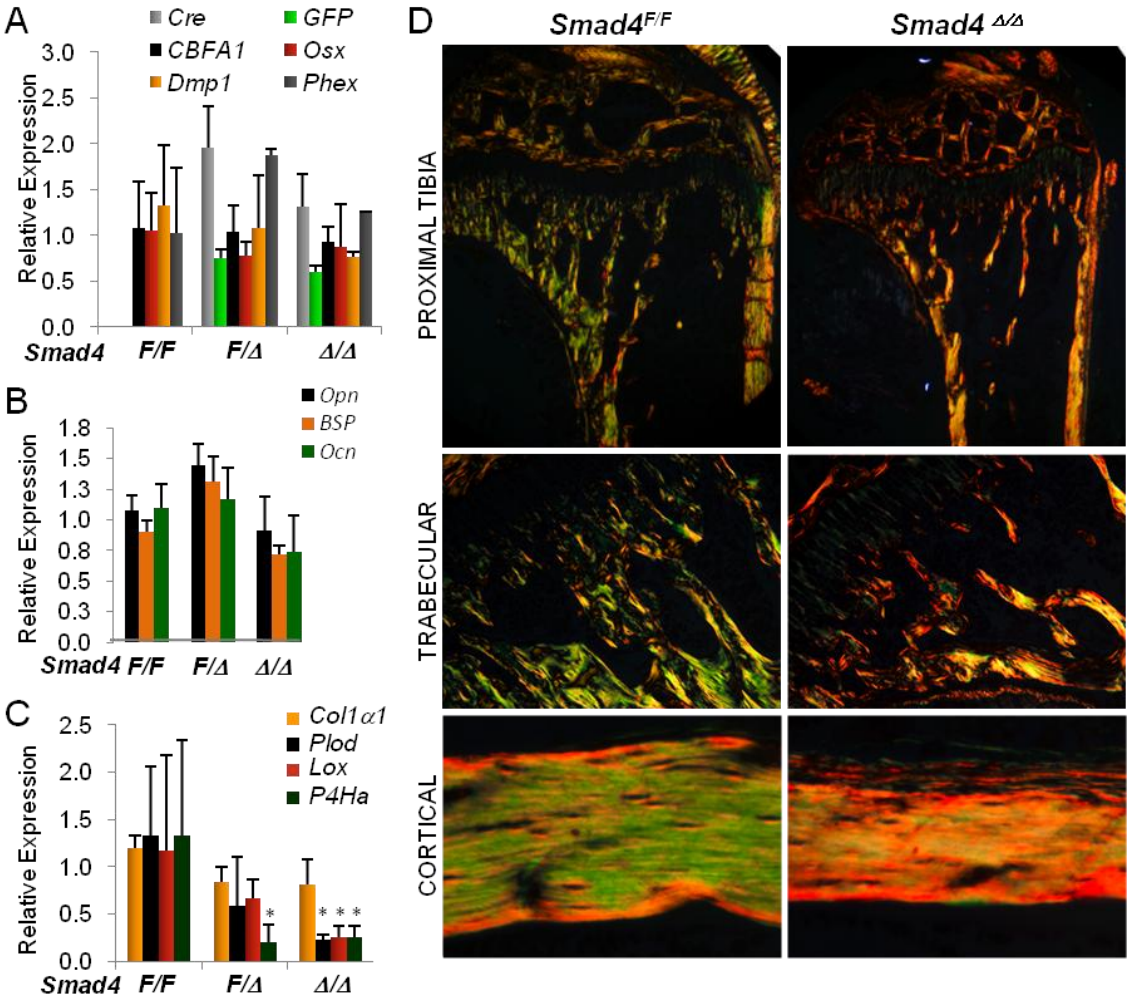
A
Cre
GFP
CBFA1
Osx
Dmp1
Phex
Relative Expression
3.0
2.5
2.0
1.5
1.0
0.5
0.0
Smad4 F/F F/Δ Δ/Δ
B
Opn
BSP
Ocn
Relative Expression
1.8
1.5
1.3
1.0
0.8
0.5
0.3
0.0
Smad4 F/F F/Δ Δ/Δ
C
Col1α1
Plod
Lox
P4Ha
Relative Expression
2.5
2.0
1.5
1.0
0.5
0.0
* * * *
Smad4 F/F F/Δ Δ/Δ
D
Smad4F/F
Smad4 Δ/Δ
PROXIMAL TIBIA
TRABECULAR
CORTICAL

Figure 4.5

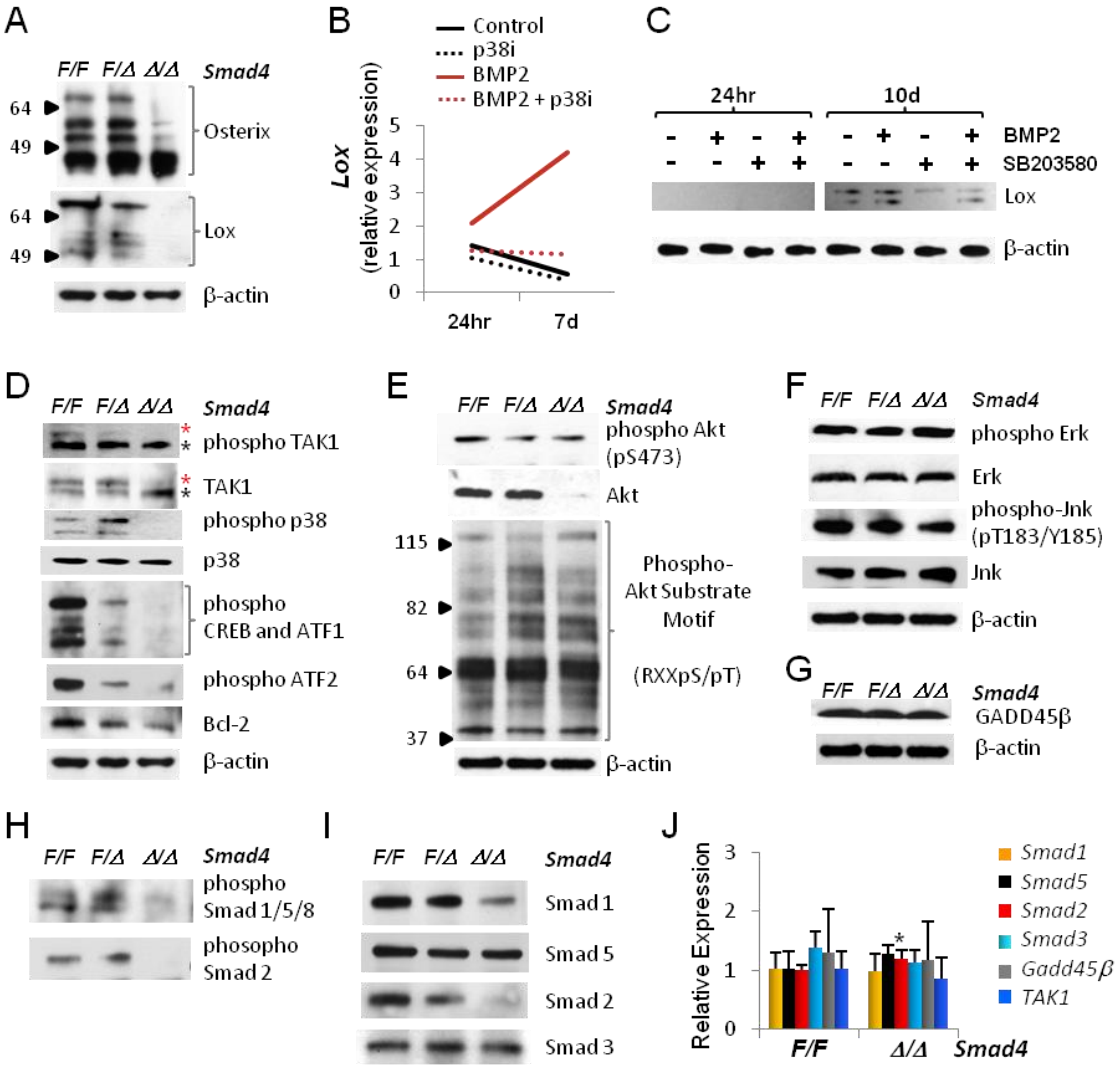
A
F/F F/Δ Δ/Δ
Smad4
64
49
Osterix
64
49
Lox
β-actin
B
Control
p38i
BMP2
BMP2 + p38i
Lox (relative expression)
5
4
3
2
1
0
24hr
7d
C
24hr
10d
- + - + - + - +
- - + + - - + +
BMP2
SB203580
Lox
β-actin
D
F/F F/Δ Δ/Δ
Smad4
phospho TAK1
TAK1
phospho p38
p38
phospho CREB and ATF1
phospho ATF2
Bcl-2
β-actin
E
F/F F/Δ Δ/Δ
Smad4
phospho Akt (pS473)
Akt
115
82
64
37
Phospho-Akt Substrate Motif (RXXpS/pT)
β-actin
F
F/F F/Δ Δ/Δ
Smad4
phospho Erk
Erk
phospho-Jnk (pT183/Y185)
Jnk
β-actin
G
F/F F/Δ Δ/Δ
Smad4
GADD45β
β-actin
H
F/F F/Δ Δ/Δ
Smad4
phospho Smad 1/5/8
phosopho Smad 2
I
F/F F/Δ Δ/Δ
Smad4
Smad 1
Smad 5
Smad 2
Smad 3
J
Relative Expression
3
2
1
0
Smad1
Smad5
Smad2
Smad3
Gadd45β
TAK1
F/F
Δ/Δ
Smad4

Figure 4.6

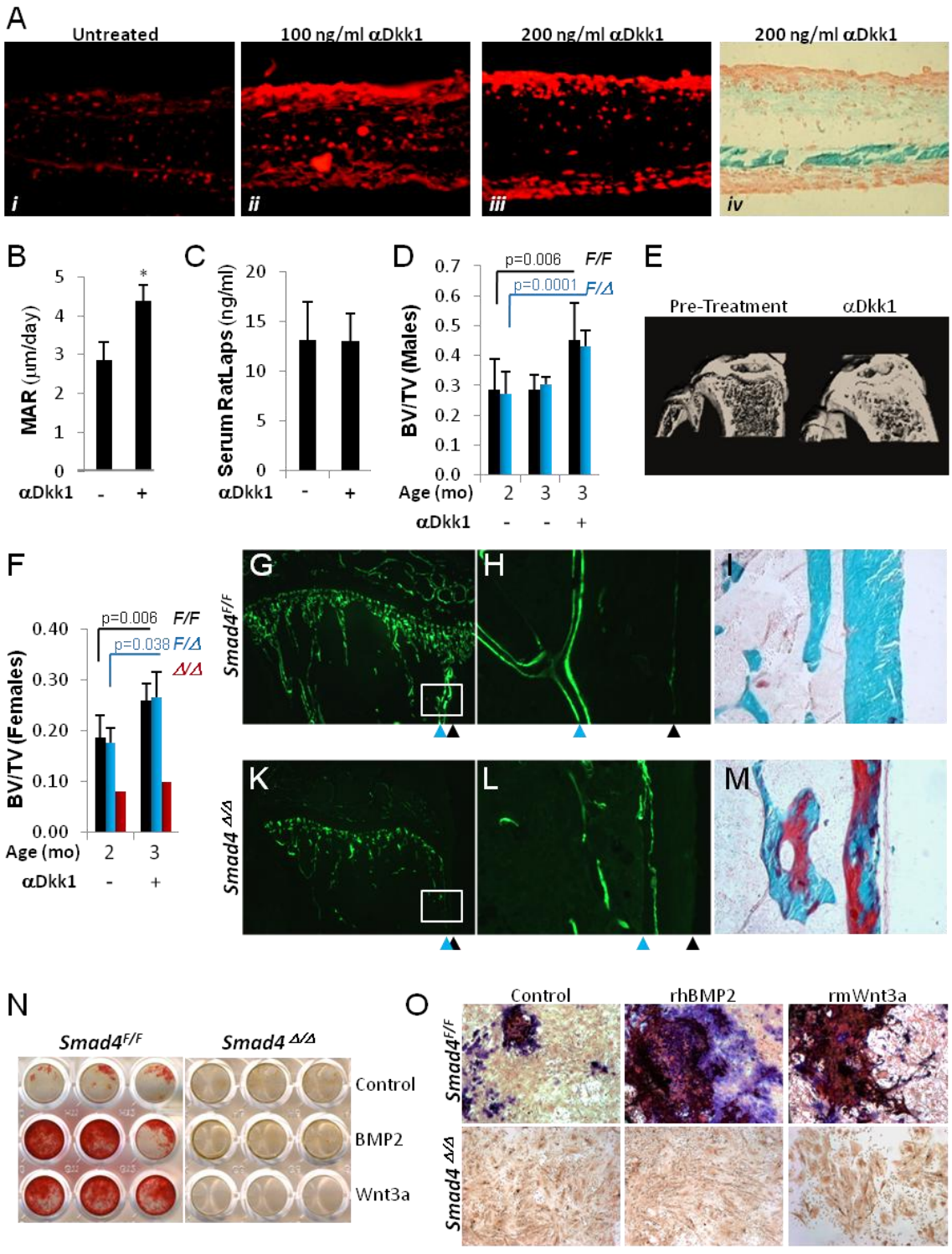
A
Untreated
100 ng/ml αDkk1
200 ng/ml αDkk1
200 ng/ml αDkk1
i
ii
iii
iv
B
MAR (μm/day)
αDkk1
C
Serum RatLaps (ng/ml)
αDkk1
D
BV/TV (Males)
p=0.006 F/F
p=0.0001 F/Δ
Age (mo)
αDkk1
E
Pre-Treatment
αDkk1
F
BV/TV (Females)
p=0.006 F/F
p=0.038 F/Δ
Δ/Δ
Age (mo)
αDkk1
G
H
I
Smad4F/F
K
L
M
Smad4 Δ/Δ
N
Smad4F/F
Smad4 Δ/Δ
Control
BMP2
Wnt3a
O
Control
rhBMP2
rmWnt3a
Smad4F/F
Smad4 Δ/Δ

Figure 4.7

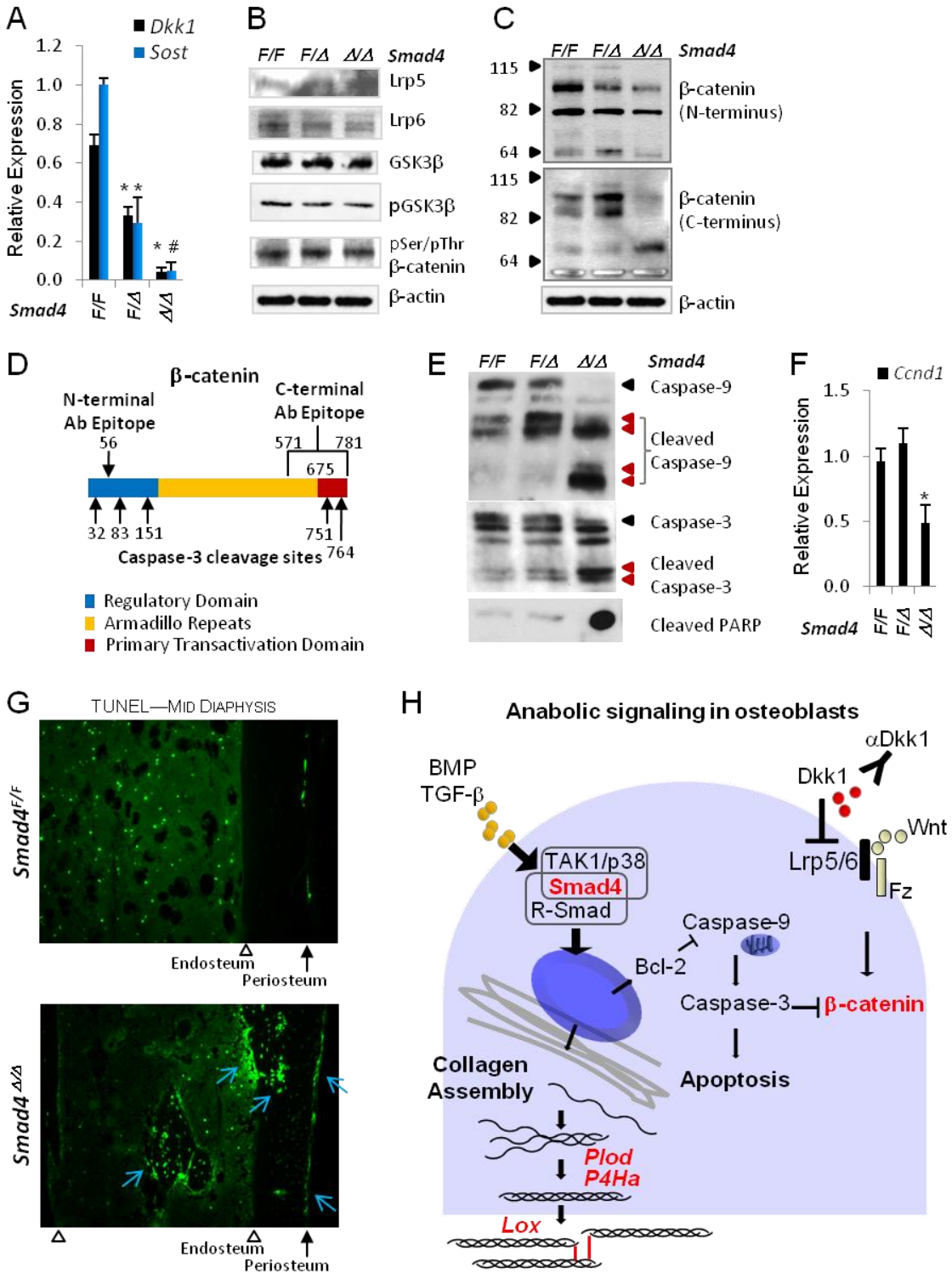
A
Dkk1
Sost
Relative Expression
1.2
1.0
0.8
0.6
0.4
0.2
0.0
* *
* #
Smad4
F/F
F/Δ
Δ/Δ
B
F/F F/Δ Δ/Δ Smad4
Lrp5
Lrp6
GSK3β
pGSK3β
pSer/pThr β-catenin
β-actin
C
F/F F/Δ Δ/Δ Smad4
115
82
64
β-catenin (N-terminus)
β-catenin (C-terminus)
β-actin
D
β-catenin
N-terminal Ab Epitope
56
C-terminal Ab Epitope
571 781
675
32 83 151
751 764
Caspase-3 cleavage sites
Regulatory Domain
Armadillo Repeats
Primary Transactivation Domain
E
F/F F/Δ Δ/Δ Smad4
Caspase-9
Cleaved Caspase-9
Caspase-3
Cleaved Caspase-3
Cleaved PARP
F
Ccnd1
Relative Expression
1.5
1.0
0.5
0.0
*
Smad4 F/F F/Δ Δ/Δ
G
TUNEL—MID DIAPHYSIS
Smad4F/F
Endosteum
Periosteum
Smad4 Δ/Δ
Endosteum
Periosteum
H
Anabolic signaling in osteoblasts
αDkk1
Dkk1
BMP
TGF-β
Wnt
TAK1/p38
Smad4
R-Smad
Lrp5/6
Fz
Caspase-9
Bcl-2
Caspase-3
β-catenin
Collagen Assembly
Apoptosis
Plod
P4Ha
Lox

4.9 TABLE 4.1

Antibody	Company	City, State	Catalog Number
β-actin	Sigma	Saint Louis, MO	A 5316
Akt	Cell Signaling	Danvers, MA	9272
Akt-substrate (RXXXS/T)	Cell Signaling	Danvers, MA	9614
Bcl-2	BD Biosciences	San Diego, CA	554218
α-catenin	Sigma	Saint Louis, MO	B 6184
β-catenin (C-terminus)	BD Biosciences	San Diego, CA	610154
β-catenin (N-terminus)	Cell Signaling	Danvers, MA	9581
Caspase 3 (Cleaved)	Cell Signaling	Danvers, MA	9661
Caspase 9	Cell Signaling	Danvers, MA	9504
Erk	BD Biosciences	San Diego, CA	610124
GADD45β	Santa Cruz	Santa Cruz, CA	sc-8775
GSK3α/β	Millipore	Temecula, CA	05-412
Jnk	Cell Signaling	Danvers, MA	9252
Lysyl Oxidase	Thermo Scientific	Rockford, IL	PA1-46020
Lrp5	Santa Cruz	Santa Cruz, CA	sc-21389
Lrp6	Cell Signaling	Danvers, MA	3395
Ncadherin	BD Biosciences	San Diego, CA	610921
Osterix	Abcam	Cambridge, MA	ab22552
p38	Cell Signaling	Danvers, MA	9212
PARP (Cleaved)	Cell Signaling	Danvers, MA	9544
Phospho-ATF2	Cell Signaling	Danvers, MA	9221
Phospho-CREB	Cell Signaling	Danvers, MA	9198
Phospho-p38	Cell Signaling	Danvers, MA	9211
Phospho-Akt (Ser473)	Cell Signaling	Danvers, MA	9271
Phospho-Erk	Cell Signaling	Danvers, MA	9101
Phospho-GSK3β	Cell Signaling	Danvers, MA	9336
Phospho-Jnk	Cell Signaling	Danvers, MA	9251
Phospho-Smad1/5/8	Cell Signaling	Danvers, MA	9511, 9516
Phospho-Smad2	Cell Signaling	Danvers, MA	3101
Phospho-Smad3	Cell Signaling	Danvers, MA	9520
Phospho-TAK1	Cell Signaling	Danvers, MA	4508
Phospho-β-catenin (S/T)	Cell Signaling	Danvers, MA	9561
Smad1	Cell Signaling	Danvers, MA	9743
Smad2	Cell Signaling	Danvers, MA	5339, 3102
Smad3	Cell Signaling	Danvers, MA	9523
Smad4	Cell Signaling	Danvers, MA	9515
Smad5	Cell Signaling	Danvers, MA	9517
TAK1	Cell Signaling	Danvers, MA	4505
α-Tubulin	Santa Cruz	Santa Cruz, CA	sc-8035

CHAPTER 5

Summary and Future Directions

5.1 Interactions between BMP and Canonical Wnt Signaling Regulate Critical Stages of the Osteoblast Lifecycle. Our lab has previously demonstrated that overexpression of β-catenin synergizes with BMP2 to stimulate osteoblast differentiation and new bone formation [1], although the molecular mechanisms behind this cooperative interaction were not clear. Thus, the central focus of this work was to examine the epistatic and molecular interactions between β-catenin and the BMP pathway that contribute to regulate cell fate, proliferation, matrix synthesis, and the death of osteoblasts. Our studies reveal that the interactions between β-catenin and BMP signals are unique at different stages of the osteoblast lifecyle, and are in large part mediated by the TGFβ/BMP transcription factor, Smad4.

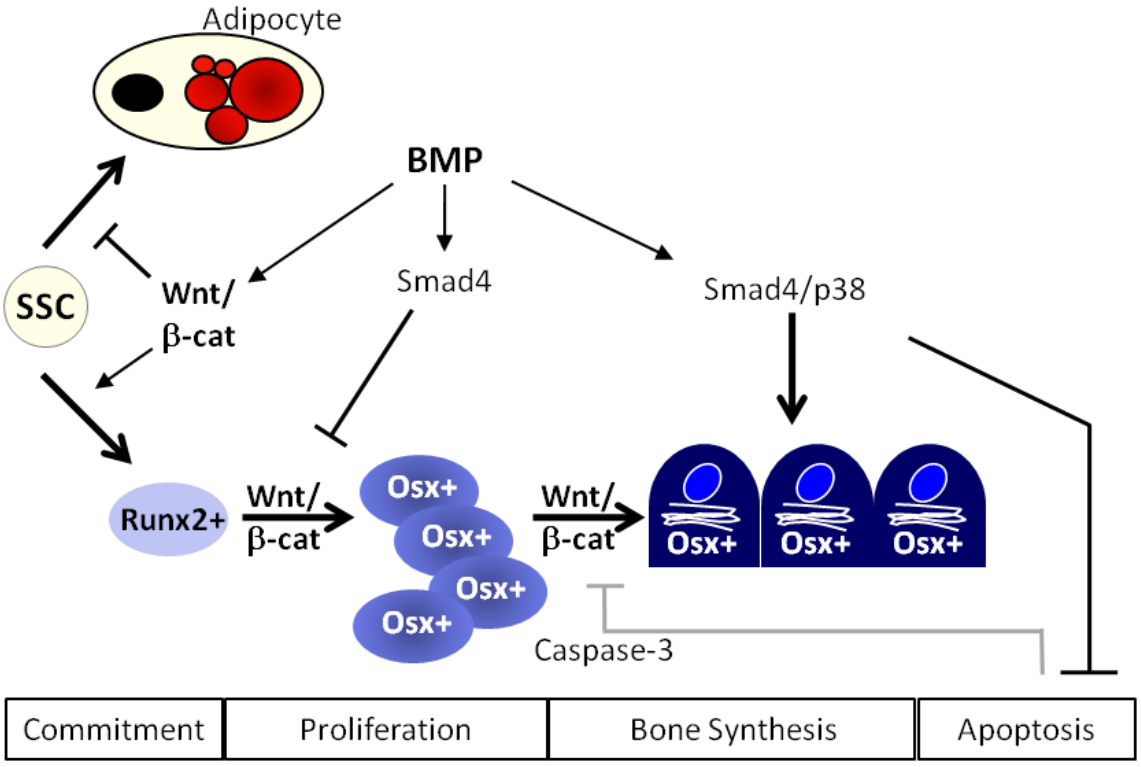

Figure 5.1 Interactions between BMP and canonical Wnt signaling regulate critical stages of the osteoblast lifecycle.

In multipotent progenitors, we find that specification of osteoblasts over adipocytes involves a lineage allocation switch that lies downstream of BMP signals and is mediated by β-catenin. Expansion of the osteoprogenitor pool by Wnt/β-catenin signaling also lies downstream of the BMP pathway, but is negatively regulated, at least in part, by BMP-dependent formation of

Smad4/β-catenin/TCF transcription complexes. This, acute removal of Smad4 increases canonical Wnt signaling at the level of Tcf/Lef dependent transcription, resulting in greater proliferation of progenitors. By contrast, long-term deficiency of Smad4 makes osteoblasts extremely susceptible to apoptosis, leading to indirect deactivation of canonical Wnt signaling via GSK3β-independent and Caspase-3 dependent cleavage of β-catenin. Thus, while pro-mitotic canonical Wnt cues are directly attenuated by BMP/Smad4 signaling, bone anabolic canonical Wnt cues are fully dependent on the integrity of the BMP/Smad4 pathway. Our study establishes that BMP pathway is epistatic to Wnt signaling during specification of osteoblast cell fate, establishment of the mitotic/post-mitotic boundary, and for control of programmed cell death. In combination with previous reports by other labs [2,3], our study further demonstrates that Wnt and BMP pathways are not epistatic during bone formation, but rather must fire simultaneously for osteoblasts to fully acquire their prototypic collagen-synthesizing and matrix-mineralizing functions. Taken together, these findings reveal that critical stages of osteoblastogenesis and bone formation are regulated by distinct and temporally-specific signaling interactions between the canonical Wnt and BMP pathways.

5.2 β-catenin acts downstream of BMP2 to suppress adipocyte cell fate and promote osteoblast differentiation. In **Chapter 2** of this thesis, we examine how β-catenin and BMP signaling coordinate to specify osteoblast cell fate and suppress adipogenesis. By performing a structure/function analysis of β-catenin, we find that stimulation of multipotent progenitors with BMP2 generates an ambiguous differentiation cue that can be amplified and refined with cell fate information by β-catenin. Specifically, overexpression of a full-length, constitutively active β-catenin mutant inhibits adipogenesis and stimulates osteoblast differentiation in mouse embryonic fibroblasts (C3H10T1/2 cells), an effect that is great enhanced by BMP2. While N-terminal truncation of β-catenin weakens its ability to transactivate Tcf/Lef activity, it does not eliminate its capacity to stimulate the osteoblast differentiation program. This is further exemplified by C-terminal truncation of β-catenin, which completely abolishes its ability to transactivate Tcf/Lefs

and suppress adipogenesis, but has no detrimental effect to the capacity of β-catenin to stimulates osteoblast differentiation. Curiously though, overexpression of this C-terminally truncated β-catenin mutant prompted spontaneous formation of adipocytes alongside alkaline phosphatase expressing osteoblasts, which the abundance of both were greatly enhanced by treatment with BMP2. Moreover, we found that C3H10T1/2 cells produce high amounts of BMP-4, and inhibition of endogenous BMP signaling by Noggin curtails differentiation of adipocytes as well as osteoblasts, even in the presence of constitutively active β-catenin. This study therefore demonstrates that BMP signaling is required for differentiation of both osteoblasts and adipocytes. Cell fate cues are provided downstream of BMP signals by β-catenin, involving both Tcf/Lef-dependent and Tcf/Lef-dependent mechanisms for inhibition of adipogenesis and enhancement of osteoblast differentiation.

5.3 Smad4 Attenuates Canonical Wnt Signaling and Proliferation in the Osteogenic Lineage. Crosstalk between BMP and canonical Wnt pathways can occur via direct interaction of Smad proteins with β–catenin. In **Chapter 3**, we tested the hypothesis that a Smad4/β–catenin physical interaction modulates Tcf/Lef-dependent transcription and biological responses. Preliminary studies in C3H10T1/2 mouse embryonic fibroblasts show that Smad4 expression inversely correlates with the ability of Wnt3a or activated β–catenin to stimulate TCF/Lef-dependent transcription, CCND1 expression, and proliferation. Immunoblot analysis in MC3T3 cells indicates that the abundance and phosphorylation status of critical components of the canonical Wnt pathway are not changed by Smad4 over-expression, thus making autocrine or paracrine regulation unlikely. In contrast to subconfluent MC3T3 cells where BMP2 can stimulate nuclear accumulation of β-catenin in approximately 75% of cells, confluent MC3T3 cells exhibit primarily nuclear localization of β-catenin, along with Smad4, TCF3, and TCF4. However, BMP-2 does not activate, and in fact inhibits lithium-stimulated TCF/Lef transcriptional activity. Pull-down experiments reveal that BMP-2 triggers recruitment of β-catenin to a heteromeric transcription complex that binds DNA oligonucleotides encoding classic Smad-binding sequences. Importantly,

this complex also contains Smad4, phosphorylated R-Smads (1/5/8), and TCF4; whereas TCF3 is not recruited. Mutational analysis demonstrates that disrupting Smad4 DNA-binding activity greatly diminishes its ability to antagonize basal CCND1 promoter activity, which is regulated by TCF/Lef promoter elements. The nuclear export signal, linker domain, and Smad4-dependent transcriptional activity are not required. Such antagonism by Smad4 on canonical Wnt signaling is also operative in vivo. And, Tamoxifen-induced ablation of Smad4 in $Smad4^{flox/flox}$; $Osx\text{-}CreER^{T2}$ mice results in a 4-fold increase in the number of BrdU+ cells in trabecular bone, an effect significantly greater than that obtained by activating LRP5/6 with a systemic anti-Dkk1 antibody treatment. Thus, Smad4 operates at the Osterix+ stage of osteoblast differentiation to dampen proliferation, a mechanism at least partially mediated by BMP-2-dependent recruitment of β-catenin/TCF4 to Smad4-containing transcriptional complexes. Our results are consistent with a competitive recruitment model whereby Smad4 can sequester the β-catenin/TCF transcriptional machinery away from canonical target genes and into BMP response elements, thus inhibiting osteoblast proliferation. Importantly, these findings imply that increased abundance of β-catenin, such as was accomplished by overexpression in Chapter 2, should alleviate the ability of BMP2 to dampen proliferation and thereby produce a greater number of osteoblast from a given starting population of progenitors.

5.4 Smad4 Coordinates p38 Signaling in Osteoblasts and is Required for a Bone Anabolic Response to Canonical Wnt Signaling. TGFß/BMP family members are potent regulators of bone cells and signal by activating cytosolic kinase cascades and Smad transcription factors, including the common mediator, Smad4. In **Chapter 3**, we report that Smad4 inhibits osteoblast proliferation in vivo, in part via direct and competitive interference with canonical Wnt signaling. To examine the role of Smad4 in bone formation (**Chapter 4**), we generated $Smad4^{Flox/Flox}$; Osx1-GFP::Cre mice ($Smad4^{\Delta/\Delta}$), where Smad4 is ablated in osteoblasts. Whole mount staining of $Smad4^{\Delta/\Delta}$ neonates reveals hypomineralization of the skull, clavicle hypoplasia, and malformations of the rib cage. At day P28, $Smad4^{\Delta/\Delta}$ mice are severely

runted and μCT indicates the cranial vault, scapulae, and sternal segment of the clavicles are still hypomineralized. Trabecular bone volume at the proximal tibia is normal relative to a smaller bone. However, Smad4$^{\Delta/\Delta}$ mice exhibit delayed development of a medullary cavity in long bones. Smad4 ablation does not impede Runx2, Col1α1, DMP1, or Phex expression in bone, but sharply decreases expression of genes involved in collagen crosslinking including Lox, Plod, and P4Ha, which is consistent with abnormal picrosirius red staining. Importantly, Smad4$^{\Delta/\Delta}$ mice fail to respond to the osteo-anabolic effect of anti-Dkk1 antibody, with sparse single calcein labels present on bone surfaces after 4 weeks of treatment as opposed to abundant wide double-labels in WT mice. Accordingly, Smad4$^{\Delta/\Delta}$ BMSCs fail to mineralize in culture, and are not rescued by either BMP-2 or Wnt3a. Mechanistically, Smad4 ablation disrupts p38 and Smad(1/5/8) phosphorylation in bone, instead enhancing Caspase-3 activity and the abundance of apoptotic TUNEL+ osteoblasts. Whereas BMP2-dependent expression of Lox is mediated by the p38 MAPK pathway, the resistance to anabolic Wnt signaling can be linked to loss of β-catenin transcriptional activity, a consequence of Caspase-3-mediated cleavage of the β-catenin C-terminal transcriptional activation domain. Thus, while that acute removal of Smad4 directly favors canonical Wnt signaling and mitosis, long-term deficiency of Smad4 indirectly impairs Wnt signaling and osteoblast function via Caspase-3. In summary, Smad4 regulates osteoblast survival and function via coupling of canonical Smad with non-canonical MAPK pathways, interactions that lie upstream of anabolic canonical Wnt/β-catenin signaling.

5.5 Future Directions. As has been extensively reviewed in this text, inhibition of osteoblast differentiation by loss of β-catenin is well documented. Thus, an immediate question prompted by the findings in **Chapter 2** is whether a transcriptionally-defective β-catenin mutant is able to restore osteoblast differentiation in Catnb-null cells. The data in **Chapter 4** could be interpreted to suggest that loss of the β-catenin C-terminal transactivation domain impedes osteoblast differentiation, which is in apparent contradiction to results in Chapter 2 showing that expression of a β-catenin mutant missing this domain is fully capable of inducing osteoblast differentiation, though alongside spontaneous adipogenesis. However, a conclusive

interpretration is elusive as it is difficult to know what components of the osteoblast defect in Smad4$^{\Delta/\Delta}$ mice are specific for loss of Smad4 and independent of β-catenin deactivation. This type of issue exemplifies a potential pitfall of analyzing protein function by overexpression on a wild type background. Thus, to directly address this question, a future objective is to determine the ability of β-catenin mutants described in Chapter 2 to rescue osteoblast differentiation in Catnb$^{\Delta/\Delta}$ primary cells.

In a similar context, we have clearly demonstrated that activation of canonical Wnt signaling, specifically at the level of the Lrp5/6 receptors, is not sufficient to rescue Smad4$^{\Delta/\Delta}$ osteoblasts. Since a critical feature of Smad4$^{\Delta/\Delta}$ osteoblasts is depletion of endogenous β-catenin, complementation of Smad4$^{\Delta/\Delta}$ osteoblasts with constitutively active β-catenin will help clarify whether the collagen-synthesizing and matrix mineralizing defects are distinct components of the overall phenotype, as we suspect collagen organization is linked to TGFβ/BMP signaling while mineralization is a function regulated by Wnt/β-catenin. This particular experimental design could also be used to determine if restoring β-catenin levels protects against apoptosis. An additional β-catenin mutant bearing Caspase-3 resistant cleavage motifs would be useful. It is important to determine if pharamacologic inhibition of Caspase-3 restores β-catenin levels in Smad4$^{\Delta/\Delta}$ osteoblasts.

Additionally, we have yet to determine the protein domain(s) of Smad4 required for its physical interaction with β-catenin. Being that we have already generated an extensive library of Smad4 mutants, this type of study should be relatively straight forward and will be conducted by evaluating which HA-tagged Smad4 mutants can co-immunoprecipate a KT3-tagged wild type β-catenin. These results will be compared to our existing data to determine whether physical interaction between Smad4 and β-catenin is required for antagonism of pro-mitotic Wnt signals.

5.6 CLOSING REMARKS In summary, these studies were undertaken in an effort to understand how β-catenin and BMP synergize to stimulate osteoblast differentiation and bone formation. To this end, the work presented here describes a systematic survey of the nature of crosstalk between BMP and β-catenin at defining stages of the osteoblast differentiation program. Our findings illuminate that complex and temporally-specific interactions between the BMP and β-catenin are in large part mediated by Smad4, and serve to regulate cell fate, proliferative capacity, function, and death of osteoblasts. These data therefore help describe the molecular mechanisms underlying osteogenic Wnt and BMP signaling in bone. Additionally, while we did not initially intend to examine the role of Smad4 in osteoblast biology, per se, we have nevertheless uncovered a fundamental role for this transcription factor of the greater TGFβ pathway in post-natal skeletal development. We provide evidence that the role of Smad4 in bone development and skeletal metabolism derives not only through an ability to modulate canonical Wnt signaling, but also because Smad4 exerts powerful influence over R-Smad and TAK1/p38 MAPK signaling in bone. Therefore, this work also provides novel evidence that current models depicting TGFβ/BMP signaling should be refined to account for a clear, but heretofore unestablished, link between canonical Smad and non-canonical MAPK pathways.

5.6 BIBLIOGRAPHY

1. Mbalaviele G, Sheikh S, Stains JP, Salazar VS, Cheng SL, et al. (2005) β-catenin and BMP-2 synergize to promote osteoblast differentiation and new bone formation. Journal of Cellular Biochemistry 94: 403-418.
2. Hill TP, Spater D, Taketo MM, Birchmeier W, Hartmann C (2005) Canonical Wnt/β-catenin signaling prevents osteoblasts from differentiating into chondrocytes. Developmental Cell 8: 727-738.
3. Chen Y, Whetstone HC, Youn A, Nadesan P, Chow EC, et al. (2007) β-catenin signaling pathway is crucial for bone morphogenetic protein 2 to induce new bone formation. Journal of Biological Chemistry 282: 526-533.
4. Nishita M, Hashimoto MK, Ogata S, Laurent MN, Ueno N, et al. (2000) Interaction between Wnt and TGF-beta signalling pathways during formation of Spemann's organizer. Nature 403: 781-785.
5. Kahler RA, Westendorf JJ (2003) Lymphoid enhancer factor-1 and beta-catenin inhibit Runx2-dependent transcriptional activation of the osteocalcin promoter. Journal of Biological Chemistry 278: 11937-11944.
6. Castro CH, Shin CS, Stains JP, Cheng SL, Sheikh S, et al. (2004) Targeted expression of a dominant-negative N-cadherin in vivo delays peak bone mass and increases adipogenesis. Journal of Cell Science 117: 2853-2864.
7. Fang LC, Cheng SL, Mbalaviele G, Donsante C, Watkins M, et al. (2006) Accentuated ovariectomy induced bone loss and altered osteogenesis in hyeterozygous N-cadherin null mice. Journal of Bone and Mineral Research 21: 1897-1906.
8. Salazar VS, Mbalaviele G, Civitelli R (2008) The pro-osteogenic action of β-catenin requires interaction with BMP signaling, but not Tcf/Lef transcriptional activity. Journal of Cellular Biochemistry 104: 942-952.
9. Ory DS, Neugeboren BA, Mulligan RC (1996) A stable human-derived packaging cell line for production of high titer retrovirus/vesicular stomatitis virus G pseudotypes. Proceedings of the National Academy of Sciences of the USA 93: 11400-11406.
10. Castro CH, Stains JP, Sheikh S, Szejnfeld VL, Willecke K, et al. (2003) Development of mice with osteoblast-specific connexin43 gene deletion. Cell Communication and Adhesion 10: 445-450.
11. Chung DJ, Castro CH, Watkins M, Stains JP, Chung MY, et al. (2006) Low peak bone mass and attenuated anabolic response to parathyroid hormone in mice with an osteoblast-specific deletion of connexin43. Journal of Cell Science 119: 4187-4198.
12. Dobrowolski R, Sasse P, Schrickel JW, Watkins M, Kim JS, et al. (2008) The conditional connexin43G138R mouse mutant represents a new model of hereditary oculodentodigital dysplasia in humans. Human Molecular Genetics 17: 539-554.

Valerie Salazar

EDUCATION

2011 (Aug) **PhD** Molecular Cell Biology
Graduate Division of Biology and Biomedical Sciences, Washington University in St. Louis, MO, USA

2000 **BA** Biology
BA Romance Languages and Literature
School of Arts and Sciences, Washington University in St. Louis, MO, USA

EMPLOYMENT POSITIONS

2004-11 **Graduate Research Assistant** Department of Internal Medicine, Division of Bone and Mineral Diseases, Washington University, St. Louis, MO, USA

2003 **Research Technician II** Department of Internal Medicine, Division of Bone and Mineral Diseases, Washington University, St. Louis, MO, USA

2003 **Associate Scientist** Department of Oncology and Pharmacology, Pfizer, St. Louis, MO, USA

2002 **Assistant Scientist** Discovery Oncology, Pharmacia, St. Louis, MO, USA

2001 **Contract Scientist** Discovery Oncology, Pharmacia, St. Louis, MO, USA

2000 **Intern** Discovery Oncology, Pharmacia, St. Louis, MO, USA

PROFESSIONAL ASSOCIATIONS

2004-pres American Society for Bone and Mineral Research

HONORS

2011 **ASBMR Young Investigator Award** for submitting a top ranking abstract to the 33rd Annual American Society for Bone and Mineral Research Conference in San Diego, California, USA

2011 **Barbara Jakschik Award** Outstanding academic performance and excellence in research of metabolic regulation. Division of Biology and Biomedical Sciences, Washington University in St. Louis, MO, USA

2010 **ASBMR Young Investigator Travel Grant** to attend the 32nd Annual American Society for Bone and Mineral Research Conference in Toronto, Ontario, Canada.

2010 **ASBMR Young Investigator Award for PhD Training** to attend a PhD Training Course for advanced bone biology in Berlin, Germany. Hosted by the European Calcified Tissue Society.

2009 **Carl Storm Fellowship** to attend the 2009 Cell Contact and Adhesion Gordon Research Conference in Waterville Valley, NH, USA.

2008-10 **Ruth L. Kirschtein National Research Service Award** Individual Pre-doctoral Fellowship from the National Institute of Health, USA. F31, Priority Score 125.

2007-09 **Lucille P. Markey Student** Honors Curriculum in Human Pathobiology, Division of Biology and Biomedical Sciences, Washington University, St. Louis, MO, USA.

2001 **Commitment and Dedication Award** Pharmacia Oncology, St. Louis, MO, USA.

2000 **Top Five Summer Intern** Pharmacia Oncology, St. Louis, MO, USA.

PEER-REVIEWED PUBLICATIONS

2011 **Salazar V**, Huang L, Norris J, Bonar S, Mbalaviele S, Civitelli R. Smad4 coordinates R-Smad and p38 signaling in osteoblasts and is required for bone anabolic response to canonical Wnt signaling. Manuscript in preparation.

2011 **Salazar V**, Zarkadis N, Huang L, Mbalaviele S, Civitelli R. Smad4 antagonizes osteoblast proliferation via competitive recruitment of β-catenin. Manuscript in preparation.

2011 **Salazar V**, Revollo L, Huang L, Norris J, Bonar S, Mbalaviele S, Civitelli R. Bone-anabolic response to anti-Dkk1 therapy is attenuated by osteoblast-specific expression of Ncadherin. Manuscript in preparation.

2010 Di Benedetto A, Watkins, M, Grimston S, **Salazar V**, Donsante C, Mbalaviele G, Radice GL, Civitelli R. N-cadherin and cadherin 11 modulate postnatal bone growth and osteoblast differentiation by distinct mechanisms. J Cell Sci 123(15):2640-2648. PMID: 20605916. PMCID: PMC2908051

2007 **Salazar V**, Mbalaviele G, Civitelli R. The pro-osteogenic action of β-catenin requires interaction with BMP signaling, but not Tcf/Lef transcriptional activity. J Cell Biochem **104**(3):942-52. PMID: 18247340.

2005 Mbalaviele G, Sheikh S, Stains J, **Salazar V**, Cheng S, Chen D, Civitelli R. β-catenin and BMP-2 synergize to promote osteoblast differentiation and new bone formation. J Cell Biochem **94**:403-418 (2005). PMID: 15526274. PMCID: PMC2647989.

2002 Trifan OC, Durham WF, **Salazar V**, Horton J, Levine BD, Zweifel BS, Davis TW and Masferrer JL. Cyclooxygenase-2 inhibition with celecoxib enhances anti-tumor efficacy and reduces diarrhea side effect of CPT-11. Cancer Res. **62**(20): 5778-84 (2002). PMID: 12384538.

CONFERENCE PROCEEDINGS

2011 **ORAL PRESENTATION, YOUNG INVESTIGATOR AWARD. V Salazar**, L Huang, G Mbalaviele, R Civitelli. Smad4 Coordinates BMP Signaling through p38 in Osteoblasts and is Required for Bone Anabolic Response to Canonical Wnt Signaling. 33rd annual ASBMR Conference in San Diego, CA, USA.

2011 **ORAL PRESENTATION. V Salazar**, N Zarkadis, L Huang, G Mbalaviele, R Civitelli. Smad4 Antagonizes Osteoblast Proliferation via Competitive Recruitment of β-catenin. 33rd annual ASBMR Conference in San Diego, CA, USA.

2010 **PLENARY POSTER. V Salazar**, J Norris, L Huang, G Mbalaviele, R Civitelli. The Osteoanabolic Effect of Systemic Dkk1 Inhibition is Associated with Canonical Lrp5/6 and Erk Signaling in Bone and is Modulated by N-cadherin in Osteoblasts. 32nd annual ASBMR Conference in Toronto, ON, Canada.

2010 **PLENARY POSTER. V Salazar**, G Mbalaviele, R Civitelli. Tamoxifen-induced Deletion of Smad4 in Osteoblasts Enhances Proliferation in the Periosteum, Growth Plate, and Bone Marrow. 32nd annual ASBMR Conference in Toronto, ON, Canada.

2009 **ORAL PRESENTATION. V Salazar**, A Di Benedetto, J Norris, G Radice, G Mbalaviele, R Civitelli. N-Cadherin and Cadherin-11 Differentially Modulate Bone Anabolic Response to Dkk1 Inhibition. 31st annual ASBMR Conference in Denver, CO, USA.

2008 **V Salazar**, G Mbalaviele, and R Civitelli. Negative Regulation of Tcf/Lef-dependent Transcription by the BMP/Smad4 Signaling Axis. 30th annual ASBMR Conference in Montreal, Quebec, Canada.

2006 **V Salazar**, G Mbalaviele, and R Civitelli. Separable Functions of β-catenin Cooperate with BMPs to Control Adipogenesis and Osteogenesis. 28th annual ASBMR Conference in Philadelphia, PA, USA.

2005 **ORAL PRESENTATION. V Salazar**, B Guillotin, G Mbalaviele, and R Civitelli. Competitive Recruitment of β-catenin to Smad-Dependent Transcription Complexes by BMP-2. 27th annual ASBMR Conference in Nashville, TN, USA.

2004 **PLENARY POSTER. V Salazar**, G Mbalaviele, and R Civitelli. Structure/Function Analysis of β-catenin in Osteoblast Differentiation. 26th annual ASBMR Conference in Seattle, WA, USA.

2002 Trifan OC, Durham WF, **Salazar V**, Horton J, Levine BD, Zweifel BS, Davis TW, and Masferrer JL. COX-2 specific inhibitor celecoxib enhances anti-tumor efficacy and reduces diarrhea side effect of CPT-11. 93rd annual AACR meeting in San Francisco, CA, USA.

RESEARCH SUPPORT

NIH F31 AR056586 Salazar (PI) 08/01/2008-07/31/2010
Antagonism of Canonical Beta-Catenin Activity by Smad4 in Osteoprogenitors